183P INCREASED α_1– AND α_2-ADRENOCEPTOR-MEDIATED CONTRACTILE RESPONSES OF HUMAN SKELETAL MUSCLE RESISTANCE ARTERIES IN CHRONIC LIMB ISCHAEMIA

Y.P.R. Jarajapu, P. Coats, J.C. McGrath*, A. MacDonald, and C. Hillier. Vascular Assessment Group, School of Biological and Biomedical Sciences, Glasgow Caledonian University, Glasgow; *Autonomic Physiology Unit, Glasgow University.

Recently we have shown that human skeletal muscle resistance arteries (SkMRAs) from distal regions of ischaemic limbs produce augmented responses to noradrenaline (NA) (Coats and Hillier 1999) confirming earlier findings in animal models of ischaemia (Sapienza *et al.*, 1996). We investigated whether either α_1- or α_2- adrenoceptors or both mediated the increased sensitivity of human SkMRAs.

SkMRAs were isolated from proximal (non-ischaemic internal control) and distal (ischaemic) sites on limbs amputated for critical limb ischaemia (CLI), mounted on a wire myograph, and normalised according to Mulvany and Halpern (1976). Viability was checked by activation with 120 mM KCl twice and 10 μM NA. Cumulative concentration response curves (CRCs) to NA (non-selective), phenylephrine (PE, selective α_1) and brimonidine (BR, selective α_2) were obtained over the range 0.001μM to 30 μM.

Maximum vasoconstrictor responses to KCl in proximal and distal SkMRAs were similar. Responses of all three agonists in distal arteries were significantly greater than those of proximal arteries (Table 1). Comparison of NA responses with PE and BR showed NA to be more efficacious than either the α_1- or the α_2- selective agonists in both proximal and distal vessels ($p<0.05$; Student's *t* test). Contractile responses of BR were small suggesting a smaller contribution of α_2-adrenoceptors to the NA-induced responses.

Table 1: Maximum responses and pEC_{50} values of adrenoceptor agonists in SkMRA (Mean ± s.e.mean).

Agonist	n	Site	pEC_{50}	Maximum Response
NA	7	Proximal	5.9±0.2	42±5
		Distal	6.2±0.3	89±5*
PE	5	Proximal	5.9±0.2	11±4
		Distal	5.7±0.2	50±12*
BR	5	Proximal	6.2±0.1	6±1
		Distal	6.4±0.2	26±8*

*Expressed as % of maximum KCl response; proximal versus distal *$p<0.05$ (Student's paired *t* test).

These results show that both α_1- and α_2-adrenoceptor mediated responses contribute to the increased reactivity to NA of SkMRA from the ischaemic limb. Increased vasoconstrictor responses to noradrenaline may contribute to reduced muscular blood flow in the ischaemic limb.

Coats, P. & Hillier, C. (1999). *Eur J Vasc Surg.* In Press.
Mulvany, M.J. & Halpern, W. (1976). *Nature (London),* **260**:617-619.
Sapienza, P., Edwards, AD., Mingoli, A. *et al.* (1996). *J. Surg. Res* **62**: 192-196.

184P ATYPICAL β-ADRENOCEPTOR-MEDIATED VASORELAXATION IN RAT ISOLATED AORTA MAY INVOLVE A cAMP-INDEPENDENT PATHWAY

L. Brawley, A.M. Shaw & A. MacDonald, School of Biological & Biomedical Sciences, Glasgow Caledonian University, Glasgow G4 0BA

Atypical β-adrenoceptors mediating relaxation co-exist with classical β-adrenoceptors in the rat thoracic aorta (Oriowo, 1995; Brawley *et al.*, 1998). Classical β-adrenoceptor -induced relaxation is mediated through a signal transduction pathway which is cAMP-dependent (Kukovetz *et al.*, 1981) but there is little information on atypical β-adrenoceptor-mediated relaxation in smooth muscle. The aim of the present study was to investigate the effects of an adenylate cyclase inhibitor, SQ 22536 (Lippe & Ardizzone, 1991), on classical and atypical β-adrenoceptor-induced relaxant responses in the rat thoracic aorta. In addition, the effects of isoprenaline and the atypical β-adrenceptor agonist, CGP 12177A (Mohell & Dicker, 1989), on cAMP levels were determined.

Male Wistar rats were stunned and killed by cervical dislocation. Thoracic aortae were removed and prepared as described previously (Brawley *et al.*, 1997). For the functional experiments, cumulative concentration-response curves (CRCs) to isoprenaline and CGP 12177A were carried out in noradrenaline-preconstricted rings (Brawley *et al.*, 1998). Some tissues were pretreated with SQ 22536 (200 μM) for 30 minutes. For cyclic nucleotide measurement, noradrenaline-constricted rings were frozen after treatment with either isoprenaline (10 μM) or CGP 12177A (100 μM) for 120 sec in the presence of IBMX (10 μM). Tissues were homogenised in 95% ethanol. After centrifugation, the supernatant was decanted and residual ethanol was evaporated. The dry extract was resuspended and cAMP levels obtained using a cAMP binding protein assay. Values given are mean ± s.e.mean. Statistical analysis was carried out using Student's *t* test (two groups) or one-way ANOVA followed by Bonferroni post tests (more than two groups).

SQ 22536 shifted the isoprenaline CRC to the right with a significant depression of the maximum response (% maximum relaxation, control, 103±4, n=7; SQ 22536, 44±1, n=7, P<0.001). Pretreatment with SQ 22536 did not alter CGP 12177-induced relaxation (% maximum relaxation, control, 96±2, n=6; SQ 22536, 97±2, n=6, P>0.05. pEC_{50}: control, 4.40±0.01; SQ 22536, 4.41±0.03, P>0.05).

Isoprenaline (10 μM) elicited 95±3 % relaxation at 120 sec. Cyclic AMP levels (pmoles/mg protein) were elevated 2.6 fold by isoprenaline (basal, 7.4±1.0, n=6; isoprenaline, 19±4, n=7, P <0.05). CGP 12177A (100 μM) produced 76±6 % relaxation at 120 sec. Cyclic AMP levels were unaltered following CGP 12177 addition (7.6±2.2, n=6, P>0.05).

In conclusion, in contrast to relaxation mediated by classical β-adrenceptors, relaxation mediated by atypical β-adrenoceptors in rat thoracic aorta appears to be mediated by a signalling pathway which is cAMP-independent.

L.B. is supported by a Glasgow Caledonian University Studentship
CGP 12177A was kindly donated by Novartis Pharma AG

Brawley, L., MacDonald, A. & Shaw, A.M. (1997) *Br. J. Pharmacol.*, **122**, 395P.
Brawley, L., MacDonald, A. & Shaw, A.M. (1998) *Br. J. Pharmacol.*, **125**, 18P.
Kukovetz, W.R., Pöch, G. & Holzmann, S. (1981) In *Vasodilatation* ed. P.M. Vanhoutte & I. Leusen, pp. 339-353. New York, Raven Press
Lippe, C. & Ardizzone, C. (1991) *Comp. Biochem. Physiol.*, **99C**, 209-211
Mohell, N. & Dicker, A. (1989) *Biochem. J.*, **261**, 401-405.
Oriowo, M.A. (1995) *Life Sci.*, **56**, PL269-PL275

185P RIGHT VENTRICULAR β-ADRENOCEPTORS IN MONOCROTALINE-TREATED RATS

T. Seyfarth, I. Heinroth-Hoffmann, H.-P. Gerbershagen, K. Pönicke, O.-E. Brodde, Institute of Pharmacology, University of Halle, D-06097 Halle, Germany

Application of the pyrrolizidine alkaloid monocrotaline (MCT) to rats leads to progressive pulmonary hypertension resulting in right ventricular hypertrophy and heart failure (Ceconi et al., 1989; Vescovo et al., 1989). The aim of this study was to investigate right ventricular β-adrenoceptor changes in MCT-treated rats. For this purpose male Wistar rats (6 weeks old) were treated with 60 mg/kg MCT i.p.; control rats received saline. Six weeks after MCT-injection rats had developed severe right ventricular hypertrophy (RVH); 50 % of these animals had pleural, pericardial and peritoneal effusions consistent with heart failure (HF). The left:right ventricle weight ratio was 1.70 ± 0.1 (n=12) in RVH and 1.58 ± 0.1 (n=13) in RVHHF versus 3.56 ± 0.1 (n=12) in controls. We assessed in right ventricular membranes of these hearts β-adrenoceptor density (by [^{125}I]-iodocyanopindolol (ICYP) binding as described by Brodde et al., 1995), the amount of β-adrenoceptors in the high affinity state (R_H, from isoprenaline ± 100 μM GTP competition curves with the ICYP binding), β_1:β_2-adrenoceptor ratio (from CGP 20712 A competition-curves with the ICYP-binding) and adenylyl cyclase activity (as described by Brown et al., 1992). β-Adrenoceptor density and the amount of β_1-adrenoceptors were significantly decreased in MCT-rats with RVH and decreased further in MCT-rats with RVHHF (Table 1). Furthermore, the amount of β-adrenoceptors in the high affinity state (R_H) decreased from 46 to 36 % in MCT-RVH rats and decreased further to 27 % in MCT-RVHHF rats ($P < 0.05$).

Table 1. Right ventricular β-adrenoceptor (AR) density, β_1-AR and R_H- β-AR in control rats and in MCT-rats with right ventricular hypertrophy (RVH) and with RVH and heart failure (RVHHF)

	β-AR (fmol/mg prot.)	β_1-AR (%)	R_H (%)
Control	35.7 ± 2.5	63.3 ± 1.6	45.7 ± 3.7
RVH	17.3 ± 2.5*)	55.6 ± 2.7*)	36.0 ± 1.9*)
RVHHF	13.6 ± 2.9*)	54.0 ± 3.2*)	27.0 ± 2.8*,a)

n=5-12; *) $P < 0.05$ vs. control; a) $P < 0.05$ vs. RVH (non-paired, two-tailed Student's t-test).

The decrease in β-adrenoceptor density and percentage in R_H-receptors was accompanied by a significant decrease in 100 μM isoprenaline-induced adenylyl cyclase activation: it was in control rats (pmol cAMP/mg protein/min): 15.7 ± 4.5 (n=5), in MCT-RVH rats 10.9 ± 1.7 (n=5) and in MCT-RVHHF rats 6.3 ± 1.1 (n=5). We conclude that in MCT rats with RVH right ventricular β-adrenoceptor number and -functional responsiveness is decreased, and decrease further in rats with RVH and heart failure.

Brodde, O.-E. et al. J. Am. Coll. Cardiol. 25: 761-767, 1995.
Brown, L. et al. J. Cardiovasc. Pharmacol. 19: 222-232, 1992.
Ceconi, C. et al. Cardiovasc. Res. 23: 674-682, 1989.
Vescovo, G. et al. J. Mol. Cell. Cardiol. 21: 1047-1061, 1989.

Supported by the Deutsche Forschungsgemeinschaft (DFG Br 526/6-1).

186P 5-HT$_{1D}$-LIKE RECEPTOR IN BOVINE PULMONARY SUPERNUMERARY ARTERIES

T. Brown, D. Bunton, A. MacDonald, A.M. Shaw. School of Biological & Biomedical Sciences, Glasgow Caledonian University, City Campus, Glasgow. G4 OBA.

Pulmonary supernumerary arteries (SA) are small muscular arteries that account for at least 40% of the total cross sectional area of all branches (Elliott & Reid, 1965) and therefore are likely to play an important role in regulating pulmonary vascular resistance. 5-hydroxytryptamine (5-HT) has been implicated in some forms of pulmonary hypertension (Herve *et al.*, 1990) and in previous studies we have shown that the response to 5-HT in SA appears to involve both a 5-HT2A and a 5-HT1 receptor (Bunton *et al.*, 1998). The aim of the present study was to further characterise the 5-HT1 receptor in bovine SA.

Bovine lungs were obtained fresh from the abattoir. Ring segments of supernumerary arteries (diameter 0.5 - 1 mm) were dissected from the lung and freed of surrounding connective tissue. The vessels were then weighed and suspended between stainless steel hooks in Krebs buffer (37°C) under a tension of 1 g and gassed with a mixture of O_2 : CO_2 (95%/5% v/v). The tissues were allowed to equilibrate for 1 hour in the presence of ritanserin (100 nM). Each tissue was then contracted with U46619 (100 nM). At the peak of contraction forskolin (1 μM) was added which completely reversed the U46619-induced contraction. Thereafter cumulative concentration response curves for reversal of forskolin-induced relaxation were constructed for 5-HT or 5-HT1-selective agonists Antagonists were added 30 min. before U46619. For pertussis toxin studies the rings were preincubated with the toxin (200 ng/ml) for 4 hours. Cyclic nucleotides were extracted from SA rings using ethanol and the cAMP content measured by protein binding assay. Results are means ± s.e. mean. The significance of differences was determined using Student's t-test.

5-HT (1 μM) produced a time-dependent reduction of forskolin (1 μM)-elevated cAMP in SA. 5-HT, 5-carboxyamidotryptamine (5-CT) and the selective agonists 8-OH-DPAT (5-HT1A), RU 24969 (5-HT1B), sumatriptan (5-HT1B/1D) and L-694247 (5HT1D) (all 0.1nM – 100μM, n=6) produced concentration-dependent contraction of forskolin-relaxed SA. The rank order of potency (-log EC50s±s.e.mean) was L-694247 (8.31±0.07) > 5-CT (7.3±0.20) > 5-HT (6.53±0.11) = RU24969 (6.31±0.05) > sumatriptan (5.94± 0.12) = 8-OH-DPAT (5.71±0.19).

The concentration response curve for 5-HT was unaffected by the antagonists BRL15572 (100 nM, 5-HT1D), cyanopindolol (1 μM, 5-HT1A/1B), SB224289A (100nM, 5-HT1B) or by pertussis toxin. In contrast GR127935T (100 nM, 5-HT1B/1D) produced a 7-fold rightward shift giving an estimated pA2 of 7.8 (-log EC50s: control 6.39±0.20 n=4; GR127935T, 5.55±0.1, n=4, p<0.001). Methiothepin (100 nM) produced a 16-fold rightward shift giving an estimated pA2 of 8.4 (-log EC50s: control 6.0±0.42, n=5; methiothepin, 4.79±0.13, n=5, p< 0.001).

The present study supports the presence of a receptor for 5-HT that is negatively coupled to adenylyl cyclase in bovine SA. The rank order of agonist potencies is consistent with the presence of a 5-HT1D receptor subtype. However, the estimated affinities of GR127935T and methiothepin are not consistent with the presence of a 5-HT1D receptor and this is supported by the lack of effect of BRL15572 and cyanopindolol. The lack of effect of pertussis toxin suggests that the negative coupling to adenylyl cyclase does not involve the Go/Gi G-proteins.

Bunton, D., MacDonald, A. M., Shaw, A., *et al.*, (1998) Br. J. Pharmacol. 125, 100P.
Herve, P., Drouet, L., Dosquet, C., *et al.*, (1990) Am. J. Med. 89, 117-120.
Elliott, F.M. & Reid, L. (1965) Clin. Radiol. 16,193-198.

187P ZOLMITRIPTAN STIMULATES A Ca^{2+}-DEPENDENT K^+ CURRENT IN C6 GLIOMA CELLS STABLY EXPRESSING RECOMBINANT HUMAN 5-HT_{1B} RECEPTORS

Bruno Le Grand, Anne Panissié, Michel Perez, Petrus J. Pauwels & Gareth W. John, Centre de Recherche Pierre Fabre, Division of Cardiovascular Diseases, 17 Av. Jean Moulin, 81106 Castres Cedex, France

Zolmitriptan is a new 5-$HT_{1B/1D}$ receptor partial agonist (Martin *et al.*, 1997) that has recently been approved for use in the acute treatment of migraine. Reduced neuronal firing is currently considered to contribute to the therapeutic migraine abortive action of zolmitriptan (Goadsby and Hoskin, 1996). The major cellular mechanism which modulates neuronal excitability following 5-$HT_{1B/1D}$ receptor activation by sumatriptan has been identified as a stimulation of an outward Ca^{2+}-dependent K^+ current ($I_{K/Ca}$; Le Grand *et al.*, 1998; John *et al.*, 1999). Therefore, the aim of the present study was to investigate whether zolmitriptan could similarly stimulate a Ca^{2+}-dependent K^+ current following h 5-HT_{1B} receptor activation.

Outward membrane currents were examined in non-transfected and in transfected C6 glioma cells using the whole-cell configuration. The internal pipette solution contained (in mM): 115 K-aspartate, 10 KCl, 3 $MgCl_2$, 1 $CaCl_2$, 2 KH_2PO_4, 5-Tris-GTP, 4 Mg-ATP, 10 HEPES, 10 D(+)-glucose, pH 7.4 (KOH). The external solution contained (in mM): 135 choline chloride, 1.1 $MgCl_2$, 0.8 $CaCl_2$, 0.001 atropine sulphate, 10 HEPES, 10 D(+)-glucose, pH 7.4 (KOH). In C6 glioma cells expressing recombinant h 5-HT_{1B} receptors, zolmitriptan increased I_K in a concentration-dependent manner (max. increase 16.3 ± 7.8 %, n=5, $p<0.001$, Dunnett's test) with a pD_2 value (geometric mean with 95 % confidence intervals) of 7.03(7.9-6.1). Zolmitriptan failed to elicit increases in I_K in non-transfected C6 cells. In the presence of the mixed 5-$HT_{1B/1D}$ receptor antagonist, GR 127935 (0.1μM), zolmitriptan (1μM) failed to significantly increase I_K in C6 cells expressing h 5-HT_{1B} receptors; confirming that zolmitriptan-evoked responses were indeed mediated by h 5-HT_{1B} receptors. In C6 cells expressing cloned h 5-HT_{1B} receptors, zolmitriptan-induced increases in I_K were prevented by the calcium chelator, EGTA (5 mM) when included in the patch pipette (max. increase -3.3±4.2 %, n=4, P=NS). The Ca^{2+}-dependent K^+ channel blockers, iberiotoxin (0.1μM) and tetraethylammonium (TEA, 1mM), prevented zolmitriptan-induced increases in I_K (4.5±7.3 %, n=4 and -0.8±1.7 %, n=4, respectively, P=NS in each case) in C6 cells expressing h 5-HT_{1B} receptors, confirming the involvement of Ca^{2+}-dependent K^+ channels.

Collectively, the present findings provide evidence that the 5-$HT_{1B/1D}$ receptor partial agonist, zolmitriptan, like sumatriptan, stimulates $I_{K/Ca}$ in C6 glioma cells stably transfected with h 5-HT_{1B} receptors suggesting increases in hyperpolarizing current.

Goadsby, P.J., Hoskin, K.L. (1996) Pain **67**, 355-359.
John, G.W., Pauwels, P.J., Perez *et al.* (1999) J. Pharmacol. Exp. Ther. **290**, 83-95.
Le Grand, B., Panissié, A., Pauwels, P.J., John G.W. (1998) Naunyn-Schmiedeberg's Arch. Pharmacol. **358**, 608-615.
Martin, G.R., Robertson, A.D., Mac Lennan, S.J. *et al.* (1997) Br. J. Pharmacol. **121**, 157-164.

188P COLLAR PLACEMENT INCREASES 5-HT_{1B} RECEPTOR mRNA LEVEL IN THE RABBIT CAROTID ARTERY

I.S. Geerts, H.R. Fret, A.G. Herman and H. Bult

Division of Pharmacology, University of Antwerp (UIA), B-2610 Wilrijk, Belgium

Serotonin (5-hydroxytryptamine, 5-HT) plays an important role in the pathophysiology of vasospasm in human coronary artery disease. A similar hypersensitivity develops in a model of intimal thickening in the rabbit carotid artery. Functional studies pointed to an increased activity of 5-HT_1- like receptors, presumably 5-HT_{1B}, which are not active in the normal rabbit carotid artery (Geerts et al., 1999). The present study addressed the expression of messenger RNA (mRNA) and protein of 5-HT_{1B} or 5-HT_{1D} receptors in this model.

Non-occlusive, silicone collars were placed around both carotid arteries of anaesthetised (sodium pentobarbital, 30 mg kg^{-1}, i.v.) male New Zealand White rabbits (2.5-3.0 kg). Seven days later the arteries were removed under anaesthesia as above. Then the rabbits were killed (overdose sodium pentobarbital). The collared vessels were divided into rings from inside (=collar) and outside (=sham) the collar. Naive (i.e. without manipulation prior to excision), sham and collar segments were frozen in liquid nitrogen after removal of blood and adhering parenchyma. The results are shown as mean ± s.e. mean, n = number of rabbits.

Total RNA was isolated (Trizol method, modification of Chomczynski & Sacchi (1987)) and treated with DNase (60 min., 37 °C, 1Uμl^{-1}). A one step reverse transcription (30 min., 50 °C) - polymerase chain reaction (28 cycles: 94°C for 30 sec, 54°C for 30 sec, 72°C for 45 sec.) (RT-PCR) was performed using the following primers: 5-HT_{1B} sense 5' GCT GTC GTC GGA TAT CAC CT 3'; 5-HT_{1B} antisense 5' CCC ACC GTG GAG TAG ACA GT 3'; 5-HT_{1D} sense 5' ACT AAG ACA CTG GGC ATC ATT 3'; 5-HT_{1D} antisense 5' CTT GCC GAA AAT CCT CAT 3'; β-actin sense 5' CCA CCT TCC AGC AGA TG 3'; β-actin antisense 5' ACC TTC ACC GTT CCA GTT T 3'. After separation on 1.8% agarose and ethidium bromide staining the optical density of the RT-PCR products was determined.

For Western blot analysis, the frozen tissue samples were homogenised and clarified by centrifugation. After SDS-PAGE and blotting onto a nitrocellulose membrane, the membranes were incubated with anti-5-HT_{1B}, anti-5-HT_{1D} or anti-5-HT_{2A} polyclonal or monoclonal antibodies (dilution range:1/1000 – 1/10000). Antibody binding was detected using horseradish peroxidase linked secondary antibodies before substrate incubation and exposure to photographic film. To check for cross-reactivity of the primary antibodies the membranes were stripped, reprobed, immunodetected and stained with India ink.

Bands at ~250 base pairs (bp) and ~270 bp were observed in naive, sham and collar samples as expected for β-actin (253 bp) and 5-HT_{1B} (270 bp) respectively. The 5-HT_{1D} RT-PCR reactions were devoid of signal. The expected 5-HT_{1D} fragment (199 bp) was only detected in a positive control (genomic DNA). Optical densitometrical analysis (ROD) revealed that manipulating the carotid artery increased the 5-HT_{1B} mRNA level. Collar placement raised it even further (ROD: 0.52±0.10, n=4; 0.88±0.04, n=5; 1.08±0.06, n=4 for naive, sham, and collar respectively; $p<0.01$ naive versus sham, $p=0.03$ sham versus collar unpaired Student's t-test). All the anti-5-HT receptor antibodies tested resulted in different patterns with multiple bands.

In conclusion, these data demonstrate that collar placement increases the amount of 5-HT_{1B} mRNA in the rabbit carotid artery. Though 5-HT receptor proteins could not be identified due to the poor selectivity of the antibodies, this indicates that up-regulation of 5-HT_{1B} expression is involved in the hypersensitivity to 5-HT in the collared segment.

Chomczynski, P. & Sacchi, N. (1987) *Anal. Biochem.*, **162**, 156-159
Geerts, I.S. et al. (1999) *Br. J. Pharmacol.*, **127**, 1327-1336

189P MOLECULAR CLONING AND PHARMACOLOGICAL CHARACTERISATION OF PORCINE 5-HT$_{1D}$ RECEPTOR

P. Bhalla, H.S. Sharma, T. Wurch*, P.J. Pauwels* & P.R. Saxena, Department of Pharmacology, Erasmus University Medical Centre, Rotterdam, The Netherlands and *Centre de Recherche Pierre Fabre, Castres cedex, France.

Sumatriptan as well as other triptans constrict porcine carotid arteriovenous anastomoses via the 5-HT$_{1B}$ receptor (De Vreis et al., 1999). In addition, the triptans may also inhibit neuropeptide release via both 5-HT$_{1B}$ and 5-HT$_{1D}$ receptors located on trigeminal ganglion (Bonaventure et al. 1998). In this investigation, we sought to clone and sequence the porcine specific cDNA encoding 5-HT$_{1D}$ receptor.

Cerebral cortex tissue, obtained from Yorkshire x Landrace pig, was snap frozen in liquid nitrogen and stored at -80°C. Total tissue RNA was isolated and the quality of RNA was ascertained by OD_{260}/OD_{280} ratio of >1.8. Poly(A$^+$)mRNA was purified from the total RNA and was used for the synthesis of cDNA and amplification of porcine 5-HT$_{1D}$ receptor by RT-PCR. Using the 5'- and 3'-end oligonucleotide primers designed from the guinea pig 5-HT$_{1D}$ receptor cDNA sequence, an expected size of 1200bp PCR product was amplified and cloned into a pGEMT easy vector. The 5'- and 3'-ends of porcine 5-HT$_{1D}$ receptor cDNA were verified by inverse PCR. Porcine cDNA sequence analysis revealed an open reading frame of 377 amino acid protein showing a 88% to 92% homology with the 5-HT$_{1D}$ receptor in other species. Using non-radioactive *in situ* hybridisation technique, we found the mRNA expression of 5-HT$_{1D}$ receptors in trigeminal ganglion.

For pharmacological studies, Cos-7 cells were transiently transfected with recombinant 5-HT$_{1D}$ receptor plasmid DNA (Wurch et. al., 1997). Membrane preparations from these cells showed high affinity for both [^{3}H]5-carboxamidotryptamine (5-CT) and [^{3}H]GR125743. The equilibrium dissociation constant (K_d) values of [^{3}H]5-CT and [^{3}H]GR125743 binding were 1.08 and 1.47, respectively; the B_{max} values were 1.74±0.40 and 2.70±0.53 pmol/mg protein (mean±s.e.m., n=3-4). The rank order of the affinity constants (pK_i) of 5-HT receptor ligands, shown in Table 1, is commensurate with the pharmacology of the human 5-HT$_{1D}$ receptor.

Table 1 Affinities of some compounds for the inhibition of [^{3}H]GR125743 (1 nM) binding to membranes prepared from cells expressing porcine 5-HT$_{1D}$ receptor.

Ligand	pK_i	Ligand	pK_i
L694247	9.50±0.03	Sumatriptan	8.06±0.04
Methiothepin	8.81±0.14	GR127935	7.98±0.17
Zolmitriptan	8.67±0.08	CP122638	7.97±0.08
5-HT	8.28±0.05	Ketanserin	7.39±0.05

5-HT, 5-hydroxytryptamine; For chemical structures of compounds, see Hoyer *et al.*, 1994.

In conclusion, we have cloned and functionally characterised the porcine 5-HT$_{1D}$ receptor, which could be a useful tool for studying potential therapeutic agents.

Bonaventure P. *et al.* (1998). Neuroreport, **9**, 641-645.
De Vreis, P. *et al.* (1999) Br. J. Pharmacol., **127**, 405-412.
Hoyer, D. *et al.* (1994). Pharmacol. Rev. **46**, 157-203.
Wurch, T. et al. (1997). J. Neurochem., **68**, 410-418.

190P DIFFERENTIAL EFFECTS OF THE 5-HT$_{1B}$ RECEPTOR ANTAGONIST SB224289 ON SUMATRIPTAN-INDUCED CONTRACTIONS IN HUMAN BLOOD VESSELS RELEVANT TO ANTIMIGRAINE THERAPY

R.W.M. van den Broek, A. MaassenVanDenBrink, R. de Vries and P.R. Saxena, Dept. of Pharmacology, Erasmus University, P.O. Box 1738, 3000 DR Rotterdam, The Netherlands.

The 5-HT$_{1B/1D}$ receptor agonist sumatriptan effectively aborts migraine headache, probably by constriction of dilated cranial arteries. Because sumatriptan also constricts coronary arteries, it may induce myocardial ischaemia in some patients. Therefore, we investigated the receptors involved in sumatriptan-induced contraction in human blood vessels indicative of therapeutic efficacy (middle meningeal artery) and coronary side effects (coronary artery and saphenous vein) using the 5-HT$_{1B}$ receptor antagonist SB224289 and 5-HT$_{1D}$ receptor antagonist BRL15572. Ring segments of human middle meningeal artery (6 patients; 2M, 4F; 30-62 years), right epicardial coronary artery (6 heart valve donors; 1M, 5F; 37-64 years) and saphenous vein (6 patients; 6M; 45-78 years) were suspended in organ baths (37°C), containing Krebs solution enriched with a cocktail of atropine, prazosin, mesulergine, imipramine, mepyramine (all 1 μM), corticosterone (10 μM) and pargyline (100 μM). Contraction was recorded isometrically and was expressed as % of contraction to 1 μM prostaglandin $F_{2\alpha}$ (middle meningeal artery) or 100 mM K^+ (coronary artery and saphenous vein). Segments were incubated with either SB224289, BRL15572, both antagonists (all 1 μM) or vehicle for at least 30 minutes prior to construction of a cumulative concentration response curve to sumatriptan. Sumatriptan-induced contraction in middle meningeal artery and saphenous vein (pEC_{50}: 6.7±0.3 and 6.1±0.1, respectively) was potently blocked by SB224289 in a non-competitive manner (Figure 1), indicating that sumatriptan contracts human middle meningeal artery and saphenous vein predominantly via the 5-HT$_{1B}$ receptor. In coronary artery, incubation with SB224289 revealed a small parallel rightward shift (pEC_{50}: 5.0±0.1 against 5.7±0.1 for control, Figure 1) yielding a pK_B value of 6.4±0.2, which is 70-fold lower than the corresponding binding affinity (pK_i: 8.1) for the 5-HT$_{1B}$ receptor (Roberts *et al.* 1997). This suggests that 5-HT$_{1B}$ receptors that are susceptible to SB224289 play a minor role in contraction to sumatriptan in coronary artery. BRL15572 did not block contraction to sumatriptan in any of the preparations (data not shown), excluding a role for the 5-HT$_{1D}$ receptor. Incubation with both antagonists together did not reveal an additional antagonism to sumatriptan compared to that observed with SB224289 alone (data not shown). We conclude that the 5-HT$_{1B/1D}$ receptor agonist sumatriptan contracts human isolated middle meningeal artery and saphenous vein predominantly by 5-HT$_{1B}$ receptors. In contrast, coronary artery contraction to sumatriptan was only partly antagonised by the 5-HT$_{1B}$ receptor antagonist SB224289, suggesting a role for another, yet uncharacterised, mechanism.

Roberts, C., Price, G.W., Gaster, L., *et al.* (1997) *Neuropharmacology* 36, 549-557.

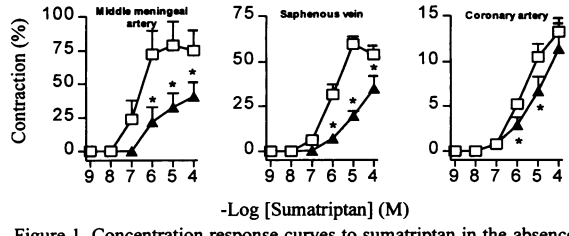

Figure 1. Concentration response curves to sumatriptan in the absence (-□-) or presence (-▲-) of 1 μM SB224289. For details see text, data presented as mean±s.e.mean. * Significantly different from respective control (paired t-test, P<0.05).

191P BRADYKININ-INDUCED CARDIOPROTECTION IS ATTENUATED IN THE RAT HYPERTROPHIED HEART

Z. Ebrahim, D.M. Yellon & G.F. Baxter. The Hatter Institute for Cardiovascular Studies, Division of Cardiology, University College London Hospital & Medical School, London WC1E 6DB

The vasodilator peptide, bradykinin (BK) is known to induce cardioprotection, analogous to Ischaemic Preconditioning (IPC). The administration of BK prior to ischaemia (Bugge & Ytrehus, 1995) has been reported to reduce infarct size in the isolated rat heart model. Additionally, IPC is recognised to exert a cardioprotective effect both in the "normal" and hypertrophied myocardium (Ferdinandy et *al.*, 1998). The aim of this study was to confirm the occurrence of IPC in our model of hypertrophy and to ascertain if exogenous bradykinin acts as a cardioprotectant in the hypertrophied rat heart.

Hypertension was induced in male Sprague-Dawley rats (300-330g) using the deoxycorticosterone acetate (DOCA)-salt regimen, which involved twice a week DOCA injections ($10mg.kg^{-1}$) and the substitution of drinking water with NaCl (0.9%), KCl (0.2%) solution for a period of 4 weeks. Hypertrophy was confirmed by an increase in the heart weight to body weight ratios ($mg.g^{-1}$), normotensive 2.94±0.12 versus hypertrophied 4.04±0.11, P<0.01.

Following the 4 week treatment protocol, animals were anaesthetised with pentobarbitone sodium ($50mg.kg^{-1}$, i.p) and killed. The hearts were excised and Langendorff perfused with Kreb's-Henseleit buffer (composition in $mmol.l^{-1}$ NaCl 118, $NaHCO_3$ 25, glucose 11, KCl 4.7, $MgSO_4$ 1.2 KH_2PO_4 1.2, $CaCl_2$ 1.8). All hearts were stabilised for 20 minutes and subjected to 35 minutes of regional ischaemia, followed by 2 hours of reperfusion. A preconditioning protocol consisting of 2 cycles of 5 minutes of global ischaemia interspersed by 10 minutes of reperfusion was employed. Bradykinin (0.1μM) was administered for 10 minutes prior to the ischaemic insult. Infarct sizes were measured using triphenyltetrazolium chloride staining, the risk zone being delineated with Evan's blue dye. The results obtained are highlighted in Table 1.

GROUP (n)	*RISK ZONE (cm^3)*	*INFARCT SIZE (%)*
Normotensive,control (7)	0.69±0.058	47.9±2.6
Normotensive,preconditioned (6)	0.65±0.052	17.1±4.0**
Normotensive,BK (0.1μM) (7)	0.64±0.082	20.8±2.7**
Hypertrophied,control (7)	0.91±0.083	47.0±3.2
Hypertrophied,preconditioned (7)	0.85±0.067	18.5±2.6**
Hypertrophied,BK (0.1μM) (6)	0.79±0.069	33.3±4.1*†

Infarct size is expressed as a proportion of the risk zone (%). Results are stated as Mean±s.e.of mean (one way ANOVA) ** = P<0.01. * = P<0.05. † = P<0.05 v corresponding normotensive group.

Although the absolute risk zone volumes of the hypertrophied hearts were larger than in the normotensive, the risk zone normalised to left ventricle volume was the same in all groups.

Both IPC and the administration of BK prior to the lethal ischaemic insult resulted in a reduction of infarct size in the normal and hypertrophied myocardium. Although BK did evoke a cardioprotective effect in the hypertrophied myocardium, the protection was less prominent. We speculate that even at this mild stage of hypertrophy signal transduction mechanisms involved in eliciting the cardioprotective effect of BK may be downregulated.

Z.E holds a British Heart Foundation Studentship (FS/98075), G.F.B is a British Heart Foundation fellow (FS97/001).

Bugge E, & Ytrehus K (1996). J.Mol.Cell.Cardiol. 28 (12), 2333-41.
Ferdinandy P, Szilvassy Z, & Baxter G.F (1998). Trends Pharmacol Sci. 19, 223-229.

192P EFFECTS OF BIIB513 ON ISCHAEMIA-INDUCED ARRHYTHMIAS AND MYOCARDIAL INFARCTION IN ANAESTHETISED RATS

Dongmei Wu, Jean Marie Stassen, Juergen Daemmgen, Henri Doods, Cardiovascular/Metabolic Research, Boehringer Ingelheim Pharma KG, 88397 Biberach, Germany

The Na^+/H^+ exchange (NHE) plays a critical role in myocardial ischaemia-reperfusion injury (Karmazyn & Moffat, 1993; Scholz & Albus, 1993). In the present study, we investigated the effects of (Benzamide,N-(aminoiminomethyl)-4-[4-(2-furanylcarbonyl)-1-piperazinyl]-3-(methylsulfonyl),methanesulfonate) BIIB513, a selective NHE-1 inhibitor on myocardial ischaemia-induced arrhythmias and myocardial infarction in anaesthetised rats.

Male Wistar rats (Chbb: Thom 350-380g) were anaesthetised with sodium pentobarbital (60mg/kg, i.p.). The trachea was cannulated and the animals were artificially respired (80 strokes/min) with room air supplemented with oxygen. The right carotid artery and left jugular vein were cannulated for the continuous measurement of arterial blood pressure and intravenous administration of test agents, respectively. Heart rate was derived from the blood pressure signal. A left side thoracotomy was performed at the level of the fifth intercostal space. The left main coronary artery was occluded for a period of 30 min followed by 2 h of reperfusion. A lead II electrocardiogram (ECG) was recorded on a computer by *Chart V3.5* program. Arrhythmias were evaluated according to the guidelines of the Lambeth conventions (Walker *et al.*, 1988). At the end of the reperfusion period, the animals were killed with pentobarbital (60mg/kg i.v.). The entire ventricle was cut, from the apex to base, into four transverse slices and incubated in 2,3,5-triphenyltetrazolium chloride (10 mg/ml in phosphate buffer) for 10 min at 37°C to visualise the infarct area. Each section was scanned with a colour image scanner and infarct size was determined. Plasma creatine phosphokinase (CPK) levels were determined by means of a CPK kit. All values are the mean ± SEM, n=5-6, p<0.05 are considered to be significant by ANOVA-test.

After the occlusion of the coronary artery, all control rats exhibited ventricular premature beats (VPB), 14 of 15 controls showed ventricular tachycardia (VT) and 12 of 15 control rats showed ventricular fibrillation (VF). Administration of BIIB513 (1.0 mg/kg) 10 min before ischaemia, reduced VPB, VT from 207 to 11 beats and 152 to 5.8 seconds, respectively, and completely prevented VF. Pre-ischaemic treatment of BIIB513 dose-dependently reduced the infarct size (Figure A). The ID50 value was 0.16 mg/kg. Administration of BIIB513 (1.0 mg/kg), 10 min before reperfusion, also reduced infarct size by 47 ± 13%. The reduction in infarct size was accompanied by a decrease in circulating CPK levels (Fig B).

The present study demonstrates the cardioprotective ability of NHE-1 inhibition during myocardial ischaemia and reperfusion by reducing serious ventricular arrhythmias and myocardial infarct size in anaesthetised rats. It may have therapeutic potential in the clinical treatment of myocardial ischaemia and the prevention of reperfusion injury.

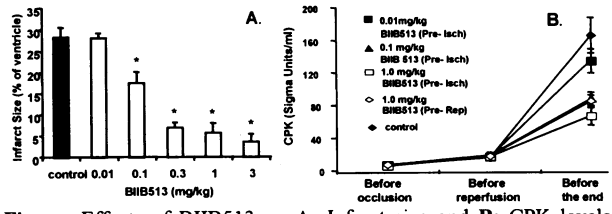

Figure: Effects of BIIB513 on **A:** Infarct size and **B:** CPK levels after left coronary artery occlusion and reperfusion. *: p<0.05.

Karmazyn, M. & Moffat, M.P. (1993) *Cardiovasc Res* 27, 915-924.
Scholz, W. & Albus, U. (1993) *Basic Res Cardiol* 88, 443-455.
Walker, M.J.A. *et al.* (1988) *Cardiovasc Res* 22, 447-455.

193P DOES SUPEROXIDE ATTENUATE CARBACHOL-MEDIATED RELAXATIONS IN HUMAN RADIAL ARTERIES?

CA Hamilton, G Berg, J Butler, V Pathi, JL Reid, AF Dominiczak. Department of Medicine and Therapeutics and Cardiothoracic Surgery, Western Infirmary, Glasgow, G1 6NT.

In human radial arteries a high proportion of relaxation to agonists such as bradykinin and acetylcholine is nitric oxide/prostanoid independent and shows pharmacological characteristics of an endothelium derived hyperpolarising factor (EDHF) (Hamilton et al, 1999). It has recently been proposed that EDHF mediated relaxations in bovine coronary arteries are resistant to increases in oxidative stress and local concentrations of superoxide (O_2^-) (Kaw and Hecker 1999)

We have investigated whether O_2^- attenuated nitric oxide dependent and/or nitric oxide independent relaxations in human radial arteries. Human radial and mammary artery segments were obtrained from patients undergoing coronary artery bypass graft surgery (CABG). Vessels were cleaned of connective tissue and cut into 4-5 mm rings for measurement of O_2^- levels by lucigenin chemiluminescence (Kerr et al, 1999) or into 2-3 mm rings for organ bath studies (Hamilton et al, 1997). Rings were contracted to their EC_{50} to phenylephrine and relaxation to carbachol 10^{-8} – 10^{-5} M studied before and after addition of superoxide dismutase SOD (45U/ml) or vehicle. Experiments were carried out either in the absence or presence of L-NAME, 200μM, to inhibit nitric oxide synthase. Results are expressed as mean ± SE of mean.

Levels of O_2^- in radial artery were 0.96±0.30 nmoles/min/mg wet weight compared to 0.91±0.09nmoles/min/mg wet weight in mammary artery samples assayed in parallel (n=6). In radial arteries in the absence of L-NAME SOD enhanced relaxations to carbachol, Emax being 70±8% and 86±7% in the absence and presence of SOD (n=8, p=0.017). Vehicle had no significant effect on Emax, values being 72±9% and 75±7% in the absence and presence of vehicle (n=8). In the presence of L-NAME neither SOD nor vehicle modified Emax values significantly, Emax being 64±7% and 63±8% in the absence and presence of SOD (n=10) and 50±5% and 43±5% in the absence and presence of vehicle (n=7). Neither vehicle nor SOD had a significant effect on EC_{50} values either in the absence or presence of L-NAME.

Levels of O_2^- were similar in radial and mammary arteries. The enhancement of relaxation by SOD in radial arteries not treated with L-NAME was similar to that previously reported in mammary arteries (Hamilton et al, 1997). The absence of an effect of SOD on relaxation in the presence of L-NAME suggests that the nitric oxide dependent component of relaxation in the radial arteries is more sensitive to O_2^- than the nitric oxide independent component. Radial arteries are used increasingly for revascularisation in CABG surgery. The resistance of EDHF relaxations to oxidative stress may contribute to long term patency of radial arteries when used in CABG surgery.

Hamilton CA, Berg G, McIntyre M et al, (1997) Atherosclerosis 113; 77-86.
Hamilton CA, Williams R, Pathi V et al, (1999) Cardiovascular Research 42; 214-223.
Kaws and Hecker M (1999) Naunyn-Schmiederbergs Arch. Pharmacol 359; 133-139.
Kerr S, Brosnan MJ, McIntyre M et al (1999) Hypertension 33; 1353-1358.

194P VITAMIN C IMPROVES ENDOTHELIAL FUNCTION IN A PRESSURE OVERLOAD MODEL OF LEFT VENTRICULAR HYPERTROPHY IN THE GUINEA-PIG

J.P. Bell, S.I. Mosfer, D. Lang & M.J. Lewis, Cardiovascular Science Research Group, Wales Heart Research Institute, University of Wales College of Medicine, Heath Park, Cardiff, CF14 4XN, UK.

Left ventricular hypertrophy (LVH) is associated with endothelial dysfunction, the latter possibly being due to an increase in oxidative stress (Bell *et al.*, 1998). The aim of this study was to investigate the effect of the antioxidant vitamin C (Vit C, 0.6 mg/ml in the drinking water) on vascular function in a guinea pig (males, Dunkin-Hartley, 200-250 g) supra renal aortic-banded (band internal diameter 0.5 mm) pressure overload model of LVH (Bell *et al.*, 1997). Treated guinea pigs received Vit C one week prior and for six weeks post-banding. All data is expressed as mean±s.e.m. and compared by either unpaired t test or one way ANOVA and a post-test where appropriate. Significant differences are identified where $P<0.05$. Heart/body weight (g x 10^2) ratios were significantly ($P<0.001$) increased in the banded untreated animals (0.46±0.02 cf. 0.31±0.01 for sham operated controls (SOC), both n≥13); Vit C significantly ($P<0.01$) reduced this increase (0.39±0.01, n=16). Plasma angiotensin II levels (pg/ml), as measured by radioimmunoassay (RIA) kit, were elevated ($P<0.01$) in banded untreated animals (14.5±0.47 cf. 10.0±0.48 for SOC, both n=8) and were significantly reduced ($P<0.01$) by Vit C (10.9±0.52, n=9). In freshly isolated coronary microvascular endothelial cells (CMVE) (Lang *et al.*, 1999), superoxide anion production (V.s/mg protein) as measured by lucigenin-chemiluminescence in the presence of excess (1 mM) NADH or NADPH (Bayraktutan *et al.*, 1998), was significantly ($P<0.05$) elevated in banded untreated animals (4098±281 & 1219±182 respectively, both n≥6 cf. 2314±154 & 653±50 respectively, both n≥6 for SOC). Vit C treatment significantly ($P<0.01$) reduced this increase (2872±282 & 742±143 respectively, both n≥6). Nitric oxide activity in the CMVE (measured indirectly using a cyclic GMP RIA kit, and expressed as fmol/μg protein) from SOC following exposure to bradykinin (BK) or calcium ionophore A23187 (A2) (both 1 μM for 90 s) increased ($P<0.01$) from 7.4±0.76 to 13.5±1.38 & 19.8±1.36 respectively (all n≥12). Both basal (5.6±0.30, n=10), BK (7.2±0.3, n=11) and A2 (7.7±0.42, n=13) stimulated increases in cyclic GMP were significantly ($P<0.01$) lower in banded untreated animals compared to SOC. Treatment with Vit C significantly ($P<0.01$) inhibited these decreases (8.3±0.64, n=12 for basal and 12.8±1.67 and 14.7±0.86 both n≥9 for BK and A2 respectively). These data suggest a role for endothelial dysfunction and oxygen free radical production in the development of pressure overload LVH. Furthermore, interventional therapy with antioxidants such as Vit C may act as a preventative measure in the control of this major life threatening condition.

Bayraktutan, U., *et al.* (1998) *Cardiovasc. Res.* 38, 256-262.
Bell, J.P., Lang, D., Lewis, M.J. (1998) *J. Mol. Cell. Cardiol.* 30, A13.
Bell, J.P., *et al.* (1997) *Br. J. Pharmacol.* 120, 99P.
Lang, D., *et al.* (1999) *Cardiovasc. Res.* 42, 794-804.

195P THE PROTECTIVE EFFECT OF THIOL-CONTAINING COMPOUNDS AGAINST OXYGEN STRESS-INDUCED DECREASE OF CONTRACTILE FORCE IN RAT ISOLATED LEFT ATRIA

C. Sand, M. Pfaffendorf & P.A. van Zwieten. Dept. Pharmacotherapy, Academic Medical Center, University of Amsterdam, Meibergdreef 15, 1105 AZ Amsterdam, The Netherlands.

Reactive oxygen species (ROS) are involved in the pathogenesis of various diseases. Radical scavengers with thiol moieties are potential therapeutics preventing ROS-induced damage. In order to quantify the protective properties of four compounds, glutathione (GSH), penicillamine (PEN), mesna (MES) and N-acetylcysteine (NAC), an in vitro model, recently established in our department (Peters et al, 1998), was employed. Isolated rat left atria, paced at 3 Hz, were subjected to ROS, induced by a constant current electrolysis (30 mA). This model offers the possibility of studying effects on the basal contractile force as well as on a specific, ROS-induced, inversion of the inotropic effect induced by α_1-adrenoceptor stimulation (Peters et al., 1998).

Furthermore, we attempted to correlate the potency of the compounds investigated with their physico-chemical properties, i.e. the octanol/water partition coefficient.

Male Wistar rats of 220-250g were sacrificed. The isolated left atria were mounted in a 5-ml organ bath and connected to an isometric force transducer. A buffer-solution of the following composition (in mM) NaCl 119; KCl 4.5; $MgCl_2$ 0.5; $CaCl_2$ 2.5; glucose 11; Tris 30 (37°C, pH 7.4), gassed with 100% O_2, was used. After an equilibration period of 15 minutes one concentration (0.1-3mM, n=5-6) of a particular scavengers or vehicle was applied. The ROS were generated for 75 s. by electrolysis via platinum electrodes at the bottom of the organ bath 15 minutes later. The α_1-selective adrenoceptor agonist methoxamine (300 µM) was added after another half an hour.

The initial force of contraction amounted to 7.60 ± 0.19 mN (n=113) and remained stable within the first 60 minutes (n=6). None of the scavengers influenced this parameter. Electrolysis, when applied 30 min. after the start of the experiment, decreased the contractile force by 67.4 ± 2.9% within the next 30 minutes. At this time point methoxamine (300 µM) induced a positive inotropic effect of 29.5 ± 4.6% in control preparations, whereas a negative inotropic effect of 24.8±3.5% was provoked in atria exposed to electrolysis. All thiols prevented the electrolysis-induced decease of contractile force in a concentration-dependent manner with a log EC_{50}(in M) of -3.67 ± 0.08, -3.48 ± 0.07, -3.29 ± 0.08 and -3.2 ± 0.06 for GSH, MES, PEN and NAC, respectively. All scavengers investigated were able to preserve the contractile force after electrolysis for 100 % of the control. The electrolysis-induced inversion of the methoxamine effect was prevented completely by all compounds, except for PEN (13.1 ± 1.9% vs. control 29.5 ± 4.5%), with a log EC_{50} of -3.61 ± 0.08, - 3.4 ± 0.08, - 3.18 ± 0.05 and -3.03 ± 0.2 for GSH, MES, PEN and NAC, respectively.

Both the log EC_{50}-values for the protective effect of the basal as well as the methoxamine-stimulated contractile force, *positively* correlate (r^2=0.846) with literature data concerning the logarithms of the partition coefficients of the compounds (-5.41, -2.18, -2.18 and –0.66 for GSH, MES, PEN and NAC, respectively). From the presented data we conclude that the protective properties of thiol-containing scavengers against ROS-induced damage are likely to depend on their physico-chemical properties, i.e. increase with hydrophilicity.

Peters et al. (1998) *Br.J.Pharmacol.*, **123**: 952-958

Estimation program LogKow, Syracuse Research Cooperation

196P 5-S-CYSTEINYL-CONJUGATES OF CATECHOLAMINES INDUCE OXIDATIVE STRESS AND DELAYED CELL DEATH IN MESENCEPHALIC DOPAMINERGIC CELLS

J.P.E. Spencer, M. Whiteman, P. Jenner, & B. Halliwell. Wolfson Centre for Age-Related Diseases, GKT School of Biomedical Sciences, Guy's Campus, London SE1 9RT.

5-S-Cysteinyl conjugates of catecholamines have been detected in the mammalian brain tissue and are observed to be elevated in post-mortem brain tissue from patients with Parkinson's disease (PD) (Spencer, *et al.*, 1998). 5-S-Cysteinyl species may undergo oxidation to form benzothiazine species, such as dihydrobenzothiazine which cross the outer mitochondrial membrane and irreversibly inhibit complex I (Li and Dryhurst, 1997). In addition, formation of these species may raise basal oxidative stress which might contribute to the death of nigral cells in PD. In the present study we have examined the effect of 5-S-cysteinyl-catecholamine adducts upon neuronal cells, measuring DNA base modification as a marker of oxidative stress.

The reversibly immortalised mesencephalic dopaminergic cell line, CSM 14.1, was used for exposures. Cells were exposed for 6 hours to 10µM of 5-S-cysteinyl-conjugates of dopamine, L-DOPA and DOPAC, and to 5-S-cysteinyl-conjugates of the methylene-dihydroxy-methamphetamine (MDMA) metabolites dihydroxy-methamphetamine (DHMA) and dihydroxy-amphetamine (DHA). Conjugates were synthesised, purified and assessed for purity as described previously (Spencer, *et al.*, 1998). After exposure, MTT assays were performed to assess cell viability. DNA isolation from cells, removal of RNA contamination and analysis of DNA base modification by GC-MS, were carried out as previously described (Spencer *et al.*, 1996). Assessment of intracellular peroxide levels was performed using 2,7-dichlorofluorescin diacetate. Statistical analysis was by one-way ANOVA with post-hoc Tukey-Kramer test.

Exposure of the dopaminergic cell line, CSM 14.1, to 5-S-cysteinyl conjugates of dopamine, L-DOPA, DOPAC, DHMA or DHA (10µM) caused extensive oxidative DNA base modification (Figure 1). Large increases in pyrimidine base oxidation products, such as thymine glycol, and purine base oxidation products such as 8-OH-guanine were observed after 6 hours of exposure. By contrast, no increases in deaminated purine products or the chlorinated products were observed. The exposures resulted in a delayed (48 hr after exposure) loss in cell viability (66.8±3.6%) even though there was no initial loss (2.6±0.8%).

Figure 1

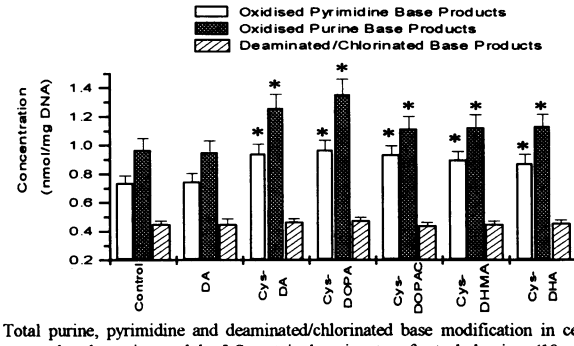

Total purine, pyrimidine and deaminated/chlorinated base modification in cells exposed to dopamine, and the 5-S-cysteinyl conjugates of catecholamines (10 µM) for 6 hours at 37°C. Values are mean ± S.D.; n=6). * indicates significant increase over control (untreated cells) ($p < 0.001$).

We propose that 5-S-cysteinyl-conjugates of catecholamines are capable of diffusing into cells and stimulating the formation of ROS. These ROS may attack DNA resulting in a pattern of base damage which suggests that hydroxyl radicals (•OH) are the major contributors to the base modification. In addition, the time course of damage suggests that ROS levels remain high in cells for up to 48 hours. The delayed cell death may proceed via an apoptotic pathway triggered by the initial oxidative damage of DNA.

Li, H. and Dryhurst, G. (1998). *J. Neurochem.* **69**, 1530-1541

Spencer, J.P.E., Wong, J. et al. (1996). *Chem. Res. Toxicol.*, **9**, 1152-1158

Spencer, J.P.E., Jenner, P., Daniel, S.E et al. (1998). *J.Neurochem.* **71**, 2112-2122

197P ASSESSMENT OF NITRATE TOLERANCE AND TOTAL ANTIOXIDANT STATUS IN THE RAT *IN VIVO*

D.W. Laight, K.M. Desai, E.E. Änggård & M.J. Carrier
The William Harvey Research Institute, Charterhouse Square, London, EC1M 6BQ

Tolerance to the haemodynamic and anti-ischaemic activities of organic nitrates, continues to restrict the clinical efficacy of these important therapeutic nitric oxide (NO) donors. We have now evaluated vascular tolerance *in vivo* following subacute exposure to isosorbide dinitrate (ISDN) in the rat. Organic nitrate-dependent vasodepression was assessed using glyceryl trinitrate (GTN); while endothelium-dependent vascular function was investigated by examining both vasodepression to acetylcholine (ACh) and the vasopressor response to the NO synthase inhibitor L-NAME. Since the development of clinically relevant nitrate tolerance has been associated with the generation of oxidant stress and in particular superoxide anion (Münzel *et al.*, 1995; Watanabe *et al.*, 1998), we additionally examined plasma total antioxidant status (TAOS) (Laight *et al.*, 1999) in our model. Reductions in rat plasma TAOS have previously been demonstrated in response to a series of pro-oxidant compounds, including superoxide anion generators, administered *in vivo* (Laight *et al.*, 1999).

Male Wistar rats (290-320 g) were treated with ISDN (30 mg kg^{-1} s.c., t.i.d.) (see Trongvanichnam *et al.*, 1996) or propylene glycol vehicle containing lactose as stabiliser (45 mg ml^{-1} kg^{-1} s.c., t.i.d.) for 3 days. Animals were then anaesthetised with thiopentone sodium (120 mg kg^{-1} i.p.). Vasodepressor responses to bolus dose ACh (0.02-2 μg kg^{-1} i.v.) and GTN (0.1-50 μg kg^{-1} i.v.) were then established, followed by the vasopressor effect of L-NAME (100 mg kg^{-1} i.v.). TAOS was determined photometrically at pH 7.4 and 37 °C, in 2 μl venous EDTA-plasma samples and expressed as an ascorbate equivalent antioxidant concentration (Laight *et al.*, 1999). Data are mean±s.e. mean and were compared using Student's unpaired t test or Welch test (n=6-7). AUC=area under dose-response curve.

Basal mean arterial pressure (MAP) was 143.0±6.0 mm Hg and 133.3±4.3 mm Hg in control and ISDN-treated animals, respectively (P>0.05). Vasodepressor responses to GTN (AUC=1960.6±15.6 units), but not ACh (AUC=448.2±10.0 units), were impaired following ISDN (AUC_{GTN}=1566.8±53.6 units, P<0.01; AUC_{ACh}=420.0±12.9 units, P>0.05) (Figure 1) while L-NAME elicited a similar rise in MAP in control (31.7±3.4 %) and ISDN-treated (32.3±2.7 %) rats (P>0.05). Plasma TAOS in control and ISDN-treated rats, was 11.7±0.3 μM and 11.0±0.6 μM, respectively (P>0.05).

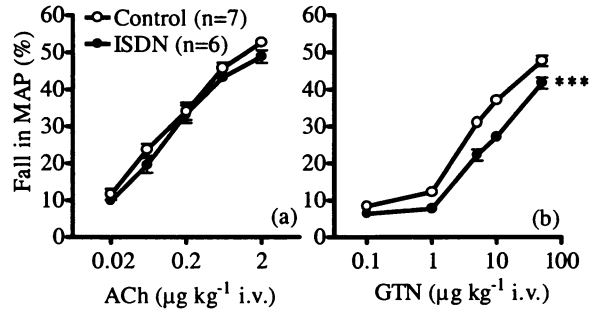

Figure 1. Vasodepression to ACh (a) and GTN (b) in anaesthetised rats with or without treatment with ISDN ***P<0.01, 2 way analysis of variance

In conclusion, subacute ISDN treatment in the rat yields a model of nitrate tolerance, as determined by the approximate 20% reduction in AUC_{GTN} *in vivo*, which may be of more clinical relevance than tolerance protocols involving acute, *in vitro* nitrate exposure (see Laight *et al.*, 1997). While the relative preservation of endothelium-dependent haemodynamic responses in ISDN-treated animals together with only a tendency to a fall in plasma TAOS, do not suggest a major role for a nitrate-mediated, pro-oxidative insult, further biomarkers of oxidant stress will be required in order to verify this observation in our tolerant model.

This work was supported by Lipha s.a., Lyon, France.

Laight, D., Carrier, M. & Änggård, E. (1997) *Br. J. Pharmacol.* **120**, 1477-1482
Laight, D., Gunnarsson, P., Kaw, A. *et al.* (1999) *Environ. Toxicol. Pharmacol.* **7**, 27-31
Münzel, T., Sayegh, H. *et al.* (1995) *J. Clin. Invest.* **95**, 187-194
Trongvanichnam, K., Mitsui-Saito, M., Ozaki, H. *et al.* (1996) *Jpn. J. Pharmacol.* **71**, 167-173
Watanabe, H., Kakihana, M., Ohtsuka, S. *et al.* (1998) *Circ.* **97**, 886-891

198P ACETYLCHOLINE-INDUCED RELAXATION IN THE CAROTID AND THE FEMORAL ARTERY OF THE MOUSE

H.M.L. Crauwels, C.E. Van Hove, A.G. Herman and H. Bult
Division of Pharmacology, University of Antwerp (UIA), B-2610 Wilrijk, Belgium

Endothelium-dependent relaxation is mediated by prostanoids, nitric oxide (NO) and endothelium-derived hyperpolarizing factor (EDHF), the identity of which is still controversial (Edwards G. *et al.*, 1998; Fisslthaler B. *et al.*, 1999). The aim of our study was to investigate the relative role of these factors in acetylcholine-induced relaxation in the carotid and the femoral artery of the mouse.

Female C57BL6 mice, aged 19-23 weeks (22.0 ± 0.1g) were anaesthetised with sodium pentobarbital (50mg kg^{-1} i.p.). Both carotid and femoral arteries were carefully removed and mounted as 2mm segments in a wire (40μm) myograph (Mulvany & Halpern, 1977) for isometric tension recording. Blood vessels were immersed in a Krebs-Ringer solution (37°C) and continuously aerated with a 95%O_2 - 5%CO_2 gas mixture (pH 7.4). Indomethacin 10μM was added to the solution unless the influence of prostanoids was investigated. Cumulative concentration response curves (3nM-30μM) were made for phenylephrine (PE) and the negative logarithm of the molar concentration (pD_2) resulting in 50% of the maximal response (E_{max}) was assessed for each vessel segment. Relaxation responses were studied by performing cumulative concentration response curves (3nM-10μM) for acetylcholine (ACh) in vessels contracted with KCl (30mM) or PE (pD_2) in the absence or presence of indomethacin 10μM, N^{ω}-nitro-L-arginine (L-NA) 300μM or the guanylate cyclase inhibitor 1H-[1,2,4]Oxadiazolo[4,3-a]quinoxalin-1-one (ODQ) 10μM. Data are presented as mean ± s.e.mean; n = number of mice.

PE evoked a maximal contraction (E_{max}) of 1.15 ± 0.15 mN mm^{-1} in the carotid (n=5), and 7.59 ± 0.29 mN mm^{-1} in the femoral artery (n=6). L-NA, in the presence of endothelial cells, significantly enhanced the E_{max} (4.35 ± 0.18 mN mm^{-1}) in the carotid (one way ANOVA, p<0.01) but not in the femoral artery. This, and the 4-fold increase in precontraction level of the carotid artery by ODQ, suggests that endogenous NO-production is much higher in the carotid artery as opposed to the femoral artery.

ACh caused complete relaxation of both the carotid (pD_2 7.58 ± 0.05, n=4) and femoral artery (pD_2 7.15 ± 0.08, n=4), contracted with PE. Indomethacin did not influence the relaxation to ACh, indicating that vasodilator prostanoids were not involved. In the carotid but not the femoral artery, elevated concentrations (≥3x10^{-7}M) of ACh caused concentration-dependent transient constrictions that were abolished by indomethacin.

Both L-NA and ODQ abolished all responses to ACh in the carotid artery, while in the femoral artery 34 ± 5% and 65 ± 4% of the relaxation persisted in the presence of L-NA and ODQ respectively (n=5). Furthermore, incubation with either inhibitor changed the shape of the relaxation response in the femoral artery from a long-lasting relaxation to a biphasic response with a fast large transient component followed by a small sustained relaxation at high ACh concentrations. Contraction with KCl (30mM), significantly reduced (paired samples t-test, p<0.05, n=5) the maximal relaxation to ACh in the carotid and the femoral artery (71 ± 4% and 83 ± 5% respectively) as compared to the relaxation of vessels precontracted with PE (105 ± 2% and 100 ± 1%). In high potassium, the ACh-induced relaxation was completely abolished by L-NA or ODQ in both arteries.

From the present observations is concluded that vasorelaxing prostanoids did not contribute to the relaxation in the carotid and the femoral artery of the mouse. In the carotid artery, the ACh-induced relaxation is mediated mainly by NO acting via cGMP-dependent pathways. In the femoral artery, part of the relaxation to ACh was L-NA- and ODQ-resistant, pointing to the existence of an EDHF different from NO, which is responsible for the initial transient part of the biphasic relaxation response.

Edwards G. *et al.* (1998) *Nature.* **396**, 269-272
Fisslthaler B. *et al.* (1999) *Nature.* **401**, 493-497
Mulvany M.J. & Halpern W. (1977) *Circ Res.* **41**, 19-26

199P OESTROGEN-INDUCED RELAXATION IN PRIMATE AORTA

P. Eseh-Sumbele, A.T. Evans and J.R. McCurrie, (Introduced by K.M. Marshall) Postgraduate Studies in Pharmacology, School of Pharmacy, University of Bradford, Bradford, BD7 1DP.

Cardiovascular protection by oestrogens in pre-menopausal women and post-menopausal women taking Hormone Replacement Therapy has been widely reported (Stampfer *et al.*, 1991). This may be related to dilator actions of oestrogens but the mechanism is unclear. Rahimian *et al.* (1997) suggested that 17β oestradiol (BEST) relaxes rat aorta via the endothelium and increased nitric oxide (NO) production, however, endothelial-dependence was not observed in rat aorta by Babaei *et al.* (1995) or in human coronary arteries by Mugge *et al.* (1993). In the present experiments we investigated the role of the endothelium and NO in oestrogen-induced relaxation in the aorta of the marmoset (*Callithrix jacchus*).

Rings of aorta 3-5mm in length were prepared from marmosets of either sex (310-380g), endothelium was removed from some rings by rubbing with forceps. Rings were set up in Krebs' solution containing indomethacin (1μM) (37°C, 95% O_2/5% CO_2) under 2g tension, equilibrated for 60 mins and reproducibility of responses was checked by repeated application of 60mM KCl. Concentration-response curves to KCl (5-100mM) were constructed in intact and de-endothelialised rings from the same animal and repeated following 5 mins incubation with BEST (20μM). No vehicle effects were observed: n = number of animals.

No significant difference in KCl E_{max} was observed between male (1.82 ± 0.22g) and female (2.6 ± 0.34g) aorta (n=8). KCl E_{max} was unchanged by endothelium removal in either sex. E_{max} in de-endothelialised male rings was 2.0 ± 0.15g and females 2.54 ± 0.26g (n=8). BEST caused a rightward shift in the KCl concentration-response curve with reduction in E_{max}. No difference in BEST-induced relaxation in intact rings of males (27.5 ± 8%) or females (22.7 ± 11.6%) was observed; relaxation was unchanged by removing the endothelium. Thus in subsequent experiments data from both sexes was pooled.

The effect of modifying NO production and cGMP concentration on oestrogen-induced relaxation was examined. Concentration-response curves to KCl were constructed in the absence or presence of BEST (20μM) as described above. Rings were then incubated for 20 mins with L-NAME (100μM) an inhibitor of nitric oxide synthase or ODQ (oxadiazolo-quinoxalin-1-one, 1μM) an inhibitor of nitric oxide-sensitive guanylyl cyclase or 8-bromo-cGMP (BcG, 10μM) a lipophilic cGMP analogue (n=6). The effect of BEST (20μM) on the KCl concentration response curve was re-tested. L-NAME (100μM) inhibited the relaxation induced by BEST (20μM) in both intact and de-endothelialised rings: this effect was reversed by incubation for 20 mins with L-arginine (1mM) (n=3). ODQ (1μM) completely inhibited relaxation induced by BEST (20μM) whereas BcG (10μM) increased maximal oestrogen-induced relaxation from 25 ± 5.7% to 34.2 ± 4.2% ($P<0.05$) in intact rings and from 23.1 ± 8.4% to 55.9 ± 9% ($P<0.001$, Student's unpaired t-test) in de-endothelialised rings.

The results show that oestradiol relaxes male and female aortae equally both in the presence and absence of the endothelium: the mechanism involves NO production and increases in cGMP. Since similar results were obtained in both intact and de-endothelialised rings we conclude that vascular muscle-derived nitric oxide is involved in oestrogen-induced relaxation in marmoset aorta.

Babaei, H. *et al.* (1995)*Br. J. Pharmacol.* 115, 152P
Mugge, A. *et al.* (1993) *Cardiovasc. Res.* 27, 1939-42
Rahimian, R. *et al.*(1997) *J. Pharmac. Exp. Therap.* 238, 116-122
Stampfer, M.J. *et al.* (1991) *N. Eng. J. Med.* 325, 756-762

200P THE EFFECTS OF NOVEL NITRIC OXIDE DONORS THE NONOATES ON ENDOTHELIN-1-INDUCED CONTRACTIONS AND BINDING CHARACTERISTICS IN HUMAN TISSUE

K. E. Wiley & A. P. Davenport. Clinical Pharmacology Unit, University of Cambridge, Level 6, Centre for Clinical Investigation, Box 110, Addenbrooke's Hospital, Cambridge, CB2 2QQ, U.K.

Endothelin-1 (ET-1) is a potent, long-acting vasoconstrictor. Nitric oxide (NO) has been shown to be an important vasodilator in large arteries. We have investigated whether NO can oppose the effects of ET-1 in human internal mammary arteries (IMA) and whether NO has a direct effect on ET-1 binding in human left ventricle using the novel NO-donor diethylenetriamine NONOate (DETA/NO).

Rings of IMA were set up in organ baths for the measurement of isometric tension. Cumulative concentration-response curves (CRC) were constructed to ET-1 (0.1- 300nM) in the absence (control) and presence of 100nM DETA/NO (preincubated with the tissue for 20 min). Experiments were terminated by the addition of a concentration of KCl (95mM) which caused a maximal contraction. ET-1 responses are expressed as %KCl response. The ability of DETA/NO (10nM-30μM) to reverse an established submaximal contraction to ET-1 (10nM) was then tested. Saturation binding experiments for [^{125}I]-ET-1 (4pM-2nM) were performed on 30μm sections of non-diseased human left ventricle alone (control), in the presence of 3mM DETA and 3mM DETA/NO.

ET-1 potently contracted IMA with an EC_{50} value of 2.6nM (95%CI; 0.52-13.1nM, n=6). In the presence of DETA/NO there was a rightwards shift in CRC ($P<0.05$; Student's paired *t*-test n=6). The maximum response to ET-1 was unaffected by preincubation with DETA/NO (87.0±9.7% and 83.3±7.6%KCl, control and in the presence of DETA/NO respectively). DETA/NO was also found to completely reverse the response to 10nM ET-1, with an EC_{50} value of 1.74μM (95%CI; 0.58-5.24μM, n=6) and caused an additional relaxation to below the original baseline (171.8 ± 37% ET-1 response).

No difference in binding affinity (K_D) was observed (control; 0.33±0.16nM, in the presence of DETA/NO; 0.47±.13nM, n=3), however DETA/NO caused a 90% (*$P<0.05$; Student's paired *t*-test) reduction in maximum binding (B_{MAX}) when compared to the control group. DETA was found to have no effect on [^{125}I]ET-1 binding.

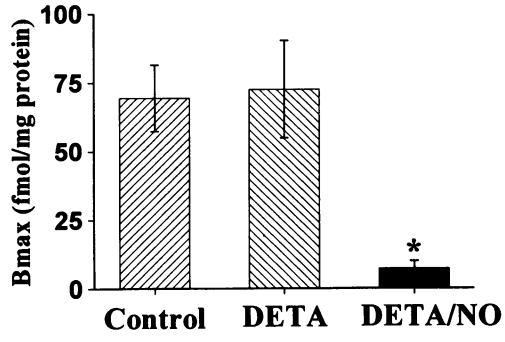

We have therefore shown that the novel NO-Donor DETA/NO is able to reverse an ET-1-induced contraction and pre-incubation with the compound causes a rightwards shift in the concentration-response curve. The binding studies indicate that there is a direct interaction between NO and either the ET-1 molecule or, more likely, the ET receptor in human ventricular tissue. NO is released continuously *in vivo*, thus this apparent modification of ET-receptor binding may provide an additional mechanism by which NO counter-balances the effects of ET.

Morely, D. & Keefer L. K. (1993). *J. Cardiovasc. Pharmacol*, **22**,(Suppl 7) S3-S9.

201P ROLE FOR CHYMASE IN THE CONVERSION OF BIG ENDOTHELIN-1 TO BIOLOGICALLY ACTIVE ENDOTHELIN PEPTIDES BY ENDOTHELIUM-DENUDED HUMAN UMBILICAL VEIN *IN VITRO*

J.J. Maguire, N. Telyatnikova & A.P. Davenport. Clinical Pharmacology Unit, University of Cambridge, Centre for Clinical Investigation, Box 110, Addenbrooke's Hospital, Cambridge, CB2 2QQ, U.K.

We have previously reported that endothelium-denuded human umbilical vein converts big endothelin-1 (big ET-1) to mature ET which produces the observed vasoconstrictor response to the precursor peptide (Maguire *et al.*, 1997). This big ET-1 response was thiorphan-insensitive but, in part, phosphoramidon sensitive. This implies a role for endothelin-converting enzyme (ECE), but not neutral endopeptidase 24.11 (NEP), in this process. More recently it has been suggested that human chymase will cleave big ET-1 to biologically active ET-1(1-31) (Nakano *et al*, 1997). We have therefore determined if the big ET-1 contractile response is due to the generation of both ET-1 and ET-1(1-31) in human umbilical vein.

Rings (4mm) of endothelium-denuded umbilical vein were set up for isometric tension recordings in 5ml organ baths containing warm (37°C), oxygenated Krebs solution. Cumulative concentration-response curves were constructed to big ET-1 in the absence (control) and presence of either 100μM chymostatin (chymase inhibitor), 30μM PD159790 (ECE-1 inhibitor; Ahn *et al.*, 1998) or a combination of both inhibitors added 30 minutes earlier. Experiments were terminated by addition of 50mM KCl to determine maximum contractile response and big ET-1 responses were expressed as a percentage of this. Data were analysed by the iterative curve-fitting programme Fig P (Biosoft, Cambridge, U.K.). Data are expressed as mean±s.e.mean and n values are the number of umbilical cords.

Big ET-1 contracted umbilical vein with a pD_2 value of 7.86±0.31 (n=4). The ECE-1 inhibitor PD159790 produced only a small rightward shift of the big ET-1 curve. A much greater effect was seen in the presence of 100μM chymostatin, with the big ET-1 curve incomplete at 700nM. The combination of PD159790 and chymostatin was more effective than chymostatin alone. (Figure 1). These data suggest that both ECE-1 and a chymostatin-sensitive enzyme, such as chymase, convert big ET-1 to biologically active forms. Additional investigation is required to determine if all of the observed contractile response to big ET-1 is due to generation of ET-1 or if there is contribution from chymase generated ET-1(1-31). ECE inhibitors alone may therefore not be sufficient to completely inhibit the synthesis of contractile ET peptides in human blood vessels.

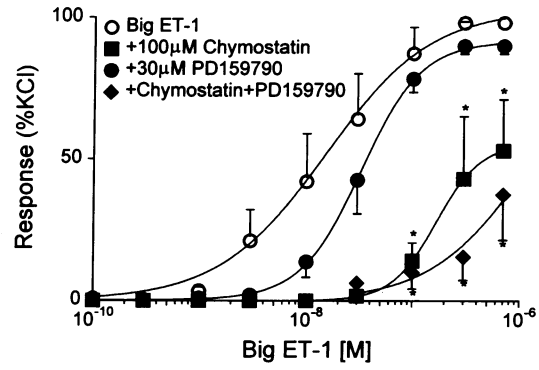

Figure 1. Inhibition of big ET-1 responses by PD159790, chymostatin or a combination of both. Data are mean±s.e.mean, n=4.

Supported by grants from the British Heart Foundation.

Ahn, K., Sisneros, A.M., Herman, S.B. *et al.*, (1998). *Biochem. Biophys. Res. Commun.*, 243, 184-190.

Maguire, J.J., Johnson, C.M., Mockridge, J.W. & Davenport, A.P. (1997). *Br. J. Pharmacol.*, 122, 1674-1654.

Nakano, A., Kishi, F., Minami, K. *et al.*, (1997). *J. Immunol.*, 159, 1987-1992.

202P INCREASED TRANSIENT EXPRESSION OF ENDOTHELIN-1 IN VENTRICULAR MYOCARDIUM ISOLATED FROM AN EXPERIMENTAL MODEL OF ENDOTOXIC SHOCK

J.P. Spiers[a], A. Dorman, J.D. Allen, E.J. Kelso*, B.J. McDermott* and B. Silke*. Departments of Physiology and *Therapeutics and Pharmacology, The Queen's University of Belfast, [a]currently at Department of Pharmacology & Therapeutics, Trinity College Dublin.

Lipopolysaccharide (LPS), a component of the outer layer of the gram-negative bacterial cell wall, is a major factor responsible for the pathogenesis of endotoxic shock by activating the release of mediators and cytokines from various cells. Circulating levels of endothelin-1 (ET-1) are elevated in both patients with endotoxic shock and LPS-treated animals (Weitzberg *et al.*, 1991). However, the role of ET-1 in the pathogenesis of endotoxic shock remains unclear. In this study, we have investigated whether the expression of ET-1 is altered, in ventricular myocardium of adults rats injected with *Escherichia coli* endotoxin (LPS), 0-14 hours following administration. An integral part of this study was to also assess the temporal expression of the ET_A and ET_B receptor subtypes.

Male Wistar rats (275-325 g; n=80) were randomly assigned to receive either 0.9 % saline (1 ml kg^{-1}, i.p.) or LPS (5 mg kg^{-1}, i.p.). The animals were sacrificed under terminal anaesthesia at 0, 2, 4, 6 and 14 hr folowing treatment. A section of the heart devoid of major blood vessels was removed and total cellular RNA isolated by acid guanidinium thiocyanate-phenol-chloroform extraction (Chomczynski & Sacchi, 1987). RNA concentration was assessed by spectrophotometry and samples standardised to 2μg μl^{-1}. Reverse transcription of total RNA was attained using a first strand cDNA synthesis kit (Reverse-iT, Abgene) and amplified by PCR using gene specific primers for endothelin-1, ET_A and ET_B receptor subtypes. PCR products were separated by electrophoresis, quantified by densitometry and normalised relative to an internal standard (GAPDH). Data are expressed as mean ± s.e.m. and analysed by one-way ANOVA with *post hoc* analysis (unpaired t-test). A value of $P<0.05$ indicates statistical significance.

The PCR products obtained were of the expected size, of 407 (ET-1), 282 (ET_A) and 293 (ET_B) base pairs, as previously reported (Maki *et al.*, 1998; Perkins *et al.*, 1997). There was a >15 fold increase ($P<0.0001$) in ET-1 mRNA expression after 2 hr in the LPS-treated group compared to saline (Figure), which returned to normal by 4 hr, and remained constant over the time period studied. LPS administration did not affect the expression of either ET_A receptor mRNA or ET_B receptor mRNA (14 hr ratio: 3.6±0.4 and 2.1±0.2, respectively) compared with saline (14 hr ratio: 3.7±0.7 and 1.8±0.3 respectively; Figure).

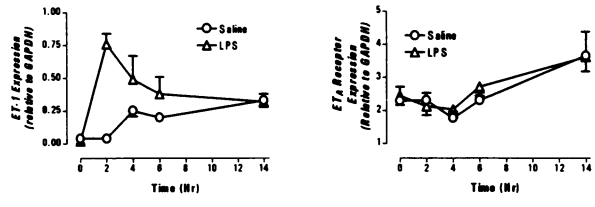

In summary, expression of endothelin-1 in the ventricular myocardium is increased in the early stages following LPS administration, but was followed by a decline to baseline, and was not accompanied by changes in endothelin receptor expression.

Chomczynski, S. & Sacchi,B. (1987) *Anal. Biochem.* 162: 156-159.

Maki, S., Miyauchi, T., Sakai, S. *et al.* (1998) *J. Cardiovasc. Pharmacol.* **31**: S412-S416.

Perkins, S.L., Sarraj, E., Kling, S.J. *et al.* (1997) *Am. J. Physiol.* **272**: E461-E468.

Weitzberg, E., Lundberg, J.M. (1991) *Circ. Res.* **33**: 222-226.

203P IL-4 AND IL-13 MODULATE CYTOKINE-INDUCED ENDOTHELIN-1 PRODUCTION IN HUMAN VASCULAR SMOOTH MUSCLE CELLS

Mandy Woods, Nicholas R. Walcot, Elizabeth G. Wood, [1]Jane A. Mitchell and Timothy D. Warner.
The William Harvey Research Institute, Charterhouse Square, London EC1M 6BQ and [1]Unit of Critical Care Medicine, Royal Brompton Hospital, London SW3 6NP.

The anti-inflammatory cytokines, interleukin-4 (IL-4), IL-10 and IL-13 have previously been shown to modulate cytokine-induced effects in a number of cell types (Jordan *et al.*, 1997; Alaaeddine *et al.*, 1999). Here we have determined whether cytokine-induced increases in endothelin-1 (ET-1) mRNA expression and peptide production in human vascular smooth muscle cells (HVSMCs; Woods *et al.*, 1999) can be modulated by either IL-4, IL-10 or IL-13.

Saphenous vein (SV) was obtained from patients undergoing coronary artery bypass graft surgery. Explants of HVSMCs were grown in DMEM supplemented with 2mM glutamine, and 15% foetal calf serum (37°C; 5% CO_2; 95% air). HVSMCs were identified by α-actin staining. HVSMCs isolated from SV were incubated with TNF-α (10ng/ml) and IFN-γ (1000U/ml) for 48 h in the presence or absence of IL-4, IL-10 or IL-13. ET-1 levels were measured by specific sandwich ELISA (R&D Systems). Total RNA was isolated by a guanidinium thiocyanate/isopropanol method with minor modifications (Chomczynski and Sacchi, 1987). Reverse transcription coupled with polymerase chain reaction was performed using standard methods.

IL-4 inhibited TNF-α and IFN-γ stimulated ET-1 release from SV with half maximal inhibition occurring at 0.11ng/ml (95% CI; 0.062-0.177ng/ml; n=4 donor patients). Similarly, IL-13 inhibited cytokine-induced ET-1 release in a concentration dependent manner with half maximal inhibition occurring at 2.15ng/ml (95% CI; 1.51-3.06ng/ml; n=4 donor patients). IL-10 did not effect cytokine-induced release of ET-1. Both IL-4 (10ng/ml) and IL-13 (30ng/ml) reduced cytokine-induced up-regulation of prepro-ET-1 mRNA expression.

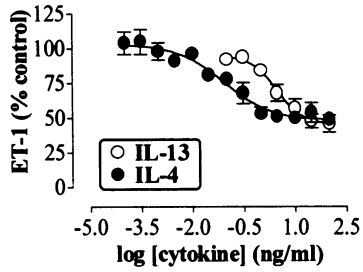

Figure 1. Effect of IL-4 and IL-13 on cytokine-stimulated ET-1 release in SV HVSMCs. Data represents mean ± s.e.m. of cells from n=4 donor patients assayed in triplicate.

In conclusion, the present study shows that cytokine-induced ET-1 mRNA expression and peptide production in HVSMCs can be modulated by the T-cell derived cytokines IL-4 and IL-13 but not by IL-10.

This work was supported by grants from The British Heart Foundation (PG/99001; FS/95003).

Alaaeddine, N., Di Battista, J.A., *et al.* (1999). *Arthritis Rheum.*, 42, 710-718.
Chomczynski, P. and Sacchi, N. (1987). *Anal. Biochem.*, 162, 156-159.
Jordan, N., Watson, M.L. *et al.* (1997). *Br. J. Pharmacol.*, 122, 749-757.
Woods, M., Mitchell, J.A., *et al.* (1999). *Mol. Pharmacol.*, 55, 902-909.

204P REGIONAL HAEMODYNAMIC RESPONSES TO GANGLION BLOCKADE IN CONSCIOUS, HYPERTENSIVE TRANSGENIC RATS

S.M. Gardiner, P.A. Kemp, J.E. March and T Bennett, School of Biomedical Sciences, Medical School, Queen's Medical Centre, Nottingham NG7 2UH.

The finding (Gardiner *et al.*, 1995) that endothelin contributes to the hypertension in male, heterozygous transgenic ((mRen-2)27) rats, in spite of the original manipulation being confined to insertion of the mouse Ren-2 gene into the rat genome (Mullins *et al.*, 1990), indicates other factors may also contribute to the hypertension in transgenic (TG) rats. In the present work we assessed haemodynamic responses to ganglion blockade following AT_1-receptor antagonism in TG rats and control Hannover Sprague Dawley (SD) rats.

As described previously (Gardiner *et al.* 1995), male, heterozygous TG rats (3-4 months old), and age-matched, male, SD rats were anaesthetised (sodium methohexitone, 60 mg kg^{-1} i.p., supplemented as required) and had pulsed Doppler probes and intravascular catheters implanted to allow assessment of changes in blood pressure (BP), heart rate (HR) and renal (R) mesenteric (M) and hindquarters (H) vascular conductances (VC) in response to i.v. administration of losartan (10 mg kg^{-1}) followed 60 min later by pentolinium (5mg kg^{-1}; 5mg $kg^{-1}h^{-1}$). Table 1 shows some of the results.

TG rats had a higher BP but a lower HR and RVC, MVC, and HVC than SD rats. Losartan caused a fall in BP in TG rats, but not in SD rats, although there was a tachycardia and vasodilatation in the kidney in both strains. Following pentolinium, there was marked hypotension in SD and TG rats, accompanied by abolition of the losartan-induced tachycardia. Under these conditions, TG rats had a higher BP, but lower HR and RVC and MVC than SD rats, although HVC was not different in the two strains.

Table 1 Baseline cardiovascular variables in SD and TG rats, and values 60 min after losartan and 30 min after pentolinium subsequently. Values are mean ± s.e. mean; $^{*}P<0.05$ versus baseline (Friedman test), $^{\dagger}P<0.05$ versus losartan value (Friedman test), $^{o}P<0.05$ versus corresponding value in SD rats (Mann-Whitney U test).

		Baseline	Losartan	Pentolinium
Heart rate	SD	375±11	412±15*	375±9†
(beats min^{-1})	TG	332±10^{o}	375±14*^{o}	342±11$^{\dagger o}$
BP	SD	109±2	110±3	80±3*†
(mm Hg)	TG	165±2^{o}	152±3*^{o}	93±4*$^{\dagger o}$
RVC	SD	79±4	88±5*	104±6*†
(kHz $mmHg^{-1}$]10^3)	TG	46±5^{o}	60±4*^{o}	88±7*$^{\dagger o}$
MVC	SD	83±6	83±7	85±8
(kHz $mmHg^{-1}$]10^3)	TG	32±4^{o}	37±4^{o}	49±5*$^{\dagger o}$
HVC	SD	39±2	40±3	48±3*†
(kHz $mmHg^{-1}$]10^3)	TG	25±2^{o}	29±2^{o}	42±2*†

These results are consistent with sympathetic hyperactivity contributing to the abnormal haemodynamic status in TG rats, but, in contrast to other reports (e.g., Zolk *et al.*, 1998), this is not manifest as an increase in resting heart rate.

Gardiner, S.M. *et al.* (1995). Br.J.Pharmacol., **116**, 2237-2244.
Mullins, J.J. *et al.* (1990). Nature, **344**, 541-544.
Zolk, O. *et al.* (1998). Br.J.Pharmacol., **123**, 405-412.

205P ANGIOTENSIN RECEPTORS AND ALTERNATIVE PATHWAYS FOR THE LOCAL GENERATION OF ANGIOTENSIN II IN THE HUMAN LEFT VENTRICLE

S. D. Katugampola & A. P. Davenport. Clinical Pharmacology Unit, University of Cambridge, Level 6, Centre for Clinical Investigation, Box 110, Addenbrooke's Hospital, Cambridge CB2 2QQ, U.K.

Conflicting results have been reported regarding the predominant enzyme involved in the conversion of angiotensin I to angiotensin II (Ang II) in the human heart (Urata et al., 1990, Zisman et al., 1995). The present study was carried out to determine the binding characteristics of Ang II receptors and to clarify the principle enzyme involved in angiotensin I to Ang II conversion in the human left ventricle using radioligand binding.

Normal human left ventricular (HLV) membranes were prepared by homogenization in 20 mM NaH_2PO_4 buffer, pH 7.4, 4°C. The homogenates were centrifuged at 40,000 g for 20 min at 4°C. The resulting supernatant was discarded and the pellet resuspended in buffer and rehomogenised and recentrifuged 3 times as described above. The final pellet was resuspended in 50 mM NaH_2PO_4, pH 7.4, containing 100 mM NaCl and 10 mM $MgCl_2$. Ang II receptor binding assay buffer consisted of 50 mM NaH_2PO_4, pH 7.4, 100 mM NaCl, 1 mM EGTA, 10 mM $MgCl_2$, 2 g/L BSA and 10 mg/L bacitracin. Competition experiments were performed at 22°C for 60 min with 0.6 mg/ml protein in a final volume of 250 µL. The labelled ligand was 0.2 nM ^{125}I-(Sar^1,Ile^8)Ang II. The non specific binding was determined using 1 µM Ang II. Competing ligands were used in a concentration range of 10^{-12} M to 10^{-4} M. For enzyme inhibitor studies, 10 µM chymostatin or 30 µM captopril were preincubated for 30 min prior to the final incubation. The binding reaction was terminated by rapid vacuum filtration using a Brandell cell harvester and Whatman GF/B filters, which were pre-soaked in wash buffer (50 mM NaH_2PO_4, pH 7.4, 4°C). The filtrates were washed three times and the radioactivity retained in the filter was measured by gamma counting. Statistical analysis was performed using Mann Whitney U-test, where the significance level was set at 95% ($p<0.05$).

The Ang II receptor antagonist, ^{125}I-(Sar^1,Ile^8)Ang II bound rapidly and specifically to HLV membranes, with a sub-nanomolar affinity. Saturation experiments yielded a mono-phasic curve with a K_D value of 0.64 ± 0.10 nM and a B_{max} value of 12 ± 3.18 fmol/mg protein (n=4). Mono-phasic competition curves, with the corresponding K_D values (nM) were obtained for saralasin (0.62 ± 1.35, n=3), Ang II (1.98 ± 1.51, n=6), angiotensin I (7.54 ± 1.4, n=6), angiotensin III (7.88 ± 1.01, n=3) and losartan (372 ± 0.42, n=3). A two site fit was preferred with CGP42112 with K_D values of 0.05 nM ± 0.60 (n=3) and less than 10 µM. Little or no [^{125}I]-angiotensin I binding was obtained and the affinity for angiotensin I reported above is mainly due to its conversion to Ang II. The binding of angiotensin I but not Ang II, was significantly inhibited by 10 µM chymostatin, with K_D values of 404 ± 23.2 nM and 39.2 ± 6.47 nM (n=3) respectively. There was no significant difference in the binding of angiotensin I compared to that of Ang II, in the presence of 30 µM captopril (n=3).

From our results it can be concluded that the AT_2 receptor predominates in the human left ventricle, with an approximate AT_1 to AT_2 ratio of 35:65. The serine protease inhibitor, chymostatin was more potent than the angiotensin converting enzyme (ACE) inhibitor captopril, at preventing the conversion of angiotensin I to Ang II in the HLV. These findings highlight the importance of alternative pathways for local generation of Ang II and AT_2 receptors in human hearts.

Urata, H., Healy, B., Stewart, R.W., et al (1990) Circ Res., **66**, 883-890.

Zisman, L.S., Abraham, W.T., Meixell, G.E., et al (1995) J Clin Invest., **95**,1490-1498.

206P PHARMACOLOGICAL CHARACTERISATION OF MUSCARINIC RECEPTORS IN FELINE AND HUMAN ISOLATED CILIARY SMOOTH MUSCLE

A. Choppin & R. M. Eglen.
Center for Biological Research, Neurobiology Unit, Roche Bioscience, Palo Alto, CA 94304, USA.

The ciliary smooth muscle from dog (McIntyre and Quinn, 1995) and man (Woldemussie *et al.*, 1993) expresses muscarinic M_3 receptors. However, recent functional studies (Choppin *et al.*, 1999a) suggest the involvement of a second receptor in dog eye. In the present study, ligands including AQ-RA 741 (Doods *et al.*, 1991), darifenacin (M_3-selective) and S-secoverine (discriminating M_5 receptors over M_3; Choppin *et al.*, 1999b) were used to examine the pharmacological characteristics of muscarinic receptors in feline and human ciliary muscle (CCM and HCM, respectively). These data were compared to those obtained in the dog ciliary muscle (DCM).

Using canine, feline and human eyes, the methodology for contractile studies was similar to that described by Choppin *et al.* (1998). Cumulative concentration-response curves to (+)-cis-dioxolane (1nM - 300µM) were established in the absence and presence of antagonists (90 min equilibration). Antagonist affinities (pK_B) were determined using the Gaddum equation (Gaddum, 1943).

(+)-Cis-dioxolane induced concentration-dependent contractions of DCM, CCM and HCM (pEC_{50} = 7.0±0.1, 6.9±0.1 and 6.6±0.1, respectively). These were antagonized by key muscarinic receptor antagonists (AQ-RA 741, S-secoverine and darifenacin; Figure 1) and the pK_B estimates are summarized in Table 1.

Table 1. pK_B estimates for muscarinic antagonists in DCM, CCM and HCM.

Antagonist	pK_B (DCM)	pK_B (CCM)	pK_B(HCM)
AQ-RA 741	5.88±0.09	5.98±0.18	6.14±0.11
S-secoverine	6.66±0.14	7.35±0.10	7.40*
Darifenacin	NC	8.35±0.15	8.34±0.15

Values shown are means ± s.e.mean, n≥3 (*: n=1).
NC: not calculated.

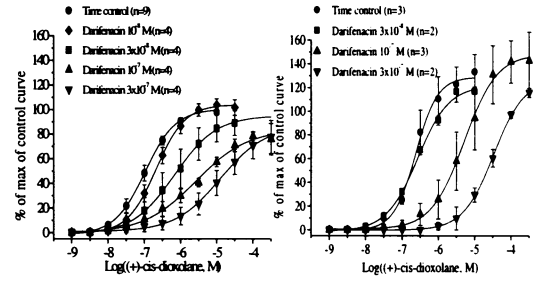

CAT HUMAN

Figure 1: Effect of darifenacin on cumulative concentration-response curves to (+)-cis-dioxolane in (left) cat ciliary muscle and (right) human ciliary muscle. Contractile effects are normalized to the control maximum. The values shown are means±s.e.mean.

In contrast to the biphasic curve obtained with darifenacin in dog ciliary muscle (Choppin *et al.*, 1999a), darifenacin exhibited a competitive antagonism, with high affinity values in feline and human tissues. The antagonist profiles obtained with all three antagonists were similar in the ciliary muscles. These data are consistent with the suggestion that contractile responses to (+)-cis-dioxolane in these tissues are mediated by a site, which has the pharmacological attributes of the M_5 muscarinic receptors. These findings thus support data from Gil *et al.* (1997) indicating the presence of M_5 receptors in human ciliary muscle

Choppin, A. *et al.* (1998). *Br. J. Pharmacol.*, 124, 883-888.
Choppin, A. *et al.* (1999a). *Br. J. Pharmacol.*, 126, 93P.
Choppin, A. *et al.* (1999b). *Br. J. Pharmacol.*, in press. 128, 33P.
Doods, H. *et al.* (1991). *Eur. J. Pharmacol.*, 192, 147-152.
Gaddum, J. H. (1943). *Trans. Faraday Soc.*, 39, 323-332.
Gil, D. W. *et al.* (1997). *Inves. Ophthalmol. Vis. Sci.*, 38, 1434-1442.
McIntyre, P. and Quinn, P. (1995). *Br. J. Pharmacol.*, 115, 139P.
Woldemussie, E. *et al.* (1993). *Exp. Eye. Res.*, 56, 385-392.

207P EFFECTS OF PRIMAQUINE DIPHOSPHATE AND ERYTHROMYCIN ON THE CARDIAC ACTION POTENTIAL RECORDED IN OVINE AND CANINE PURKINJE FIBRES AND GUINEA-PIG PAPILLARY MUSCLES

A.V. Lancaster, D. Mair, K.A. Lansdell, N. Gillard, S. Fraser, D. Templeton*, S. Parker*, A.G.B. Templeton and L. Patmore, Department of Pharmacology, Quintiles Scotland Limited, Edinburgh and * SmithKline Beecham Pharmaceuticals, Welwyn Garden City, UK

We have compared the effects of primaquine and erythromycin on the cardiac action potential recorded from Purkinje fibres and endocardial tissue from different species. These preparations are used to assess the potential of novel compounds to interact with cardiac ion channels which contribute to the ventricular cardiac action potential and define QT interval. Primaquine, an anti-malarial agent and erythromycin, an antimicrobial agent have been reported to cause cardiac arrhythmias (Luzzi & Peto, 1993; Nilsen, 1987) have been studied over a concentration range pertinent to the plasma levels achieved in man.

Recordings were made from left ventricular Purkinje fibres from hearts of adult Suffolk sheep and Beagle dogs, or right ventricular papillary muscles from Dunkin-Hartley Guinea pigs, as previously described (Lansdell *et al.*, 1999). The effects of primaquine (0.3-100 μM) and erythromycin (10-200 μg/ml) were assessed on action potential duration (APD), maximum rate of depolarization (MRD), upstroke amplitude (UA) and resting membrane potential (RMP), compared with time-matched vehicle recordings.

Exposure of isolated ovine and canine (A, B) Purkinje fibres to 1-10 μM primaquine resulted in decreases in APD_{90}, UA and MRD. Concentrations of 30 μM and above were associated with a marked depolarization of the resting membrane potential that led to a loss of excitability. Exposure of guinea pig papillary muscles to 30 μM primaquine was associated with decreases in UA and MRD but no effect on APD_{90} or RMP was observed at any of the concentrations tested.

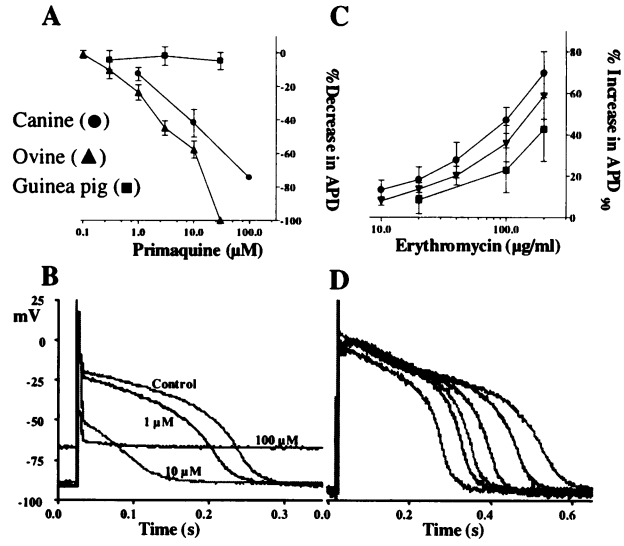

Exposure of isolated ovine or canine (C, D) Purkinje fibres and guinea pig papillary muscles to erythromycin resulted in a concentration dependent significant prolongation of APD_{90} (EC_{15} ~20 μg/ml). This is similar to the plasma levels achieved following 900 mg i.v. in healthy volunteers (Rubart et al., 1993).

These data indicate that ovine and canine Purkinje fibre preparations display similar sensitivities to primaquine and erythromycin whilst guinea pig papillary muscle is a less sensitive preparation.

Lansdell *et al.*, (1999), *Br J Pharmacol* **127**, 111P
Luzzi & Peto, (1993) *Drug Safety*, **8**, 295-311
Nilsen (1987) *J. Antimicrob. Chemother.*, **20**, 81-88
Rubart, M. et al., (1993) *Circulation*, **88 (1)**, 1832-1844

208P AN AORTIC-BANDED PRESSURE OVERLOAD MODEL OF LEFT VENTRICULAR HYPERTROPHY IN THE RAT: VASCULAR RESPONSES PROXIMAL AND DISTAL TO THE STENOSIS COMPARED

F. Donaldson, L McEvoy, D. Lang, & M.J. Lewis, Cardiovascular Science Research Group, Wales Heart Research Institute, University of Wales College of Medicine, Heath Park, Cardiff, CF14 4XN, UK.

Increases in blood pressure and humoral agents such as angiotensin II (Ang II) are thought to be intrinsic to the development of left ventricular hypertrophy (LVH), though the extent to which these factors contribute to this condition and its associated vascular dysfunction is unknown. In the present study we have measured vascular responses in isolated aortic rings from a rat (male, Wistar, 150-200g at the time of banding) aortic-banded (AB, band internal diameter 0.4mm) pressure overload model of LVH (method as used by Bell *et al.*, 1997 for guinea pigs). In this model, the aorta proximal to the band is exposed to increases in both blood pressure and circulating humoral agents such as Ang II, whilst that distal to the band experiences effects of the humoral changes only. Six weeks post-banding, endothelium-intact rings (2-3mm wide) were prepared from aortic tissue immediately (within 1cm) proximal and distal to the stenosis. Similar tissue was taken from sham operated controls (SOC). Rings were mounted (resting tension 1g) in 8ml tissue baths containing Krebs buffer (with 10μM indomethacin) and gassed with 95% CO_2/5% O_2 at 37°C for isometric tension recording. All rings were preconstricted with phenylephrine (PE, 1μM) until a reproducible constriction was achieved. They were then exposed to increasing concentrations of PE (1nM to 10μM), washed and reconstricted to approximately 70% of the maximum response (Cmax) to PE (0.3 to 1μM). On reaching a steady plateau rings were exposed to acetylcholine (ACh, 1nM to 10μM). All rings were then washed, re-equilibrated then reconstricted to 70% of the Cmax to PE followed by exposure to sodium nitroprusside (SNP, 1nM to 10μM). PE-induced increases in tension are expressed in g and relaxation responses expressed as a percentage of the PE-induced (70% of Cmax) constriction. All data is expressed as mean±s.e.m. and Cmax and maximum relaxation (Rmax) responses compared by paired t test. Significant differences are identified where $p<0.05$. In tissue taken from SOC rats, no difference was observed in either the Cmax to PE or the Rmax to ACh between rings proximal and distal to the site of aortic band placement (2.0±0.4 & 1.6±0.1g respectively, both n=6 for Cmax and 97.6±1.4 & 94.5±3.9% respectively, both n=6 for Rmax). However, in tissue taken from AB rats, a significant decrease was observed in both the Cmax to PE ($p<0.05$) and the Rmax to ACh ($p<0.001$) in rings proximal as compared to distal to the band (0.8±0.1 & 1.8±0.4g respectively, both n=6 and 76.0±1.3 & 96.9±1.7% respectively, both n=7 for Rmax). Following exposure to SNP, no differences in Rmax values were observed between proximal and distal band rings from either group of rats (104.0±2.9 & 105.7±3.0% respectively for SOC, both n=6 and 102.5±1.9 & 106.2±3.5% respectively for AB, both n=6). These data demonstrate impairment of both vasoconstriction and vasorelaxation responses in proximal aortic tissue from AB rats only. This suggests that increased blood pressure may be the greatest contributory factor to the observed vascular dysfunction

Bell. J.P., *et al.* (1997) *Br J Pharmacol*, 120, 99P.

209P INOSITOL PHOSPHATE FORMATION IN RAT THORACIC AND ABDOMINAL AORTA

K. Becker, C. Giessler, K. Pönicke, O.-E. Brodde, Institute of Pharmacology, University of Halle, D-06097 Halle, Germany

The aim of this study was to find out whether increases in inositol phosphates (IP) evoked by stimulation of $G_{q/11}$-coupled receptors might be different in rat thoracic versus abdominal aorta. For this purpose we assessed the effects of noradrenaline (NA), endothelin-1 (ET) and the thromboxane A_2-mimetic U 46619 on IP-formation in rings of rat thoracic and abdominal aorta. Male wistar rats (12 weeks old) were killed by cervical dislocation; the thoracic and abdominal aorta was rapidly removed and placed in oxygenated Krebs-Henseleit solution. The aorta was cut into rings of 1 mm in width with a tissue shopper, maintained at 37° C and incubated with [^{3}H]-myo-inositol (5 µCi/ml) for 1 hour. After wash-out of the radioactivity three rings of each aorta were incubated in a total volume of 330 µl in the presence or absence of agonists and antagonists for 45 min at 37°C. Incubation was stopped by addition of methanol/chloroform (1:2 v/v) and [^{3}H]-IP's were isolated by Dowex AG 1-X8 column chromotography as described previously (Becker et al., 1996). In both preparations NA (10^{-8} - 10^{-4} M), ET-1 (10^{-9} - 10^{-6} M) and U 46619 (10^{-8} - 10^{-5} M) concentration-dependently increased IP-formation; for all three agonists effects in thoracic aorta were significantly higher than in abdominal aorta (see Table 1).
In both preparations ET-1 (0.1 µM)-induced IP-formation was inhibited by the ET_A-receptor antagonist BQ-123 (Moreland, 1994; pK_B-values 8.16 ± 0.24 and 8.10 ± 0.35), U 46619 (1 µM)-induced IP-formation by the TP-receptor antagonist SQ 29548 (Ogletree et al., 1985; pK_B-values 8.20 ± 0.3 and 8.48 ± 0.2), and NA (10 µM)-induced IP-formation by the α_{1D}-adrenoceptor antagonist BMY 7378 (Goetz et al., 1995; pK_B-values 8.11 ± 0.39 and 8.25 ± 0.46).

Table 1. Agonist-induced IP-formation in rat thoracic and abdominal aorta

	A. thoracica		A. abdominalis	
	pEC_{50}	E_{max}	pEC_{50}	E_{max}
NA	5.8 ± 0.1	407 ± 57	5.8 ± 0.1	203 ± 36*)
ET-1	7.5 ± 0.1	1190 ± 139	7.7 ± 0.1	522 ± 87*)
U 46619	6.9 ± 0.1	928 ± 189	6.8 ± 0.2	348 ± 24*)

E_{max} = % stimulation of basal (=100 %); n= 4 –6; *) $P < 0.05$ vs. A. thoracica (non-paired, two-tailed student's t-test).

We conclude that, in rat aorta, ET-1-effects are predominantly mediated by ET_A-receptors, U 46619-effects by TP-receptors and NA-effects by α_{1D}-adrenoceptors; however, responses in thoracic aorta are much more pronounced than in abdominal aorta.

Becker, K. et al. Naunyn-Schmiedeberg's Arch. Pharmacol. 354: 572-578, 1996.
Goetz, A. S. et al. Eur. J. Pharmacol. 272: R5-R6, 1995.
Moreland, S. Cardiovasc. Drug Res. 12: 48-69, 1994.
Ogletree, M. L. et al. J. Pharmacol. Exp. Ther. 234: 435-441, 1985.

Supported by the Deutsche Forschungsgemeinschaft (DFG Br 526/6-1).

210P COMPARISON OF THE DIFFERENTIAL TIME COURSE OF NIFEDIPINE IN HUMAN AND RAT VASCULAR MODELS

R. van der Lee[¶], M. Pfaffendorf[¶], G.A. van Montfrans[†], J.J. van Lieshout[†], R.P. Koopmans[†] & P.A. van Zwieten[¶]. [¶]Dept. Pharmacotherapy, [†]Dept. Internal Medicine, Academic Medical Center, University of Amsterdam, Meibergdreef 15, 1105 AZ Amsterdam, The Netherlands.

In a previous study we investigated the differential time course of various calcium antagonists (CA) in small isolated rat mesenteric arteries (Van der Lee *et al*, 1998). We concluded that the differences observed were most probably due to differences in lipophilicity between the CA studied. The aim of this study was to compare the time course of nifedipine of the previous study with data from a study in small isolated subcutaneous human arteries and human forearm venous occlusion plethysmography in healthy subjects. Human small subcutaneous arteries (internal diameter 529±107µm, n=6 for each concentration) were derived from tissue leftovers from plastic surgery. The vessels were mounted in an isometric wire myograph in the same way as described by Van der Lee *et al.* (1998). After a training procedure (twice 120mM KCl, once 3µM phenylephrine and again once 120mM KCl) the vessels were precontracted with 120 mM KCl. After stabilization of the contraction, one concentration of nifedipine (range 1nM-0.3µM) was added and the effect was studied for 120 min. Healthy male non-smoking volunteers (age 31±7yrs, n=7) were studied in the supine position with both forearms stabilized slightly above the heart level. Informed consent was obtained prior to each experiment from all subjects. The arteria brachialis was cannulated; the cannula remained in position throughout the study protocol for direct measurement of blood pressure (MAP 88±3mmHg) and infusion of nifedipine. ECG tracings were measured continously and forearm blood flow (FBF) was measured at 15-second intervals by R-wave triggered venous occlusion plethysmography. After an ischemia-hyperemia protocol in which maximal possible vasodilation was observed, the study commenced with the vehicle of nifedipine (NaCl 0.9%). In four subsequent runs increasing concentrations of nifedipine were studied for 20 min each, with an infusion rate of 0.3 ml/min. During experiments both hands were excluded from the circulation using small wrist cuffs, inflated to 200mmHg.
Nifedipine dilated both depolarized human and rat small isolated small arteries by 100% at the highest concentrations. In the human forearm nifedipine-induced mean increase in blood flow was 63±15% at the highest concentration infundated. $LogIC_{50}$-values were -8.23±0.02 and -8.49±0.07 for small isolated rat and human arteries, respectively. In the human forearm, the $logIC_{50}$-value amounted to -7.27±0.18. All these values were significantly different from each other ($p<0.01$). The time nifedipine needed to reach equilibrium was 10.3±1.7 min and 6.4±1.4 min for human subcutaneous artery and human forearm vascular bed, respectively. For the rat mesenteric artery the value was 8.8±1.3 min. The differences between these values did not reach statistical significance.
We conclude that the time course of action of nifedipine is inherent to the drug rather than the system studied. The difference in effectivity of nifedipine between isolated vessel preparations and the human forearm vascular bed might be explained by differences in contractile conditions.

Van der Lee R *et al.* (1998), *Fundam. Clin. Pharmacol.* **12**, 607-612

211P TIME-DEPENDENT CHANGES OF THE FUNCTIONAL PROPERTIES OF ISOLATED SAPHENOUS VEIN PREPARATIONS EXPOSED TO VARIOUS PRESERVATION SOLUTIONS

M. Rinia-Feenstra[1], M. Pfaffendorf[1], T.M. van Gulik[3], B.A.J.M. de Mol[2], P.A. van Zwieten[1,2]. Dept. Pharmacotherapy[1], Dept. Cardiopulmonary Surgery[2] and Dept. Experimental Surgery[3], Academic Medical Center, Meibergdreef 15, 1105 AZ Amsterdam, The Netherlands.

The patency of saphenous vein (SV) grafts depends partially on their reactivity to spasmogens and endothelial function (Motwani & Topol, 1998). In a previous study we found that the endothelial function of human SV remnants obtained during aortocoronary bypass surgery (CABG), was reduced and independent of the surgical technique applied (Rinia-Feenstra *et al.*). In the present study another determinant of functional properties of SV, namely the exposure to different solutions during CABG was investigated, in an in vitro animal model.

New Zealand white rabbits (2-3 kg) (n=28) were sacrificed and the lateral SV of both hind limbs was dissected and cut into four segments. The vessels were investigated immediately (0h) or after cold (4°C) preservation for 1h, 24h or 48h, respectively, in a physiological salt solution (NaCl) (n=5-9), cardioplegic solution of St. Thomas (CST) (n=5-8), heparinized Ringer's lactate (RL) (n=4-8) or University of Wisconsin solution (UW) (n=7-9). Each segment was cut into three rings (length 3 mm) and mounted into 8 ml organ baths filled with oxygenated Krebs solution of 37°C and connected to an isometric force transducer. After a priming procedure cumulative concentration-response curves (CRC) were constructed for the α_1-adrenoceptor agonist phenylephrine (Phe) (0.1μM-1mM). For the CRC of the nitric oxide (NO)-donor sodium nitroprusside (SNP) (1nM- 10μM) and the endothelium-dependent vasodilator metacholine (MCh) (1nM- 10μM), the SV rings were precontracted with Phe (30μM). Data were analyzed by means of ANOVA for unpaired data with Newman-Keuls' post-test for multiple comparisons.

The potency (expressed as pD_2-values) of Phe, SNP and MCh in the non-incubated segments, was 5.0±0.02, 7.5±0.05, 7.4±0.02, respectively, and did not alter after preservation. The maximal responses to KCl, Phe, SNP and MCh of the segments incubated in RL, CST and UW (Table 1) did not change after storage, and were identical for the three solutions. Preparations incubated in NaCl showed a decline in contractile response to a potassium solution (KCl) (60mM), while the Phe-induced contractions remained intact (Table 1). The relaxations to SNP of the segments incubated in NaCl remained stable in contrast to the responses to MCh.

Table 1: *E_{max} of segments preserved in NaCl or UW for different time intervals (expressed as absolute value (mN) for KCl and Phe, and for MCh as % of the precontraction). *p<0.05 compared to non-incubated segments and segments stored in the other solutions.*

		0h	1h	24h	48h
NaCl	KCl	31±2	26±3	21±2*	13±2*
	Phe	19±2	15±3	16±2	12±2
	MCh	97±5	97±5	72±8*	62±9*
UW	KCl	28±2	24±1	27±2	26±2
	Phe	22±4	16±2	17±1	15±2
	MCh	94±5	96±3	95±2	92±3

In conclusion this study demonstrated that the preservation in a physiological salt solution produced a decline in the depolarization-induced contractile responses, and the endothelial function.

The exposure to RL and CST, which are the solutions applied during aortocoronary bypass surgery for preservation and check for structural integrity, did not change the viability of the lateral SV, in the rabbit model used. For the preservation of SV for transplantation or reoperation purposes, CST and RL might be as effective as UW.

Motwani J.G. & Topol E.J. (1998), *Circulation* **97**, 916-931
Rinia-Feenstra M. *et al.* (in press), *Ann. Thorac. Surg.*

212P BLOCK OF THROMBOXANE A_2-INDUCED CONTRACTION BY A Rho-KINASE INHIBITOR IN HUMAN INTERNAL MAMMARY ARTERY

R Sadaba, A Ishola, [+]C Munsch, [*]P Pacaud & DJ Beech. School of Biomedical Sciences, University of Leeds, Leeds LS2 9JT, UK. [+]Leeds General Infirmary, UK. [*]Faculte des Sciences et Techniques, University of Nantes, France.

Thromboxane A_2 may be important in vasospasm of conduit arteries used for cardio-pulmonary bypass surgery because its plasma level is elevated during and after surgery and it is a potent vasoconstrictor. The aim of this study was to elucidate the major cellular mechanisms underlying contraction evoked by thromboxane A_2 in human left internal mammary artery (LIMA), a conduit commonly used in bypass surgery.

Discarded segments of LIMA were obtained with ethical permission. Isometric tension recordings were made from rings of LIMA in Krebs solution gassed with 95 % O_2 / 5 % CO_2 at 37 °C. Krebs solution contained (mM): NaCl 118.3, KCl 4.6, $MgSO_4$ 1.2, $NaHCO_3$ 25, KH_2PO_4 1.2, $CaCl_2$ 2.5, and glucose 11. Low Ca^{2+} solution was the same except it contained 5 mM EGTA (calculated free Ca^{2+} = 100 nM). All experiments were performed in the presence of 10 μM diltiazem, which strongly inhibits L-type Ca^{2+} channels but has a minor inhibitory effect on contraction evoked by the stable thromboxane A_2 mimetic U46619.

It has been shown that endothelin-1 evoked contraction of rat aorta is strongly inhibited by 30 μM SKF96365, a blocker of capacitative Ca^{2+}-entry and receptor-operated channels (Iwamura et al., 1999). Therefore, U46619 concentration-response curves were constructed for LIMAs in control conditions and then in 30 μM SKF96365 or vehicle only, but there was no effect on the EC_{50} or maximum response (n=4 for each). These data suggested that Ca^{2+}-influx had only a minor role in U46619-evoked contraction and this hypothesis was supported by the observation that U46619-evoked contractions were preserved in 100 nM-Ca^{2+} Krebs solution (n=3). An alternative source of Ca^{2+} for contraction could be Ca^{2+}-released from sarcoplasmic reticulum. However, U46619-evoked contractions persisted after treatment with 10 μM cyclopiazonic acid, which depletes stored Ca^{2+} by inhibiting SERCA (n=4). Another mechanism for contraction that does not require an elevation of $[Ca^{2+}]_i$ is Rho kinase-mediated inhibition of myosin phosphatase, resulting in Ca^{2+}-sensitisation of contractile proteins (Somlyo et al., 1999). This effect is inhibited by the Rho-kinase inhibitor Y27632 (Uehata et al., 1997). Strikingly, 10 μM Y27632 abolished contraction evoked by 10 nM U46619 (n=6).

The findings suggest that Rho kinase-mediated Ca^{2+}-sensitisation plays a major role in thromboxane A_2-evoked spasm of human left internal mammary artery.

The work is funded by the National Heart Research Fund.

Iwamuro Y et al, 1999, *Br J Pharmacol* **126(5)**:1107-14
Somlyo AP et al, 1999, *Rev Physiol Biochem Pharmacol* **134**: 202-234.
Uehata M et al, 1997, *Nature* **389**:990-994

213P SPHINGOSINE-1-PHOSPHATE-INDUCED VASOCONSTRICTION IN ANAESTHETIZED RATS IS PERTUSSIS TOXIN-SENSITIVE

A. Bischoff, D. Meyer zu Heringdorf, K. H. Jakobs, M. C. Michel, Depts. of Medicine and Pharmacology, Univ. Essen, 45122 Essen, Germany

We have reported that i.v. injection of the sphingolipid sphingosine-1-phosphate (SPP) reduces renal (RBF) and mesenteric blood flow (MBF) in anaesthetized rats without changes in mean arterial pressure (MAP) or heart rate (HR, Bischoff et al. 1998). Since some SPP effects *in vitro* are mediated by receptors of the EDG-family and blocked by pertussis toxin (PTX) treatment (Gonda et al. 1999), we have investigated the effects of PTX treatment on SPP-induced vasoconstriction in anaesthetized rats.

Male Wistar rats (320-470 g) were anaesthetized with ketamine (100 mg kg^{-1}), and given PTX (10 µg kg^{-1}) or vehicle via the jugular vein (n = 5-6 per group). Three days later the rats were anaesthetized with thiobarbital (100 mg kg^{-1}) and surgically prepared as previously described (Bischoff et al.1996). Briefly, the femoral artery was catheterized for MAP measurements by a Statham transducer, the femoral vein was catheterized for volume substitution and bolus injections. RBF, MBF and HR were determined by flow sensors placed on the right renal and the mesenterial artery, respectively. SPP bolus injections (1-100 µg kg^{-1} i.v.) were given in 3 min intervals. These intervals were sufficient to allow all haemodynamic parameters to return to baseline values. Statistical significance between the basal values was determined by an unpaired t-test, significance of the main treatment effect was determined by a two-way analysis of variance with $P < 0.05$ considered significant. Data are mean ± s.e.m.

PTX-treatment did not significantly alter basal MAP (101±10 mm Hg) , HR (374±8 bpm), RBF (6.2±0.2 ml min^{-1}) or MBF (5.5 ±0.9 ml min^{-1}). Systemic SPP bolus injection did not markedly alter MAP or HR in vehicle- or PTX-treated rats. In contrast SPP dose-dependently reduced RBF in vehicle- but not in PTX-treated rats ($P < 0.05$; Fig. 1). Similarly, SPP dose-dependently lowered MBF by maximally 2.4±0.3 ml min^{-1} at a dose of 100 µg kg^{-1} in vehicle- but not in PTX-treated rats.

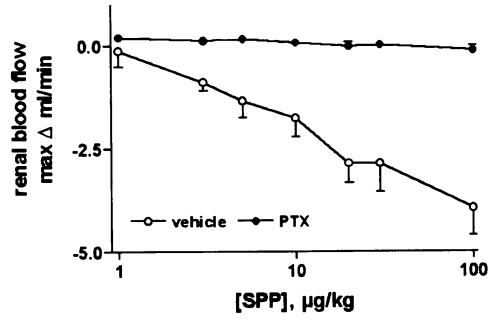

Fig. 1: Effect of PTX treatment on SPP-induced RBF reduction

We conclude that SPP-induced vasoconstriction in anaesthetized rats is PTX-sensitive and therefore likely to occur via receptors coupling to G-proteins of the $G_{i/o}$ type.

Bischoff, A. et al. (1996) *J.Physiol.* 495: 525-534
Bischoff, A. et al. (1998) *Naunyn-Schmiedeberg's Arch.Pharmacol.* 357 Suppl.: R112
Gonda, K. et al. (1999) *Biochem.J.* 337: 67-75

214P IDENTIFICATION OF Na^+, K^+ ATPase SUBTYPES IN RAT HEPATIC AND MESENTERIC ARTERIES

G. R. Richards, C. D. Glen, G. Brady, M. Burnham, G. Edwards, M. J. Gardener, J. Lloyd & Arthur H. Weston. School of Biological Sciences, University of Manchester, G38 Stopford Building, Manchester, M13 9PT, UK.

Vascular endothelial cells release an "endothelium-derived hyperpolarizing factor" (EDHF), which hyperpolarizes the underlying vascular smooth muscle. Recent studies in rat hepatic and mesenteric arteries identified EDHF as endothelium-derived K^+ (Edwards *et al.*, 1998; 1999a,b), and proposed the endothelial K^+-release channels to be the small- and intermediate-conductance calcium sensitive potassium channels (SK_{Ca}, IK_{Ca}). In addition, the smooth muscle cell hyperpolarization was attributed to the subsequent activation of Na^+,K^+ ATPases and inwardly-rectifying K^+ channels on the muscle.

A reverse-transcription, polymerase chain reaction (RT-PCR) approach, based on existing protocols (Brady & Iscove, 1993), has been developed by us to allow the direct investigation of mRNA in freshly-isolated, vascular smooth muscle cells. In the present study we have applied this methodology to identify the Na^+,K^+ ATPase subunit mRNA in vascular smooth muscle cells freshly-isolated from the rat hepatic and mesenteric arteries. Briefly, the method comprised enzymatic digestion of freshly-dissected arteries to yield isolated cells, followed by collection of a small number of vascular smooth muscle cells in a narrow-bore glass pipette. Cells were transferred directly to a lysis buffer, and a three-step process was used to produce an unbiased global amplification of the mRNA present in the cells. cDNA was then quantified and used in gene-specific PCR.

Using this approach in morphologically-identified smooth muscle cells from both hepatic and mesenteric arteries we found the presence of α_1-, α_2-, α_{1T}-, β_1-, and β_2-subunit mRNA, but failed to detect α_3- and α_4-subunit mRNA (see figure 1). In conjunction with information regarding variations in Na^+, K^+ ATPase α-subunit ouabain sensitivity (Blanco & Mercer, 1998), and the ouabain-sensitivity of the EDHF-response (Edwards *et al.*, 1999b) the results suggest that a smooth muscle Na^+, K^+ ATPase containing an α_2-subunit is specifically involved in mediating the EDHF response.

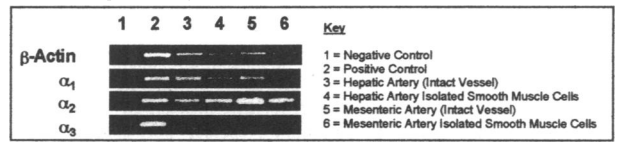

Figure 1: Gel images showing presence of α_1- and α_2-, and absence of α_3-Na^+/K^+ ATPase subunit mRNA in rat arteries. β-Actin was included as a PCR positive control.

Supported by the British Heart Foundation and the Medical Research Council.

Blanco, G. & Mercer, R.W. (1998) *Am.J.Physiol.* 275 F633-F650
Brady, G. & Iscove, N.N. (1993) *Methods.Enzymol.* 225 611-623
Edwards, G., Dora, K.A., Gardener, M.J., *et al.*, (1998) *Nature* 369 269-272
Edwards, G., Feletou, M., Gardener, M.J., *et al.*, (1999a) *Br.J.Pharmacol.* 128 1788-1794
Edwards, G., Gardener, M.J., Feletou, M., *et al.*, (1999b) *Br.J.Pharmacol.* 128 1064-1070

215P A COMPARISON OF POLY-L-LYSINE (PLL) AND *ALTERNARIA TENUIS*-INDUCED RESPONSES IN RABBIT SKIN

H. Jones, C.P. Page & W. Paul, Sackler Institute of Pulmonary Pharmacology, GKT School of Biomedical Sciences, King's College London, SE1 9RT.

We have reported previously that the polycation poly-L-lysine (PLL) and Alternaria tenuis (AT) extract cause plasma exudation (PE) and neutrophil accumulation when injected intradermally (i.d.) in, respectively, normal and AT sensitised rabbits (Jones *et al*, 1998, Jones *et al*, 1999). Here, we have used colchicine treatment to assess the neutrophil dependency of PE responses to PLL and AT, with PE responses to the formyl peptide f-met-leu-phe (fMLP) and bradykinin (BK), respectively, as neutrophil dependent and independent controls. We have also studied the duration of the PE response to AT in relation to that produced by PLL, which was shown previously to persist for up to at least 2 h (Sasaki *et al*, 1991).

Intradermal injections (0.1 ml) were made in the shaved skin of pentobarbitone anaesthetised, AT immunised NZW rabbits (3.0 - 3.8 kg). PE was measured as local accumulation of i.v. injected ^{125}I-albumin (0.1 MBq kg^{-1}) and expressed as µl plasma. Responses were induced by i.d. injection of PLL (30 - 100 µg site^{-1}), AT (50 - 500 protein nitrogen units (p.n.u.) site^{-1}), BK (4.7 x 10^{-10} mol site^{-1}) + prostaglandin (PG) E_2 (3 x 10^{-10} mol site^{-1}) or fMLP (10^{-11} mol site^{-1}) + PGE,. Colchicine (1 mg kg^{-1} i.v.), or saline, were injected 10 min prior to i.d. injections and PE responses were measured over 3 h. In time course experiments, i.d. injections were made 2.5, 1.5, 0.5 or 0 h prior to i.v. injection of ^{125}I-albumin and responses measured over 30 min. Values are mean ± s.e.m. (n = 4 - 6). Significance of differences was assessed by paired or unpaired t-test.

In colchicine treated animals, responses to fMLP + PGE_2 and AT 50, 200 or 500 p.n.u. (36 ± 12, 69 ± 11, 110 ± 12, 176 ± 27 µl) were significantly ($P < 0.05$ - 0.01) reduced compared to those in control animals (128 ± 24, 113 ± 15, 208 ± 25, 278 ± 28 µl). In contrast, responses to BK + PGE_2 and PLL 30 or 100 µg (171 ± 31, 67 ± 6, 124 ± 11 µl) were not significantly affected by colchicine (190 ± 36, 61 ± 15, 103 ± 15 µl). PE in skin sites pre-injected with AT (200 p.n.u. site^{-1}) was significant at all times compared with saline (sal) injected sites (e.g. 0 - 0.5 h: sal; 6.4 ± 1.8 µl, AT; 54 ± 7 µl, $P < 0.01$; 2.5 - 3 h: sal; 3 ± 1.4 µl, AT; 23 ± 5µl, $P < 0.05$). PE in sites injected with PLL (100 µg site^{-1}) was also significant up to 2.5 - 3 h: sal; 3.3 ± 1.4 µl, PLL; 16 ± 2.4 µl, $P < 0.05$.

These results show that the PE response to PLL is, like that to BK, neutrophil independent. In contrast, the active cutaneous anaphylactic (ACA) response to AT is partially neutrophil dependent, as has been reported for passive cutaneous anaphylactic responses in rabbit skin (Hellewell *et al*, 1992). However, the PE response in ACA, unlike that reported for PCA, persists for up to 3 hours.

Hellewell, P.G., Jose, P.J. & Williams, T.J. (1992) *Br. J. Pharmacol.*, 107, 1163 - 1172.
Jones, H., Wang, Y.C., Douglas, G.J., Paul, W. & Page, C.P. (1998) *Br. J. Pharmacol.*, 123, 167P.
Jones, H., Paul, W. & Page, C.P. (1999) *Am. J. Respir. Crit. Care Med.*, 159, A35.
Sasaki, M., Paul, W., Douglas, G.J. & Page, C.P. (1991) *Br. J. Pharmacol.*, 104, 444P.

216P PHARMACOLOGICAL MODULATION OF INFLAMMATORY CELLS AND VASCULAR PERMEABILITY DURING ALLERGIC REACTION IN RAT AIRWAYS

Amilcar S Damazo, Wothan Tavares de Lima & Sonia M Oliani
Department of Biology, IBILCE-UNESP, S.J. Rio Preto, and Department of Pharmacology, ICB-USP, São Paulo, SP, Brasil.
[Introduced by Mauro Perretti]

There is a renewed interest in the central role that tissue mast cells play in the initiation and progress of the allergic inflammatory reaction (Galli *et al.*, 1999). The aim of this study was to relate the efficacy of several anti-inflammatory drugs to their potential effect on mast cell stability and morphology in a rat model of allergic inflammation. In particular, known inhibitors of the catabolism of arachidonic acid were used.

Male Wistar rats (n=10; 200-230 g body weight, USP, São Paulo) were sensitised by i.p. injection of 10 µg of ovalbumin (OVA; grade III, Sigma Chemical Co., St. Louis, IL) suspended in 10 mg aluminium hydroxide. After 14 days, animals were challenged by aerosol administration of OVA (1%; 15 min application at 0.75 ml min^{-1}). Control rats (n=5) were challenged with saline. Evans blue (EB) was injected i.v. (20 mg/kg) immediately before OVA, to determine vascular permeability. For pharmacological modulation, rats (n=5) were treated with the following drugs prior to OVA challenge at the time indicated: the connective tissue mast cell degranulator compound 48/80 was given at the dose of 2 mg/kg i.p., twice a day for 5 days; the glucocorticoid dexamethasone (DEX) was given at 1 mg/kg i.v. 12 h before; the 5-lipoxygenase inhibitor nor-dihydroguaiaretic acid (NDGA) was used at 30 mg/kg i.p., and the non-selective cyclo-oxygenase inhibitor indomethacin (4 mg/kg i.v.) were both given 30 min prior to OVA. In all cases, rats were sacrificed at the end of the 15 min inhalation period, and several tissues collected (larynx, trachea, external and internal bronchi) and wet weighted. Fragments were also dried up into a stove, to determine the dry weight. Other fragments were fixed in formamide (4 ml per gram of tissue), and the stain extracted for 24 h in room temperature. Absorbance was quantified at 620 nm wavelength in a spectrophotometer, and results expressed as µg EB extracted per g of dry weight tissue. For the morphological and statistical analysis, segments of trachea were fixed in 2.5% paraformaldehyde-glutaraldehyde for 24 h. Following embedding in historesin (Technovit 2000, São Paulo), 2 µm serial sections (n=10) were cut and stained with 0.25% toluidine blue in 1% sodium borate (Sigma).

Data were analysed by ANOVA followed by the Bonferroni test taking a P value less than 0.05 as significant.

OVA challenge produced a significant increment in vascular permeability well above the one measured in rats with saline challenge (data are µg EB g^{-1}): 91±11 and 252±8 for saline- or OVA-challenged groups in the larynx ($P<0.05$). Similar increases were seen in the other tissues: 94±23 and 252±18 for the trachea, 38±8 and 302±70 for the external bronchi, 87±8 and 172±15 for the internal bronchi, in saline and OVA-treated groups, respectively ($P<0.05$ in all cases). Morphological analysis in the trachea of control animals showed intact connective tissue mast cells (CTMC, 20.7±1.0 cells per section), and mucosa mast cells (MMC, 14.9±0.9 cells), whereas a high incidence of mast cell degranulation was seen in the tissue sections prepared from the OVA-challenged rats (CTMC, 21.3±1.5 cells; MMC, 11.2±0.9 cells). This was also associated to a marked infiltration of leukocytes. The central role of the MMC was confirmed by depletion of CTMC with compound 48/80, since no changes in EB extravasation and leukocyte infiltration were seen in this group. In contrast, DEX and NDGA treatment produced a similar effect on EB extravasation, with the following degrees of inhibition: 64±6% and 71±6% for the larynx, 74±7% and 64±3% for the trachea, 76±3% and 82±8% for the external bronchi, and 79±5% and 82±2% for the internal bronchi, for DEX and NDGA, respectively (n=5, $P<0.05$ vs. respective OVA-challenge group). Indomethacin treatment was ineffective on EB extravasation in any of these tissues. Morphological analysis demonstrated that treatment with either DEX or NDGA, but not indomethacin, reduced mast cell degranulation and leukocyte influx.

In conclusion, this study confirms the central role that MMC, but not CTMC play in this model of allergic inflammation in the rat. In addition, we propose a link between the expected inhibition exerted by classical anti-inflammatory drugs and the integrity of mast cells, therefore proposing that an action on this cell type can at least contribute to the overall anti-allergic effect of DEX and NDGA. Finally, these results support a major involvement of leukotriene, rather than prostanoid, metabolism in experimental allergic inflammation.

Galli S. et al., (1999). *Curr. Opin. Immunol.* **11**, 53-59.
This work was supported by FAPESP and CNPq

217P LEUKOTRIENE PRODUCTION IN HUMAN BLOOD IS REDUCED BY NO-ASPIRIN BUT NOT ASPIRIN: COMPARISONS BETWEEN RESPONSES IN HEALTHY VOLUNTEERS AND ASPIRIN-SENSITIVE ASTHMATICS

P. A. Gray, T.D. Warner, I. Vojnovic, [1]A. Parikh, [1]G. Scadding, [2]P. Del Soldato and [3]J.A. Mitchell

Vascular Inflammation, The William Harvey Research Institute, London EC1M 6QB; [1]Royal National Throat, Nose and Ear Hospital, London; [2]NicOx, SophiaAntipolis, France; [3]Department of Critical Care Medicine, the Royal Brompton Hospital, London.

Cyclo-oxygenase-1 activity is highly expressed in human blood, where it is inhibited by a range of nonsteroidal anti-inflammatory drugs (NSAIDs) including aspirin (Warner *et al.*, 1999). Inhibition of cyclo-oxygenase activity in most individuals results in anti-inflammatory and analgesic effects, with a small risk of gastric damage. However, in a sub-population of asthmatics NSAIDs, primarily aspirin, induce symptoms of asthma. This response of aspirin-sensitive asthmatics has been attributed to an over production of leukotriene (LT) C_4, due to an over expression of LTC_4 synthase (Cowburn *et al.*, 1998). However, it is not clear how the production of LTC_4 correlates with inhibition of cyclooxygenase in these patients. Thus, in the current study, we have compared the ability of blood from aspirin-sensitive asthmatics with that of tolerant donors to release LTC_4 and derivatives. Furthermore, we have assessed the effects of aspirin and NO-aspirin (a nitrobutylester derivative) to inhibit cyclo-oxygenase-1 activity and to influence LTC_4 production.

Blood was collected into heparinised tubes and 100µl added to each well of a 96-well plate. Blood was incubated for 1hr at 37°C in the presence of different concentrations of aspirin, NO-aspirin or vehicle (0.1 or 1%DMSO). The blood was then stimulated with the calcium ionophore, A23187 (50µM) for 30 min. The blood was then centrifuged at 3,000rpm for 5min and thromboxane B_2 (TXB_2; index of cyclo-oxygenase-1 activity; Warner *et al.*, 1999) or LTC_4, D_4 and E_4 measured by radioimmunoassay or ELISA respective.

Blood from aspirin tolerant or aspirin-sensitive donors contained low levels of TXB_2 (controls, 3±1; aspirin-sensitive, 4±2ng/ml) or LTs (controls, 3±1; aspirin-sensitive, 3±0 ng/ml). However, when blood was stimulated with A23187 large amounts of TXB_2 (control, 56±10; aspirin-sensitive, 54±20 ng/ml) and LTs (control, 35±6; aspirin-sensitive, 39±4 ng/ml) were released. Pre-treatment of the blood with aspirin prior to A23187, induced concentration-dependent reductions in TXB_2 formation in controls (log IC_{50}, -5.8 ±0.1 M), similar observations (log IC_{50}, 4.9±0.1 M) were observed using NO-aspirin (n=6). Both forms of aspirin also inhibited TXB_2 production by blood from aspirin-sensitive donors (log IC_{50}; aspirin, -5.8±0.08 M; NO-aspirin, -4.5±0.16M), (n=6). LT production in blood from control or aspirin-sensitive patients was not altered by aspirin at concentrations up to 10^{-3}M (control, 77±18% of control; aspirin sensitive, 82±19% of control; n=4). By contrast, treatment with NO-aspirin (10^{-3}M) reduced LT production by blood from aspirin tolerant donors to 16±4% of control (n=4), similar results were observed for aspirin-sensitive donors (reduced to 35±6% of control; n=4).

Thus, we have shown that the capacity of blood from aspirin-sensitive individuals to produce LTs is comparable with that from tolerant individuals. Moreover, we have shown that LT production in not increased when blood is treated with aspirin. This observation suggest that in peripheral cells, at least, there is no evidence for an inhibitory effect of cyclo-oxygenase products on LT formation and that there is no over-expression of LTC_4 synthase in aspirin-sensitive patients. Whether, the over-expression identified in the airways of aspirin-sensitive patients (Cowburn *et al.*, 1998) is exclusive to this tissue remains to be established. The findings here, that NO-aspirin actually reduces the amount of LTs produced in, suggests that it may be a useful therapy for patients sensitive to aspirin.

Cowburn *et al.*, (1998). *J. Clin. Invest.* **101**, 834-846.
Warner *et al.*, (1999). *Proc. Natl. Acad. Sci. USA*, **96**, 7563-8

This work was supported by NicOx, France.

218P HEPATOCYTE GROWTH FACTOR/SCATTER FACTOR (HGF/SF) ACCELERATES ANGIOGENESIS IN SPONGE IMPLANTS IN MICE: MODULATION BY L-NAME AND NS398

Shiladitya Sengupta[1], Ermanno Gherardi[2] and Tai-Ping Fan[1].
Departments of [1]Pharmacology & [2]Oncology, University of Cambridge, Cambridge CB2 1QJ

HGF/SF binds to the Met-receptor and mediates multiple effects at both developmental and adult stages (Trusolino *et al.*, 1998). It has also been implicated as an angiogenic factor in the rabbit cornea (Bussolino *et al.*, 1992). Here, we examined (i) the effects of HGF/SF on neovascularisation in a mouse sponge model, and (ii) the possible involvement of nitric oxide (NO) and cyclooxygenase-2 (COX-2) in the angiogenic signalling pathway of HGF/SF.

Male Balb/c mice (c. 20 g) were anaesthetised with isoflurane and two bilateral polyether sponges were implanted subcutaneously, following creation of two air-pockets on the dorsal subscapular region. Starting 24h post-surgery (day 1), HGF/SF, drugs or vehicle (control) was injected daily into sponges till day 10, according to the protocol in Tables 1 and 2. Angiogenesis into the sponge implants was assessed on days 7, 15 and 28 by a ^{133}Xe clearance technique (Hu *et al.*, 1995). This functional assessment was supported by gross anatomical count of vessels entering the sponges and confirmed histologically by immunostaining the sponge sections for von Willebrand factor.

Data on vessel counts and % ^{133}Xe clearance at the end of 560s following injection into the sponges showed that HGF/SF enhanced angiogenesis on Day 15 as compared with control group (Table 1).

Table 1 Effect of HGF/SF on sponge-induced angiogenesis

Days	Vehicle (0.1%BSA in PBS)		HGF/SF (30ng/sponge/d × 10d)	
	Vessel count	%133Xe clearance	Vessel count	%^{133}Xe clearance
7	4.0±1.2(n=10)	38.9±4.2(n=12)	5.6±1.3(n=12)	45.7±7.2(n=12)
15	16.6±3.6(n=12)	52.8±6.4(n=6)	27.5±4.9(n=11)**	72.1±4.2(n=6)**
28	19.6±4.0(n=10)	82.5±1.6(n=6)	25.9±6.0(n=14)	79.2±3.6(n=6)

** $P < 0.01$ vs vehicle controls

To assess the involvement of NO and COX-2 in HGF/SF-induced angiogenesis, L-NAME (a non-selective NO-synthase inhibitor) or NS398 (a selective COX-2 inhibitor) was co-injected with HGF/SF. Table 2 shows that L-NAME produced a dose-dependent inhibition of HGF/SF-induced angiogenesis, and at 50 ng/sponge/d, it reversed the HGF/SF-mediated increase in vessel count to basal value (control). This was reflected in the findings of the ^{133}Xe clearance experiments and confirmed by histology. However, at this dose, L-NAME had no effect on basal angiogenesis. NS398, at doses 3mg/kg (b.i.d.) and above, also reversed HGF/SF-induced increase in vessel count and ^{133}Xe clearance.

Table 2 Effects of ten daily doses of L-NAME (intrasponge) and NS398 (p.o.) on HGF-induced angiogenesis on Day 15.

Treatment	Vessel Count	%^{133}Xe clearance
HGF (30ng/sponge/d)	27.5±4.9(n=11)	72.1±4.2(n=6)
HGF+L-NAME (5ng/sponge/d)	23.7±3.4(n=12)	58.8±6.7(n=8)*
HGF+L-NAME(50ng/sponge/d)	16.7±4.6(n=13)**	51.0±2.9(n=6)**
L-NAME (50ng/sponge/d)	19.3±3.5(n=10)	56.9±6.0(n=5)
HGF+NS398(3mg/kg/d)	21.8±3.8(n=11)	62.8±10.2(n=6)
HGF+NS398(3mg/kg, b.i.d.)	20.6±1.9(n=5)*	58.3±15.0(n=5)
HGF+NS398(10mg/kg)	19.3±3.5(n=10)*	52.3±7.7(n=5)**

* $P < 0.05$, ** $P < 0.01$ vs HGF-treated group (ANOVA followed by Dunnett post-test)

The present findings suggest that HGF/SF accelerated the process of angiogenesis in the sponge implants but did not alter the maximal angiogenic response. It is also evident that both NO and COX-2 are involved in the signalling pathway by which HGF/SF accelerates angiogenesis *in vivo*.

Bussolino, F. *et al.* (1992) *J. Cell Biol.*, **119**, 629-641.
Hu, D.E. *et al.* (1995) *Lab. Invest.*, **72**, 601-610.
Trusolino, L. *et al.* (1998) *FASEB J.*, **12**, 1267-1280.

SS is a Cambridge Nehru Scholar. We thank the Wellcome Trust and the Medical Research Council for support.

219P THE ROLE OF INTERCELLULAR ADHESION MOLECULE (ICAM) IN NERVE GROWTH FACTOR (NGF)-INDUCED HYPERALGESIA

Foster, P.A., and Brain, S. D. Centre for Cardiovascular Biology and Medicine, King's College London, New Hunts House, Guy's Campus, London SE1 1UL

Nerve growth factor (NGF) is a mediator of hyperalgesia (Lewin and Mendell 1993). Work in this laboratory has focused on the role of neutrophils in thermal hyperalgesia, induced by NGF in the rat paw (Bennett et al., 1998). Hyperalgesia was not observed in the absence of circulating neutrophils. The current study investigates, by use of an anti-ICAM antibody, whether neutrophil-endothelial interactions are necessary for the neutrophil-dependent NGF-induced hyperalgesia.

Male Wistar rats (70-100g) were anaesthetised with halothane (2%) in gas (95% O_2, 5% CO_2) and treated either with anti-ICAM-1 monoclonal antibody mAb, (2mg/kg i.v., Serotec, UK) or anti-rat irrelevant Ab (2mg/kg i.v.) or saline (0.2ml i.v.) 15 min prior to intraplantar injection of NGF (40 pmol 100 μl^{-1}) into a hind paw. Nociceptive threshold testing was performed according to Hargreaves & coworkers (1988) and as modified by Bennett & coworkers (1997). Thermal nociceptive threshold was determined by use of an automatic heat source attached to a timer which records the time of paw withdrawal from the heat source. Measurements, either basal (prior to treatments) or at selected time points after intraplantar injection were the mean of three readings. Statistical analysis was by ANOVA followed by Bonferroni's post test. Results are shown in Table 1.

NGF induced a time-dependent hyperalgesia in saline-treated rats as shown in Table 1. The NGF-induced response was abolished in anti-ICAM-treated rats, but not in anti-rat irrelevant Ab treated rats.

Table 1: Effect of anti-ICAM-1 mAb on NGF (40 pmol)-induced thermal hyperalgesia. Results (mean ± s.e. mean of (n)) are expressed as difference in withdrawal time (sec.) of test compared with contralateral paw *P<0.05 compared to IgG treated rats; †P<0.05 compared to saline treated rats.

Treatment (i.v.)	Saline (0.2ml i.v.)	anti-rat irrelevant Ab (2mg kg^{-1} i.v.)	Anti-ICAM Ab (2mg kg^{-1} i.v.)
Basal	0.55± 0.67 (7)	-0.20± 0.90 (7)	0.47± 0.99 (5)
30 min	-1.78± 0.49 (7)	0.34± 0.57 (7)	0.80± 0.79 (5)
90 min	-3.10± 0.99 (7)	-2.90± 0.88 (7)	0.45± 0.78*†(5)
180 min	-2.65± 0.75(7)	-2.50± 0.35 (7)	0.63± 1.56* (5)
270 min	-4.03± 0.80(7)	-3.13± 0.66 (7)	0.55± 0.87 *†(5)

The results confirm the importance of neutrophils in NGF-induced hyperalgesia. They demonstrate that ICAM-1 plays a significant role in mediating the neutrophil-dependent hyperalgesia. Thus it is suggested that adhesion and possibly emigration of circulating neutrophils is required for NGF-induced hyperalgesia.

P. Foster is supported by a BBSRC/Rhône-Poulenc Rorer studentship.

Bennett, G.S. *et al.*, (1998) *Pain* 77, 315-322
Hargreaves, K. *et al.*, (1988) *Pain* 32, 77-88
Lewin, G.R. & Mendell, L.M. (1993) *Trends. Neurosci.*, 16, 353-359

220P STIMULATED EQUINE EOSINOPHILS PRODUCE IL-1 AND TNFA-LIKE ACTIVITY: EFFECTS ON ENDOTHELIUM-DEPENDENT ADHERENCE

S.R. Bailey, F.M. Cunningham, Department of Veterinary Basic Sciences, The Royal Veterinary College, Hawkshead Campus, Hertfordshire AL9 7TA

Eosinophils accumulate in large numbers in the skin of horses with the allergic skin disease, sweet itch. This study has examined whether equine eosinophils stimulated by mediators that have been implicated in allergic disease may contribute to further cell recruitment by producing cytokines such as IL-1 and TNFα which increase endothelial adhesion molecule expression.

Blood eosinophils (10^6 /ml) obtained from 4 native breed adult ponies were incubated for 18h with rhIL-5 (10 ng/ml), substance P (0.1 mM), histamine (1 μM) or medium. Cell-free medium containing each mediator was used as a control. After centrifugation (900x g, 15 min) supernatants were incubated with equine endothelial monolayers (Bailey and Cunningham, 1999) for a further 18h. The endothelial cells were then washed three times with PBS and adherence of fresh unstimulated eosinophils (10^6 /ml) from the same 4 ponies quantified after 25min as previously described (Foster *et al*, 1997). Cell supernatants were also assayed for IL-1 and TNFα using murine T-lymphocyte (D10) and fibroblast (L929) cell line bioassays, respectively (Landoni *et al*, 1996).

Supernatants from stimulated eosinophils caused significantly greater adherence of eosinophils (expressed as % of the total added) to endothelial cell monolayers than that induced by addition of the mediators alone (2.3±0.2 %, 3.5±0.6 % and 4.2±0.8 % adherence for rhIL-5, substance P and histamine compared with 0.9±0.1 %, 1.8±0.3 % and 1.8±0.1 % adherence for cell-free samples, paired *t*-test P<0.05; supernatants from unstimulated eosinophils caused 1.2±0.2 % adherence compared to 1.1±0.1 % with cell-free medium). Stimulated eosinophils also released both IL-1- and TNFα-like biological activity (Table 1). At similar concentrations the recombinant human (rh) forms of these cytokines increased equine eosinophil adherence (EC_{50} values: 0.3±0.04 ng/ml for rhIL-1 (Bailey and Cunningham, 1999); 1.8±0.6 ng/ml for rhTNFα).

Table 1.

Eosinophils +	medium	rhIL-5 (10ng/ml)	substance P (0.1 mM)	histamine (1 μM)
IL-1 (pg/ml)	37.4 ±11.1	288.5 ±80.0*	179.9 ±38.7*	76.5 ±20.7
TNFα (pg/ml)	34.5 ±4.6	142.7 ±36.7*	149.3 ±57.9*	66.0 ±6.2*

P<0.015 vs unstimulated cell supernatant; 2 way ANOVA followed by a paired t-test, applying Bonferroni's'correction factor.

These data suggest that activated eosinophils may contribute to further cell recruitment in allergic disease by the release of mediators which alter endothelial cell function.

The authors would like to thank the Home of Rest for Horses for their financial support.

Bailey, S., Cunningham, F. (1999) *Brit J Pharmacol* 128, 270P
Foster, A.P., McCabe, P.J., Sanjar, S., Cunningham, F.M. (1997) *Vet Immunol Immunopathol* 56, 205-220
Landoni, M.F., Foot, R., Frean, S., Lees, P. (1996) *Equine Vet J* 28, 468-75

221P INHIBITION OF TUMOUR NECROSIS FACTOR α(TNFα) RELEASE BY DRUGS USED IN THE TREATMENT OF ULCERATIVE COLITIS (UC)

C.J.Whelan and S.Klee. Dept. of Biosciences, University of Hertfordshire, Hatfield, Herts, AL10 9AB U.K,

Ulcerative colitis is frequently treated by aminosalicylates, such as sulphasalazine or by glucocorticoids (Ardizzone and Porro, 1998). Nicotine, administered percutaneously, also has a beneficial effect in the treatment of colitis (Birtwistle, 1996). However, the mechanism of action of underlying the therapeutic effect of these drugs in this disease remains unclear. Recent, clinical studies have shown that humanised antibodies to TNFα are effective in the treatment of UC (Evans, *et.al.*, 1997). Thus, we have investigated whether these drugs, used therapeutically, inhibit the release of TNFα from THP-1 cells *in vitro*.

THP-1 cells were cultured in RPMI 1640 medium containing penicillin (50 U.ml^{-1}), streptomycin (50 μg.ml^{-1}) and amphoteracin B (25μg ml^{-1}). Cells were suspended in fresh medium (1 x 10^6 cells ml^{-1}) and incubated with drugs, or vehicle, for 2h prior to the addition of lipopolysaccharide (LPS; 3μg ml^{-1}). Cell free supernatants, recovered 2h after addition LPS, were assayed for TNFα by ELISA.

Two h after addition of LPS the amount of TNFα released by THP-1 cells had increased significantly (P<0.05; t test) from 310 ± 77.6 (n=6) to 556.7 ± 59.0 (n=6) pg ml^{-1}.

Sulphasalazine (10^{-9} to 10^{-5} M) caused a concentration-related inhibition of LPS-induced TNFα release from THP-1 cells with concentrations greater than 10^{-8} M causing a significant inhibition of TNFα release (P<0.05; ANOVA). At a concentration of 10^{-6} M, sulphasalazine reduced TNFα release from 560.0 ± 5.8 (n=6) to 115.3 ± 8.9 (n=6) pg ml^{-1}, a reduction of 80%.

Dexamethasone (10^{-9} to 10^{-6}M) also caused a concentration-related inhibition of LPS-induced TNFα release from THP-1 cells *in vitro*. Concentrations of dexamethasone greater than 10^{-8} M caused a significant (P<0.05; ANOVA) inhibition of TNFα release with the highest concentration tested (10^{-6} M)causing a reduction from 570.0 ± 122.5 (n=6) to 215.8 ± 194.0 pg ml^{-1} (n=6; 62% reduction). Thus, dexamethasone was approximately 10 times less potent as an inhibitor of TNFα release than sulphasalazine.

Nicotine (10^{-13} to 10^{-10} M) caused a concentration-related reduction in LPS-induced TNFα release from THP-1 cells. Concentrations greater than 10^{-12} M significantly (P<0.05; ANOVA) reduced TNFα release and the highest concentration of nicotine tested (10^{-10} M) reduced release from 586.9± 64.6 (n=11) to 46.7 ± 7.7 pg ml^{-1} (n=6, 93% reduction). Thus nicotine is approximately 5 orders of magnitude more potent than sulphasalazine as an inhibitor of TNFα release.

In conclusion, the data presented show that, of the three drugs tested, nicotine is the most potent inhibitor of TNFα release followed by sulphasalazine and dexamethasone. Since these agents have beneficial effects in UC and antibodies to TNFα are also an effective therapy for UC we suggest that inhibition of the release of TNFα may play a key part in the therapeutic effect of these agents.

Ardizzone, S.; Porro, G.B. (1998). Drugs,**55**, 519-542
Birtwistle, J., (1996); Postgrad. Med. J., **72**, 714-718
Evans, R.C., *et.al.*, (1997); Aliment. Pharmacol. Ther., **11**, 1031-1035

222P SEPHADEX-INDUCED AIRWAY EOSINOPHILIA IN THE RAT: MOLECULAR AND CELLULAR CHARACTERISATION OF THE MODEL

S.L. Underwood. E.-B. Haddad. D. Dabrowski. S. Webber. M. Foster & M. Belvisi. Discovery Biology. Rhône-Poulenc Rorer Ltd. Dagenham. Essex RM10 7XS.

Intratracheal sephadex instillation causes pulmonary eosinophilia in the rat. but the mechanism of action is not well understood. Since T cells are generally held to promote airway eosinophilia in asthma. we have investigated the role of T cells in the sephadex model. We measured sephadex-induced changes in gene expression of putative T cell-derived cytokines and the chemokine eotaxin in rat lung. and the effects on eosinophilia of prior T cell depletion and treatment with T cell-suppressing drugs.

Pulmonary eosinophilia was induced in rats (male. Sprague-Dawley. 300-350g) by intratracheal sephadex (5 mg/kg in saline. 1 ml/kg). Rats were killed with pentobarbitone overdose (200 mg/kg. i.p.). Cells were then recovered from lung tissue by enzymatic disaggregation (incubation with collagenase 1 mg/ml and DNase 25 μg/ml. 37°C. 1h). Eosinophils (Wright/Giemsa-stained) were counted by light microscopy. T cells (CD2$^+$ cells) were counted by flow cytometry. Lung tissue cytokine mRNA was amplified by RT-PCR. The products were separated by agarose gel electrophoresis. The intensities of the signals were quantified by laser densitometry using ImageMaster™ software (Pharmacia) and expressed as a ratio to the housekeeping gene GAPDH used as an internal standard. For all data. group results are presented as mean ± s.e.m. (n = 6-8) with statistical significance of differences determined using the Kruskal-Wallis test (P < 0.05 accepted as significant).

Inflammation was assessed 2. 4. 6. 12. 24. 48 and 72 h post-sephadex and compared to that in vehicle-treated controls. Levels of IL-4. IL-5. IL-13 and eotaxin mRNA were each significantly increased by sephadex. Peak changes were: IL-4 from 0.39±0.28 to 3.30±0.52 after 12 h; IL-5 from 0.65±0.27 to 5.28±0.63 after 24 h; IL-13 from 0.06±0.02 to 0.17±0.03 after 24 h; eotaxin from 4.47±0.23 to 8.13±1.29 after 24 h. The eosinophil number was significantly increased after 12 h (peak increase from 0.2±0.1 to 2.6±0.3 x10^3/mg after 48 h) and remained significantly elevated at 72 h.

T cells were partially depleted (by 66% from 1.6±0.3 x10^3/mg) with an antibody against the ab-T cell receptor (R73. 1 mg/kg. i.v., 24 h before sephadex). Gene expression for IL-4 and eosinophilia measured 24 h after sephadex were each significantly suppressed by this treatment (Table 1). Cyclosporin A (50 mg/kg. p.o.) or budesonide (30 mg/kg. p.o.) given 24 h and 2 h before sephadex significantly suppressed gene expression for IL-4. IL-5 and IL-13 and eosinophilia measured 24 h after sephadex (Table 2).

Our data suggests that T cells play a role in orchestrating sephadex-induced pulmonary eosinophilia in the rat. This model may be useful for rapid evaluation of anti-asthma drugs that affect T cell function.

Table 1. Effects of T cell depletion on sephadex-induced pulmonary inflammation in the rat.

Treatment	RT-PCR product ratio		Eosinophils
	IL-4	IL-5	(x10^3/mg)
Saline	0.15±0.09	0.71±0.13	0.2±0.1
Sephadex	0.76±0.20 †	1.13±0.22	1.7±0.3 †
Sephadex + R73 antibody	0.10±0.06 *	0.77±0.10	0.8±0.1 *

Table 2. Effects of cyclosporin A and budesonide on sephadex-induced pulmonary inflammation in the rat.

Treatment	RT-PCR product ratio			Eosinophils
	IL-4	IL-5	IL-13	(x10^3/mg)
Saline	0.13±0.05	0.18±0.05	0.22±0.29	0.2±0.1
Sephadex	0.75±0.35 †	0.72±0.15 †	1.10±0.29 †	2.2±0.3 †
Sephadex + cyclosporin A	0.24±0.10 *	0.37±0.06 *	0.17±0.05 *	0.1±0.0 *
Sephadex + budesonide	0.14±0.13 *	0.14±0.05 *	0.11±0.07 *	0.3±0.1 *

† P < 0.05 compared with saline-treated group; * P < 0.05 compared with sephadex-treated group.

223P MEDIATOR INVOLVEMENT IN ANTIGEN-INDUCED MICROVASCULAR LEAKAGE INTO THE AIRWAYS AND BRONCHOSPASM IN OVALBUMIN SENSITISED BROWN NORWAY RATS

D.J. Hele, M.A. Birrell, S.E. Webber, M. Foster and M.G. Belvisi. Rhône-Poulenc Rorer Ltd, Pharmacology Department, Dagenham Research Centre, Rainham Road South, Dagenham, Essex.

The leakage of plasma proteins from the microvasculature into airways tissue and the airway lumen and bronchospasm are seen as important consequences of allergic airways inflammation. Intravenously administered ovalbumin (OA) in the antigen sensitised Brown Norway (BN) rat causes bronchospasm (Nagase *et al*, 1996) and microvascular leakage (MVL) into the airways (Taylor *et al*, 1997). In these studies we have attempted to elucidate which mediators drive the responses to antigen by the use of a histamine H1, a 5HT and a cys-leukotriene receptor antagonist (mepyramine, methysergide and montelukast respectively).

Male Brown Norway (BN) rats (250-350g) were sensitised on days 0, 12 and 21 with antigen (OA, 100 µg i.p., administered with aluminium hydroxide adjuvant, 100 mg, i.p.). From day 28 animals received mepyramine (1 or 3 mg kg^{-1} i.v.) or methysergide (0.1 or 0.3 mg kg^{-1} i.v.) 5 min. prior to OA challenge (1 mg kg^{-1} i.v.) or montelukast (30 mg kg^{-1} p.o.) 90 min. prior to OA challenge or relevant vehicle (saline or 0.5% methyl cellulose plus 0.2% Tween 80). For the combination studies all three compounds were given at doses shown to be effective against MVL and bronchospasm and at the timings shown above. In the MVL studies animals received Evans blue dye (20 mg kg^{-1} i.v) 1 min prior to OA challenge (1 mg kg^{-1},i.v.). All i.v. administrations were made via the tail vein under brief isofluorane anaesthesia. Animals were killed by pentobarbitone (200 mg kg^{-1} i.p.) 15 min after OA administration. The lungs were perfused with saline until free of blood, dissected free and the parenchyma scraped from the intra-pulmonary airways (IPA). The IPA and bronchi were placed in formamide at 37°C for 16h to extract Evans blue dye. The absorbances of the resulting extracts were determined against standard concentrations of Evans blue at 620nm. Results are expressed as concentration of Evans Blue (ng mg^{-1} of tissue). In the bronchospasm studies changes in airways resistance (measured on the Buxco LS20 system), induced by OA challenge (1 mg i.v.), were in anaesthetised (pentobarbitone, 105 mg kg^{-1} i.p.), artificially respired animals. The doses of antagonist used in these studies have been shown to selectively inhibit their relevant agonist (histamine, 5HT or leukotriene D4) in preliminary experiments. Statistical analysis was by one way analysis of variance with a correction for multiple comparisons using Dunnett's critical values.

These studies shows that in the sensitised BN rat OA challenge causes MVL into the trachea, bronchi and IPA (5.32 ± 0.53 increased to 36.14 ± 5.38, 9.45 ± 0.55 increased to 41.16 ± 5.43 and 5.66 ± 0.83 increased to 45.64±4.57 ng mg^{-1} of tissue respectively, $p < 0.001$) and an increase in airways resistance (0.419 ± 0.059 cmH_2O ml^{-1} s^{-1}, $p < 0.01$). In the MVL study, mepyramine (1 mg kg^{-1} i.v.) had no significant effect, methysergide (0.1 mg kg^{-1} i.v.) reduced leakage in the trachea (36.14 ± 5.38 ng mg^{-1} of tissue reduced to 22.25 ± 1.91 $p < 0.05$), and montelukast (30 mg kg^{-1} p.o.) reduced leakage to basal levels in all three airway regions ($p < 0.001$). A combination of all three antagonists also reduced leakage to basal levels. In the airways mechanics studies mepyramine (3 mg kg^{-1} i.v.) had no significant effect, methysergide (0.3 mg kg^{-1} i.v.) produced 58% inhibition compared to vehicle (0.176 ± 0.058 cmH_2O ml^{-1} s^{-1}) and montelukast (30 mg kg^{-1} p.o.) caused 50% inhibition compared to vehicle (0.211 ± 0.088 cmH_2O ml^{-1} s^{-1}), both of which did not reach statistical significance. A combination of all three caused 91% inhibition compared to vehicle (0.033 ± 0.019 cmH_2O ml^{-1} s^{-1}, $p < 0.01$).

Table 1 The effect of mepyramine, methysergide and montelukast on OA-induced microvascular leakage and bronchospasm in sensitised BN rat airways

Drug	Dose mg kg^{-1}	Bronchospasm (% change)	Microvascular leakage (% change)
Mepyramine	1		Trachea -26
			Bronchi -21
			IPA -16
	3	0	
Methysergide	0.1		Trachea -38**
			Bronchi -19
			IPA -10
	0.3	58	
Montelukast	30	50	Trachea -78***
			Bronchi -70***
			IPA -72***
Combination	-	91**	Trachea -80***
			Bronchi -72***
			IPA -72***

* $p < 0.05$, ** $p < 0.01$, *** $p < 0.001$, $n = 4$.

These studies show that antigen induced MVL and bronchospasm appear to be mediated by 5-HT and cys-leukotriene-1 receptors. Antigen-induced bronchospasm appears to equally involve 5-HT and cys-leukotriene-1 receptors whereas antigen-induced MVL appears to be predominantly mediated by cys-leukotriene-1 receptors.

Nagase, T., Dallaire, M.J. and Ludwig M.S. (1996) *J. Appl. Physiol.*, 80/2, 583-590.
Taylor, B.M., Kolbasa, K.P., Chin J.E., *et al* (1997) *Am. J. Respir. Cell. Mol. Biol.* 17/6, 757-766.

224P EFFECT OF THE p38 KINASE INHIBITOR, SB203580, ON SEPHADEX-INDUCED AIRWAY INFLAMMATION IN THE RAT

M.A. Birrell, C.H. Battram K. McCluskie. M. Pecoraro, S.E. Webber. M.L. Foster and M.G. Belvisi. Pharmacology Department. Rhone-Poulenc Rorer Research and Development. Dagenham research Centre. Dagenham. Essex RM10 7XS.

We have previously shown that a p38 inhibitor. SB 203580. (Badger *et al*., 1996) blocks LPS-induced systemic TNFα release in rats (Haddad *et al*., 1999). Increased levels of TNFα in the airways following sephadex treatment have been suggested to play a causative role in sephadex-induced lung pathology (Gater and Renzetti. 1998). In this study we have examined the effect of SB 203580 on sephadex-induced airway inflammation in the rat.

Male Sprague Dawley rats (400g, n = 8) were orally dosed with vehicle (0.5% methyl cellulose and 0.2% tween 80. 2 ml kg^{-1}) or compound (3 - 100 mg kg^{-1}) 1 hour prior to and 5 hours after saline (1 ml kg^{-1}. i.t.) or sephadex (5 mg kg^{-1}). Dexamethasone (1 mg kg^{-1}) was included as a positive control and was orally dosed 24 and 2 hours prior to i.t challenge. Saline or sephadex instillation was performed while the animals were anaesthetised with halothane (4% in oxygen for 4 minutes). Twenty four hours after challenge the animals were culled with an overdose of pentobarbitone (200 mg kg^{-1}. i.p.). the lungs removed. cleaned and weighed. The lung was perfused with ice cold RPMI to remove any blood and then finely chopped. A 300 mg aliquot of lung was weighed and kept at 4°C. the remaining lung flash frozen in liquid nitrogen and stored at -80°C. The amount and type of white blood cell in the lung tissue was determined by incubating the aliquot of lung with 10 ml of RPMI containing collagenase 1 mg ml^{-1} and DNase 25 µg ml^{-1} in a shaking water bath at 37°C for 1 hour. The resulting mixture was then passed through a 70 µm cell sieve and then spun at 1900 g for 10 minutes at 4°C. The supernatant was discarded. 10 ml of RPMI added and the pellet re-suspended. The pellet washing step is carried out twice to remove the collagenase and DNase. After the final wash the pellet was re-suspended in 1 ml of RPMI. Total white blood cell counts were determined on an automated cell counter. the Argos Cobas. Differentiating the types of white blood cells was performed by examination. under light microscopy. of the slide preparations made from the samples.

TNFα and IL-1β levels in the lung tissue were determined using rat specific ELISA's (TNFα kits from R&D sytems and IL-1β kits from Lifescreen).

Statistical analysis was by one way analysis of variance with a correction for multiple comparisons using Dunnett's critical values. Values are expressed as mean ± s. e. mean.

Lung wet weight was significantly increased from 0.473 ± 0.056 to 0.571 ± 0.084 wet weight (g) body weight (g) $^{-1}$ (21 %. $p<0.01$) by sephadex treatment. this was accompanied by a significant increase in lung tissue TNFα levels from 150.6 ± 27.2 to 1104.7 ± 243.9 pg g of lung tissue $^{-1}$ (733 %. $p<0.01$) and an increase in eosinophils from 0.795 ± 0.264 to 2.395 ± 0.777 $*10^3$ cell g of lung tissue $^{-1}$ (249 %) and macrophages from 5.232 ± 0.582 to 10.548 ± 1.903 $*10^3$ cell g of lung tissue $^{-1}$ (167 %) which failed to reach significance in this study. The positive standard. dexamethasone. significantly reduced lung oedema and TNFα levels (from 0.571 ± 0.084 to 0.389 ± 0.007 wet weight (g) body weight (g) $^{-1}$ $P<0.01$ and from 1104.7 ± 243.9 to 207.95 ± 20.91 pg g of lung tissue $^{-1}$, $P<0.01$; respectively). SB 203580 inhibited the sephadex-induced oedema in a dose-dependent manner which reached statistical significance at 30 and 100 mg kg^{-1} (from 0.571 ± 0.084 to 0.497 ± 0.012 or 0.476 ± 0.020 wet weight (g) body weight (g) $^{-1}$ $P<0.01$. repectively). The ED_{50} value (18 mg kg^{-1}) achieved in this model compares well with that obtained in models of arthritis where this effect is attributed to inhibition of p38 kinase (Badger *et al*., 1996). In contrast. SB 203580 had no impact on inflammatory cell infiltration and TNFα production in the lungs of sephadex-treated animals. These data are in agreement with studies suggesting that SB 203580 failed to impact on TNFα levels and the associated inflammatory cell recruitment into the BAL fluid following aerosolised LPS (Haddad *et al*., 1999). These data suggest that the increase in TNFα and lung oedema are separate processes which both contribute to sephadex pathology and that the development of lung oedema is not dependent on the release of this cytokine.

In conclusion. p38 kinase is involved in the generation of lung oedema following sephadex. Compounds of this class may be of use in pulmonary pathologies in which lung oedema is a feature.

Badger. A.M., Bradbeer. J.N., Volta. B. *et al*., (1996) J. Pharmacol. Exp. Ther., 279:1453-1461.
Gater. P.R. and Renzetti. L.M.. (1998) *Agents Actions Suppl.*, 49. 67-71.
Haddad. E-B.. Birrell. M.A.. Ling. A., *et al*., (1999) *Am. J. Respir. Crit. Care Med*., 159:A331.

225P THE ROLE OF INDUCIBLE NITRIC OXIDE SYNTHASE IN SEPHADEX-INDUCED AIRWAY INFLAMMATION IN THE RAT

M.A. Birrell. C.H. Battram. EB. Haddad. K. McCluskie. G.A. Bohme. S.E. Webber. M.L. Foster and M.G. Belvisi. Pharmacology Department. Rhone-Poulenc Rorer Research and Development. Dagenham Research Centre. Dagenham. Essex. RM10 7XS.

Excessive local production of nitric oxide (NO) due to the expression/activation of inducible NOS (iNOS) may play a role in airway inflammatory diseases such as asthma (Barnes & Belvisi. 1993). Until recently there were no selective iNOS inhibitors available to investigate this hypothesis. In this study we examined the effects of the selective iNOS inhibitor. 1400W (Garvey *et al.*. 1996) compared with that of a non-selective inhibitor L-NAME. on sephadex-induced airway inflammation.

Male Sprague Dawley rats (400g. n = 8) were dosed i.p. with vehicle (saline. 2 ml kg^{-1}) or compound (3 - 100 mg kg^{-1}) 2 hours prior to and 4 and 12 hours (Laszlo & Whittle. 1997) after saline (1 ml kg^{-1}. i.t.) or sephadex (5 mg kg^{-1}) treatment. Dexamethasone (0.3 mg kg^{-1}) was included as a positive control and was orally dosed 24 and 2 hours prior to i.t challenge. Saline or sephadex instillation was performed while the animals were anaesthetised with halothane (4% in oxygen for 4 minutes). Twenty four hours after challenge the animals were culled with an overdose of pentobarbitone (200 mg kg^{-1}. i.p.). the lungs removed. cleaned and weighed. The lung was perfused with ice cold RPMI to remove any blood and then finely chopped. A 300 mg aliquot was weighed and kept at 4°C. the remaining lung flash frozen in liquid nitrogen and stored at -80°C for cytokine protein measurement and analysis for iNOS mRNA expression by RT-PCR. The amount and type of white blood cell (WBC) in the lung tissue was determined using a method described by Underwood (1997). TNFα and IL-1β levels in the lung tissue were determined using rat specific ELISA (TNFα kits from R&D sytems and IL-1β kits from Lifescreen). Statistical analysis was by one way analysis of variance with a correction for multiple comparisons using Dunnett's critical values. Values are expressed as mean ± s. e. mean.

Lung wet weight was significantly increased from 0.437 ± 0.016 to 0.547 ± 0.017 wet weight (g) body weight (g) $^{-1}$(25%, $p<0.01$) by sephadex treatment. this was accompanied by a significant increase in lung tissue TNFα levels from 80.3 ± 8.3 to 1868.8 ± 282.0 pg g of lung $tissue^{-1}$ ($p<0.01$). IL-1β levels from 3284.7 ± 400.5 to 5951.2 ± 445.3 pg g of lung $tissue^{-1}$ ($p<0.01$) and eosinophil cell numbers from 0.209 ± 0.096 to 1.069 ± 0.119 * 10^3 cell mg of lung tissue $^{-1}$ ($p<0.01$). The positive standard. dexamethasone. significantly reduced lung oedema. eosinophilia and TNFα levels when compared to vehicle (to 0.382 ± 0.010 lung wet weight (g) body weight (g) $^{-1}$. $p<0.01$: to 0.188 ± 0.086 * 10^3 cell mg of lung tissue $^{-1}$. $p<0.01$ and to 149.4 ± 12.4 pg g of lung $tissue^{-1}$. $p<0.01$ respectively). L-NAME inhibited the sephadex-induced oedema in a dose-dependent manner which reached statistical significance at 30 and 100 mg kg^{-1} (figure 1, ED_{50} = 21 mg kg^{-1}). In a previous study D-NAME. the inactive isomer,

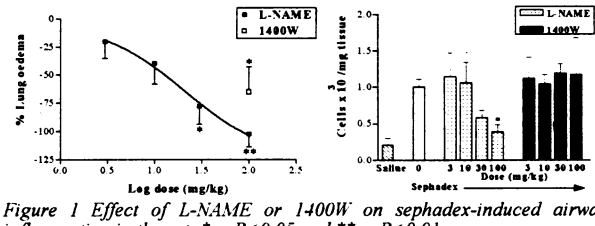

*Figure 1 Effect of L-NAME or 1400W on sephadex-induced airway inflammation in the rat. * = P<0.05 and ** = P<0.01.*

had no effect in this model when tested at the same doses. In contrast. the selective iNOS inhibitor. 1400W. only impacted on lung oedema at 100 mg kg^{-1} (reduced to 0.476 ± 0.025 lung wet weight (g) body weight (g) $^{-1}$. $p<0.05$). L-NAME also inhibited the sephadex-induced eosinophilia in a dose-dependent manner which reached statistical significance at 100 mg kg^{-1} (figure 1, ED_{50} = 24 mg kg^{-1}), whereas 1400W had no effect at the doses tested. L-NAME. and to a lesser extent 1400W. reduced TNFα levels in the lung tissue at the top dose only (to 300.7 ± 90.1 and 904.1 ± 359.7 pg g of lung $tissue^{-1}$; $p<0.01$. $p<0.05$. respectively). iNOS gene expression. as measured by RT-PCR. was not induced in the lung after sephadex treatment at all time points investigated whereas LPS-treated rats (0.3 mg ml^{-1} w v^{-1}. aerosolised for 30 minutes and lungs sampled 4 hours after) showed a marked induction of iNOS mRNA. The absence of iNOS mRNA after sephadex treatment and the reduced activity of 1400W compared to L-NAME does not highlight a role for iNOS activation in this model.

In conclusion. these data suggest that activation of the constitutive isoforms of NOS play a role in sephadex induced cellular inflammation and lung oedema.

Barnes. P.J. and Belvisi. M.G. (1993) *Thorax.*. 48. 1034-1043.
Garvey. E.P.. Oplinger. J.A.. Furfine. E.S.. *et al* (1996) *J. Bio. Chem.*, 272. 8. 4959-4963.
Laszlo F. and Whittle B. J. (1997) Eur. J. Pharm.. 334. 99-102.
Underwood. S.L.. Raeburn. D.. Lawrence. C.. et al (1997) Br. J. Pharm.. 122. 439-446.

226P A NATURAL AGONIST OF THE MC3 RECEPTOR INHIBITS ACUTE INFLAMMATION

Stephen J Getting, Roderick J Flower, & Mauro Perretti
Department of Biochemical Pharmacology, St. Bartholomew's and the Royal London SMD, Charterhouse square, London, EC1M 6 BQ.

We have recently reported that a fragment of adrenocorticotropic hormone (ACTH), ACTH4-10 (MEHFRWG), exhibits anti-inflammatory properties *via* activation of the melanocortin type 3 receptor (MC3-R) expressed on mouse peritoneal macrophages (MØ) (Getting *et al.*, 1999). In this study we extend this finding using selective depletion of resident cells as well as selective agonists (γ_2-melanotropic stimulating hormone, γ_2-MSH, and MTII) and an antagonist (SHU9119) at this receptor subtype (Fan *et al.*, 1997).

Male Swiss Albino mice (28-32g) were depleted of resident mast cells or macrophages using a recently published protocol (Ajuebor *et al.*, 1999). Briefly, mast cells (MCS) were reduced by ≥90% by i.p. administration of 10 µg of compound 48/80 (given 72h prior to experiment) whereas the number of resident macrophages (MØ) was reduced by ≥85% by i.p. administration of 100 µl liposome preparations containing clodronate for three consecutive days. On the day of the experiment, mice received s.c. ACTH4-10 (104 nmol) or PBS (100 µl), 30 min prior to i.p. injection of 3 mg monosodium urate (MSU) crystals. In other cases mice were pre-treated with γ_2-MSH (104 nmol) or MTII (1-27.9 nmol). Some other animals were also given the antagonist SHU9119 (9nmol i.p.). Cell influx into the peritoneal cavities was measured 6 h later (Getting *et al.*, 1999). The CXC chemokine KC was measured in cell-free lavage fluids by a specific ELISA (R&D Systems, Abingdon, UK). *In vitro*, MØ were purified by a 2 h adherence at 37°C, prior to incubation with ACTH4-10 (104 µM), MTII (9.3 µM) or γ_2-MSH (104 µM) in the presence or absence of 9 µM SHU9119. After 30 min, 1 mg/ml of MSU crystals were added and KC release measured 2 h later in cell free supernatants by ELISA. The effect of these peptides on MØ phagocytosis was also determined using a 15 min incubation period at 37°C with similar concentrations to those listed above, and addition of RED Oxyburst™ (Molecular Probes, Eugene, OR). Phagocytosis was monitored in real time by flow cytometry. Values were analysed by ANOVA and Bonferroni test with *P<0.05 taken as significant.

Depletion of resident MCS and MØ led to a 19% and 37% reduction, respectively, in the number of emigrating neutrophils compared to control mice (13.5 ± 0.70 $x10^6$, n=6). KC levels in cell free supernatants was also reduced in MCS (30%) and MØ (41%) depleted animals compared to control values (1163 ± 99 pg per cavity, n=6). In animals pre-treated with ACTH4-10 (104 nmol) a significant reduction in cell migration (6.25 ± 0.44 $x10^6$ cells per cavity, *P<0.05, n=6) was seen compared to control mice, with a similar inhibition (52%) being observed in MCS-depleted mice *P<0.05, n=6). In contrast, no signifcant effect of ACTH4-10 was seen in MØ-depleted mice (n=6). With respect to KC release, ACTH4-10 inhibited KC release by 43% (668 ± 134 pg per mouse, *P<0.05, n=6) in control mice, with 20% reduction being observed in MCS-depleted mice respectively. No effect was observed in MØ depleted animals. The anti-inflammatory action of ACTH4-10 was mimicked by the more selective agonists. MSU crystals-induced cell accumulation (6.54 ± 0.91 $x10^6$ cells, n=10) was dose-dependently inhibited by ACTH4-10 and MTII with approximate ED50s of 104 and 9.3 nmol respectively. γ_2-MSH was equipotent with ACTH4-10 at the dose tested of 104 nmol (42% of inhibition, n=8, *P<0.05). All these effects were blocked in the presence of SHU9119. A similar pattern was obtained with respect to KC levels in the 6 h exudates. *In vitro*, all peptides inhibited MØ phagocytosis in a concentration-dependent manner, with approximate IC40 of 104 µM for both ACTH4-10 and γ_2-MSH. A maximal inhibition of 20% was obtained for MTII. The inhibitory effect displayed by these peptides on MØ phagocytosis was also blocked by co-addition of 9 µM SHU9119. MSU stimulation of MØ primary cultures produced an intense release of KC as measured after 2 h (6.10 ± 1.20 ng/ml^{-1}). Addition of 104 µM ACTH4-10 or γ_2-MSH, or MTII (9.3 µM) produced the following inhibitions: 52%, 32% and 63%, respectively (n=4; *P<0.05 in all cases). This inhibitory effect on adherent MØ was again absent in cells co-incubated with the MC3/4 antagonist SHU9119 (9 µM).

In conclusion, these results show that in the experimental inflammation induced by MSU crystals, MC3-R and the resident peritoneal MØ are the target sites for the anti-inflammatory action of melanocortin peptide agonists.

Ajuebor, M.N. *et al.* (1999) *J.Immunol.* **162**:1685-1691.
Fan, W.B. *et al.* (1997). *Nature* **385**: 165-168.
Getting, S.J. *et al.* (1999). *J. Immunol.* **162**: 7446-7453.
This work was supported by the Arthritis Research Campaign (grant P0537). MP is an ARC Post-doctoral fellow whereas RJF is a Wellcome Principal Research Fellow.

227P THE EFFECT OF THE SELENO-ORGANIC COMPOUND EBSELEN ON LPS-INDUCED AIRWAY INFLAMMATION

K. McCluskie, E-B. Haddad, M.A. Birrell, S.E. Webber, M. Foster, M.G. Belvisi. Pharmacology Department, Rhone-Poulenc Rorer, Dagenham Research Centre, Dagenham, Essex RM10 7XS.

Ebselen is a seleno-organic compound which possesses anti-oxidant and anti-inflammatory properties (Gao *et al*, 1993). Its anti-inflammatory activities include inhibition of human polymorphonuclear leukocyte (PMNL) transendothelial migration *in vitro*, PMNL migration to arthritic joints and dermal inflammatory reactions in rats (Belvisi *et al*, 1998). The aim of this study was to determine the activity of ebselen in a model of lipopolysaccharide (LPS)-induced airway inflammation in the rat.

Male Wistar rats (250g) were dosed with vehicle (25% dimethylsulfoxide with 75% polyethylene glycol or 0.5% carboxymethylcellulose with 0.2% Tween 80, 0.5 ml kg^{-1}, i.p.), ebselen (1-100 mg kg^{-1}, i.p.) or dexamethasone (1 mg kg^{-1}, p.o.) which was used as a positive control. Doses were administered 2 hours prior and 1 hour post exposure to aerosolised saline or LPS (0.3 mg ml^{-1} w/v for 30 minutes). 4 hours after LPS challenge animals were killed by overdose of pentobarbitone (200 mg kg^{-1} i.p.) and bronchoalveolar lavage (BAL) was performed. Inflammatory cell recruitment was evaluated by differential counting of cells by light microscopy of cytocentrifuge preparations stained with Wright-Giemsa stain. IL-1β levels in the BAL were assessed by rat specific ELISA. Myeloperoxidase (MPO) activity, which is a measure of neutrophil degranulation was determined in cell-free BAL (Bradley *et al*, 1982). Lungs were removed and flash frozen prior to Northern blot analysis of gene expression of the CXC chemokines, CINC and MIP-2. The intensities of the signals were quantified by laser densitometry using ImageMaster™ software (Pharmacia) and expressed as a ratio of the housekeeping gene GAPDH which was used as an internal standard to account for differences in loading or transfer efficiencies of the mRNA (n= 3-4). Statistical analysis was carried out by Kruskal-Wallis with a correction for multiple comparisons using Dunnett's critical values.

LPS inhalation caused a significant increase in total white cell numbers, eosinophils and neutrophils in BAL (0.17 ± 0.01 increased to 0.80 ± 0.08, 0 to 0.01 ± 0.01 and 0.005 ± 0.002 to 0.72 ± 0.08 cells 10^6 ml^{-1} respectively, $p<0.01$) (figure A). Ebselen (100 mg kg^{-1}) and the synthetic steroid, dexamethasone, reduced neutrophil influx to a similar level (0.72 ± 0.08 reduced to 0.35 ± 0.08 and 0.95 ± 0.10 reduced to 0.29 ± 0.03 cells 10^6 ml^{-1} respectively, $p<0.001$). A significant increase in MPO activity was also observed in cell-free BAL ($1.25 \pm 0.45 \times 10^{-3}$ increased to $9.4 \pm 0.8 \times 10^{-3}$ units l^{-1}, $p<0.01$). This was significantly inhibited by ebselen at 10, 30 and 100 mg kg^{-1} by 67, 80 and 53% respectively ($9.4 \pm 0.8 \times 10^{-3}$ reduced to $3.12 \pm 0.58 \times 10^{-3}$, $1.9 \pm 1.1 \times 10^{-3}$ and $4.4 \pm 1.2 \times 10^{-3}$ units l^{-1} respectively $p<0.05$). Dexamethasone produced a 45% inhibition in MPO activity ($12 \pm 1.7 \times 10^{-3}$ reduced to $6.6 \pm 1.0 \times 10^{-3}$ units l^{-1}) which did not reach statistical significance.

The significant increase in BAL IL-1β levels (below detection increased to 13.29 ± 3.3 pg ml^{-1}) was significantly inhibited by ebselen at 10, 30 and 100 mg kg^{-1} (figure B)). Ebselen at 100 mg kg^{-1} and dexamethasone at 1 mg kg^{-1} completely abrogated IL-1β levels (13.29 ± 3.3 pg ml^{-1} reduced to below detection for both).

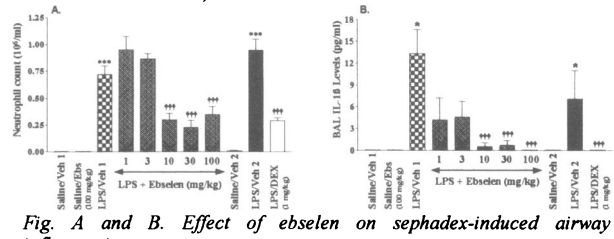

Fig. A and B. Effect of ebselen on sephadex-induced airway inflammation.
(* indicates significant difference from saline control group at *p<0.05, ***p<0.001, ††† indicates significant difference from LPS/vehicle group (p<0.001), n=8) Values are expressed as mean ± s. e. mean.

Following LPS inhalation there was an induction of CINC and MIP-2 mRNA (change in ratio of 0.68 ± 0.12 and 1.17 ± 0.15 respectively). Ebselen or dexamethasone did not affect the level of expression of either transcript in the lung although there was a trend towards a decrease in CINC gene expression following dexamethasone treatment (0.31 ± 0.04). The effect of ebselen and dexamethasone on neutrophils does not appear to be associated with an inhibition of the mRNA of the neutrophil chemoattractants CINC and MIP-2. This suggests that additional mechanisms may be responsible for neutrophil influx. The inhibition of neutrophilic inflammation by ebselen is not achieved through inhibition of the CXC chemokines but may be due to an inhibition of the potent neutrophil recruiting mediator, IL-1_β (Hybertson,*et al*, 1997).

Belvisi, M.G., Haddad, E-B., *et al.* (1998) *Naunyn. Schmiedeberg's. Arch. Pharmacol.*, 358 (Suppl 1), R329
Bradley, P.P., Priebat, D.A., *et al.* (1982) *J. Invest. Dermatol.*, 78(3), 206-209.
Gao, J.X., Isselkutz, A.C., (1993) *Int. J. Immunopharmacol.* 15, 793-802.
Hybertson, B. Jepson, E.K., *et al.* (1997) *Am. J. Respir. Crit. Care. Med.*, 155, 1972-76.

228P THE ROLE OF NO ON CHANGES IN AIRWAY REACTIVITY INDUCED BY EXPOSURE OF GUINEA-PIGS TO INHALED LPS

T.J. Toward & K.J. Broadley, Pharmacology Division, Welsh School of Pharmacy, Cardiff University, Cathays Park, Cardiff CF10 3XF.

We have demonstrated that guinea-pigs exposed to aerosolised lipopolysaccharide (LPS) produce features of chronic obstructive pulmonary disease (COPD) and asthma (Toward & Broadley, 1999), namely neutrophil and macrophage airways infiltration (COPD) and airway hyperreactivity (AHR) to histamine (Hist) (asthma and COPD). After exposure to antigen, asthmatics (Alving *et al.*, 1993) and atopic guinea-pigs (Iijima *et al.*, 1998) exhale increased nitric oxide (NO) levels. Schuiling *et al.* (1998) suggested, that in atopic guinea-pigs, over-production of NO benefits recovery from AHR. We therefore studied the LPS-induced changes in airway reactivity and NO.

Specific airway conductance (sGaw) was measured in groups (n=6) of conscious Dunkin-Hartley guinea-pigs (male 300-350g) by whole-body plethysmography (Griffiths-Johnson *et al.*, 1988). Baseline sGaw values were obtained and 30min later they received a nose-only exposure to a threshold dose of nebulised (0.2ml.min^{-1}) Hist (1mM, 20s) and sGaw was recorded at 0, 5 and 10min afterwards. 24h later, the animals were box-exposed (60min), to either nebulised LPS (30μ $g.ml^{-1}$) or vehicle (0.9% LPS-free saline) and airway reactivity to Hist was re-assessed at 0.5, 1, 2, 4, or 24h post exposure. A bronchoconstrictor dose of Hist (3mM, 20s) was used pre and 48h post exposure to test for airway hyporeactivity (AHOR). In other animals, LPS or vehicle were followed at 2h by nebulised NO synthase inhibitor, N^G-nitro-L-arginine methyl ester (L-NAME: box exposed, 15min, 1.2 or 12mM). Airway reactivity to Hist (1mM, 20s) was re-assessed a further 2h later. Animals were then overdosed with pentobarbitone sodium (0.6mg.$100g^{-1}$, i.p.), the lungs lavaged (1% EDTA, 1ml.$100g^{-1}$, twice) and the bronchoalveolar fluid (BALF) centrifuged (1000r.p.m., 6 min). Supernatant NO metabolites (NO_2 and NO_3) were assayed based on the spectrophotometric Griess reaction (NO_2) and reduction (*Aspergillus* nitrate reductase) of NO_3 to NO_2 (Grisham *et al.*, 1996).

Hist produced an increased bronchoconstriction (-26.3±7.9 peak % change from baseline sGaw) 1h after LPS exposure, compared with pre exposure (+16.1±5%), ie AHR. There was AHOR to Hist at 48h (pre: -56.8±5.1, post:-35.6±7.7%). Combined NO metabolites in BALF (per 100μl) increased ($p<0.01$) 1h after vehicle exposure (74.2±5.7μM, naive: 52.7±5.9μM), but were reduced 1h (25.5±5.1μM, $p<0.01$) and 2h (16.8±14.4μM, $p<0.01$) after LPS. 4h after LPS, levels were elevated (74.4±3.2μM) compared to naïve ($p<0.01$), but by 24h levels (51.6±1.2μM) were equivalent ($p>0.05$). 48h later, NO levels (94.8±9.3μM) were raised compared to naïve ($p<0.001$). Airway reactivity to Hist was slightly increased ($p>0.05$) 4h after vehicle exposure followed by L-NAME. However, there was significant AHR ($p<0.01$) 4h after LPS exposure followed by L-NAME (1.2mM; pre +16.8±5.6, post -8.6±5.2; 12mM; pre +13.7±5.6, post -16.1±5.1 peak % change from baseline sGaw). Combined NO metabolites in BALF were reduced, after LPS or vehicle exposure followed by L-NAME (1.2mM: 18.2±6.9, 13.2±2.8; 12mM: 19.1±7.6, 0.2±2.2μM, respectively), to levels found during AHR after LPS only (1 and 2h).

This study demonstrates that LPS-induced AHR and AHOR coincide with a respective reduction and elevation in airway NO (metabolites). NO may benefit recovery from AHR as inhibition of its production prolongs AHR to at least 4h. However, NO deficiency alone is not responsible for LPS-induced AHR.

Supported by a GlaxoWellcome Studentship to TJT

Alving, K et al. (1993) Eur. Respir. J. **6,** 1368-70.
Griffiths-Johnson DA et al. (1988) *J Pharmacol Meth* **19,** 233-42.
Grisham, MB *et al.*, (1996) *Methods in Enzymology* **268,** 237-46.
Iijima H, et al. (1998) *Br. J. Pharmacol.* **124,** 1019-28.
Schuiling et al. (1998) *Br. J. Pharmacol.* **123,** 1450-56.
Toward TJ & Broadley KJ (1999) *Br. J. Pharmacol.* Leeds BPS meeting 27P.

229P REGULATION OF 15-LIPOXYGENASE ISOENZYMES BY CYTOKINES IN HUMAN CULTURED NORMAL BRONCHIAL EPITHELIAL CELLS

C Brown, I Kilty, S Jenkinson. (Introduced by M. Trevethick).
Discovery Biology, Pfizer Central Research, Sandwich, Kent, CT13 9NJ.

Previous studies have described the regulation of the 15-lipoxygenase (15-LO) enzyme by the pro-inflammatory cytokines IL-4 and IL-13 in a number of cell types (Jayawickreme *et al.*, 1999). The recent discovery of a second isoenzyme of 15-LO (Brash *et. al.*, 1997), termed 15-LOb (original now termed 15-LOa), raises the question of whether the expression of this second isoenzyme is also under similar transcriptional regulation by cytokines. Therefore, we have examined the effect of a panel of inflammatory cytokines on the expression of both 15-LO isoenzymes in primary cultures of normal human bronchial epithelial (NHBE) cells.

NHBE cells (Clonetics) were seeded onto transwell tissue culture inserts ($5cm^2$; Corning) in supplemented basal epithelial growth medium (Clonetics) until they reached confluency. Subsequently, the cells were grown at an air liquid interface for 12 days before cytokines were added (IL-4 10ng/ml, IL-8 160ng/ml, IL-13 10ng/ml, IL-1β 100pg/ml, TNFα 50pg/ml). After a further 72 h incubation, cells were either examined for 15-LO whole cell enzymatic activity, or harvested for mRNA and protein analysis. To measure 15-LO activity, whole cells were incubated with 100μM linoleic acid in Hanks' balanced salt solution for 10 min at 37°C. Following termination of the reaction by addition of acidified methanol, the 15-LO product, 13-HODE, was extracted and quantified by HPLC/UV detection, measuring the area under the curve. Levels of mRNA of both 15-LO isoenzymes were measured using quantitative PCR (TaqMan RT-PCR) with isoenzyme specific primer/probe sets. Protein levels were measured by Western blot analysis using isoenzyme selective antibodies. Statistical analysis was performed using Students t-test (*P<0.05; **P<0.01). Data represent the mean +/- standard error of three independent experiments.

15-LOa mRNA and protein expression were increased significantly in NHBE cells incubated with either IL-4 (42.7 & 8.6-fold compared with controls) or IL-13 (36.2 & 6.6-fold compared with controls) (figure 1), but not with IL-8 and TNFα. IL-1β produced a significant decrease in 15-LOa protein expression, but no change in mRNA levels. In contrast, none of the cytokines examined had an effect on either 15-LOb mRNA or protein expression. In parallel with the above results, 15-LO whole cell activity was selectively enhanced by IL-4 and IL-13 (1.7 & 1.7-fold compared with control [control value 96.3 ± 11.9ng/10^6cells]).

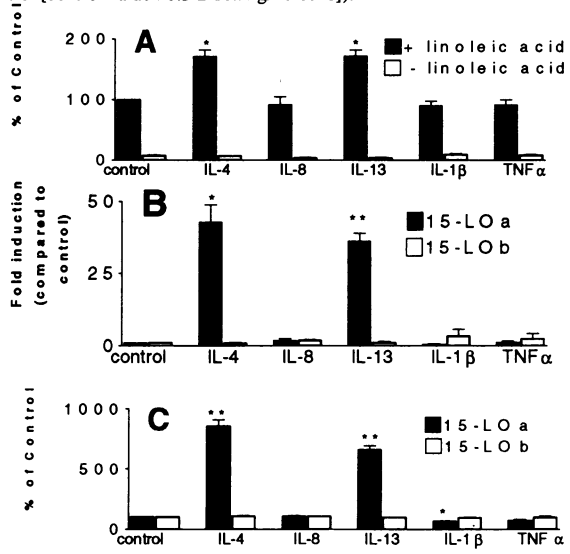

Figure 1: Effect of cytokines on 15-LO activity (A), 15-LOa and 15-LOb mRNA (B) and protein expression (C).

These results demonstrate that IL-4 and IL-13 selectively upregulate 15-LOa isoenzyme expression in primary cultures of NHBE cells. Moreover, the increased expression of this specific isoenzyme is responsible for the enhanced 15-LO activity observed in the presence of these cytokines.

Brash *et al.* (1997) *Proc. Natl. Acad. Sci. USA.*, 94, 6148-6152
Jayawickreme *et al.* (1999) *Am. J. Physiol.*, 276, L596- L603

230P COMPARATIVE EFFECTS OF THE LEUKOTRIENE D_4 RECEPTOR ANTAGONISTS IRALUKAST AND ZAFIRLUKAST IN A MODEL OF OZONE-INDUCED AIRWAY HYPERREACTIVITY AND INFLAMMATION

C.A. Lewis[#§] & K.J. Broadley[#]. Division of Pharmacology, Welsh School of Pharmacy, Cardiff University, Cardiff[#] and Novartis Horsham Research Centre, Horsham , UK[§].

Airway hyperresponsiveness and inflammation to ozone (O_3) can be demonstrated in animals (Campos et al, 1992), however the role of leukotrienes remains controversial (Yeadon et al, 1992; Asano et al, 1993). The aim of this study was to compare the effects of the LTD_4 receptor antagonists, iralukast and zafirlukast on the direct bronchoconstriction, hyperreactivity and inflammation following O_3 exposure in guinea-pigs.

Male Dunkin-Hartley guinea-pigs (300-400g) were exposed to O_3 (0.5-1.2ppm) for 2h. Lung function was measured as specific airway conductance (sGaw) by plethysmography over 2 hours. Animals then received inhaled U-46619 (30ng/ml for 1 min) and lung function measured for 20 mins. They were then overdosed (Sagatal[R]) and the lungs lavaged for total and differential cell counts. Two hours before O_3, guinea-pigs received iralukast (0.1, 0.3 or 1.0% i.e. 1, 3 or 10 mg/ml) or water for injection by inhalation for 20 min. Alternatively they received oral zafirlukast (1, 10 or 100 mg/kg suspension in methylcellulose) or vehicle. Data expressed as mean ± s.e.mean were analysed using two factor ANOVA with replication and Mann Whitney Rank Sum test.

O_3 caused a marked bronchoconstriction with a peak sGaw value (-55.1±10.8%) at 15 min (n=4). Baseline returned by 2h. Iralukast (0.1%, n=4) had no effect, whereas 0.3% significantly (P<0.005) decreased the bronchoconstriction over the 2h period compared to the vehicle-treated group. The sGaw peak at 5 min (–45.4 ± 9.5%, n=4) resolved to baseline by 15 min. 1% iralukast substantially attenuated the constriction (P < 0.0005, n=4) with a peak sGaw value of -21.3±17.9% at 15 min. Zafirlukast did not inhibit the direct bronchoconstriction to O_3 at any of the doses tested.

U-46619 caused a bronchoconstriction after O_3 not seen in unchallenged animals. Iralukast (0.1%) or zafirlukast (1mg/kg) did not affect this airway hyperreactivity. 0.3% iralukast and 10mg/kg zafirlukast (P<0.05) reduced the response and 1% and 100mg/kg abolished the response (P<0.01). The 5 min peak at the highest concentrations was significantly (P<0.05) reduced to reveal bronchodilations +15.4±11.7% and +47.7 ± 38.4% for iralukast and zafirlukast, respectively compared with vehicle controls (-37.6 ± 10.0% and –45.0±7.2%, both n=4).

Significant increases (P<0.05, n=4) in total cells ($3.1\pm0.6 \times 10^6$) including macrophages, neutrophils and eosinophils were observed following O_3 exposure compared to air ($0.8\pm0.1 \times 10^6$, n=4).Total and differential counts were not significantly reduced by any concentration of iralukast, zafirlukast or vehicle.

Iralukast and zafirlukast inhibited the airway hypereactivity following ozone exposure, supporting the role for LTD_4 antagonists in respiratory disease therapy. Interestingly, iralukast but not zafirlukast caused a dose-dependent inhibition of the direct bronchoconstriction to ozone exposure. The route of administration may be important in this observation. Finally, the cell influx was not inhibited by these compounds, indicating a lack of activity against ozone-induced inflammation.

Campos M.G. et al. (1992) J. Appl. Physiol. 73, 354-361
Yeadon M. et al. (1992) Pulm. Pharmacol. 5, 39-50
Asano M. et al. (1993) Agents Actions 38, 171-177

231P SYNERGISTIC EFFECTS OF THE TWO NON-PEPTIDE TACHYKININ ANTAGONISTS, CI-1021 AND GR159897, ON CAPSAICIN-INDUCED BRONCHOCONSTRICTION IN THE ANAESTHETISED GUINEA-PIG

S. Purbrick, R.G. Williams, A.T. McKnight and K. Meecham. Parke-Davis Neuroscience Research Centre, Cambridge University Forvie Site, Robinson Way, Cambridge, CB2 2QB.

Neurogenic bronchoconstriction in the guinea-pig is predominantly mediated via NK_2 receptor activation, with NK_1 receptors playing a minor role. Boni *et al.*, 1995 have demonstrated that synergy exists between NK_1 and NK_2 receptor antagonists in blocking neurogenic bronchoconstriction, whereas Vieira *et al.*, 1997 report no such effect against pulmonary resistance or dynamic elasticity. We examined the effects of the highly selective NK_1 antagonist CI-1021 (Singh *et al.*, 1997) and the NK_2 antagonist GR159897 (Beresford *et al.*, 1995) against capsaicin-induced and agonist-induced bronchoconstriction in the anaesthetised guinea-pig.

Male Duncan Hartley guinea-pigs (300-450 g) were anaesthetised with pentobarbitone (45 $mgkg^{-1}$ i.p.) and respiration was artificially maintained. Insufflation pressure was constantly monitored via a transducer placed in the closed air circuit. Blood pressure and heart rate were monitored continuously via the carotid artery. All compounds were administered via the jugular vein. All animals were pre-treated with atropine (1 $mgkg^{-1}$ iv) and phosphoramidon (2.5 $mgkg^{-1}$ iv). Vehicles and antagonists were administered 5 minutes prior to cumulative administration of an agonist.

Administration of capsaicin, [Sar^9, Met $(O_2)^{11}$]-substance P and [β-Ala^8]-NKA(4-10), produced dose related increases in bronchcoconstriction. CI-1021 1.0 $mgkg^{-1}$ caused a 10-fold rightward shift of the [Sar^9, Met $(O_2)^{11}$]-substance P dose response curve, (pED_{50}: 8.44 ± 0.04 to 7.43 ± 0.05 $nmolskg^{-1}$, n=4/5), but showed no activity against [β-Ala^8]-NKA(4-10). In contrast GR159897 1.0 $mgkg^{-1}$ caused a rightward shift of the [β-Ala^8]-NKA(4-10) dose response curve, (pED_{50}: 8.88 ± 0.07 to 6.87 ± 0.13 $nmolskg^{-1}$, n=3) but showed no activity against [Sar^9, Met $(O_2)^{11}$]-substance P. GR159897 (1.0 $mgkg^{-1}$) also caused significant inhibition of capsaicin-induced bronchoconstriction, but only a 3-fold shift in the curve; higher doses (3.0 and 10.0 $mgkg^{-1}$) had no additional effect. CI-1021 (0.1 and 1.0. $mgkg^{-1}$) had no significant effect on capsaicin-induced bronchoconstriction. By comparison however, when given together the combination of GR159897 with CI-1021 significantly reduced the level of bronchoconstriction with an almost complete block of the response (Figure 1). The combination of GR159897 and CI-1021 did not show significant synergistic activity against the selective agonists.

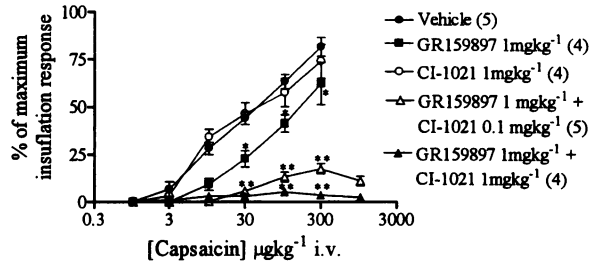

Figure 1. Effect of GR159897 +/- CI-1021 (iv.) on capsaicin-induced bronchoconstriction *P<0.05, **P<0.01 (ANOVA followed by Dunnet's test).

These studies demonstrate that high doses of the NK_2 receptor antagonist GR159897 cause significant, though clearly limited, attenuation of capsaicin-induced bronchoconstriction in the anaesthetised guinea-pig. However, co-administration of GR157897 with the NK_1 receptor antagonist CI-1021, at doses that were ineffective against the neurogenic stimulus alone, resulted in substantially greater inhibitory effects. These findings are consistent with previous studies indicating synergy between NK_1 and NK_2 receptor antagonists (Boni *et al.*, 1995) and further suggest that a substantial part of the capsaicin-mediated response was mediated by the NK_1 receptor, though apparently masked by the NK_2-mediated response.

Beresford, I.J.M *et al.* (1995) *Eur. J. Pharmacol.* **272**, 241-248.
Boni, P. *et al.* (1995) *J. Auton Pharmacol.* **15**, 49-54.
Singh, L. *et al.* (1997) *Eur. J. Pharmacol.* **321**, 209-216.
Vieira, J.E. *et al*, (1997) *Exp. Lung. Res.* **23(1)**, 85-99.

232P INFLUENCE OF RECEPTOR RESERVE ON H_1-HISTAMINE ANTAGONISM BY CETIRIZINE: COMPARISON BETWEEN ISOLATED GUINEA-PIG TRACHEA AND ILEUM

B. Christophe, M. Gillard, D. Smeyers, B. Carlier, P. Chatelain, M. Peck & R. Massingham, UCB Pharma, Chemin du Foriest, B-1420 Braine l'Alleud, Belgium

Cetirizine has previously been described as a competitive H_1-histamine antagonist in isolated guinea-pig ileum (Abe *et al.*, 1994) but as a non-competitive H_1-histamine antagonist in guinea-pig trachea (Kalher & Du Plooy, 1994). The aim of the present work was to determine if a difference in the amount of receptor reserve might explain this disparity.

Receptor reserve was determined as described by Furchgott (1966) using dibenamine as the alkylating agent. Strips of ileum or rings of trachea were isolated from male Dunkin-Hartley guinea-pigs (250-350 g, killed by cervical dislocation) and mounted in organ baths (at 1 g resting tension) filled with Tyrode (ileum) or Krebs' (trachea) solution (37 °C, 95-5 % O_2-CO_2) for isometric tension measurement. Concentration-response (C-R) curves to histamine were non-cumulatively (ileum) or cumulatively (trachea) constructed in the presence or absence of dibenamine. Similarly, H_1 antagonism was determined by constructing C-R curves to histamine in the absence and presence of cetirizine (60 min incubation) on the isolated ileum and trachea as described by Van Rossum (1963). H_1 binding profiles and kinetics were determined as described by Moguilesky *et al.* (1995) and Motulsky & Mahan (1984) Data are presented as mean ± s.e.m.

Cetirizine showed competitive (pA_2 = 8.10 ± 0.10, n = 18) or mixed (competitive and apparent non-competitive : pA_2 = 7.25 ± 0.38, n = 28, apparent pD'_2 = 6.65 ± 0.32, n = 27) H_1-antagonism on the ileum and trachea respectively.

This mixed antagonism was not readily explained by additional, non-H_1 properties of cetirizine as its binding profile was relatively selective for the H_1 receptor: (pK_i for H_1 : 8.2, no binding at 10 μM for A_1, β_1, D_2, H_3, 5-HT_{1A}, M_3, B_2, Na^+ channel or Ca^{2+} channel and 20-50 % inhibition at 10 μM for α_1, α_2 or H_2). The dissociation $t_{1/2}$ of cetirizine from the H_1 receptor was measured to be 95 min at 37°C.

Dibenamine (3 μM) produced an irreversible inhibition of the maximal contraction to histamine (21.8 ± 10.7 %, n = 6 after 180 min on the ileum and 35.8 ± 6.3 %, n = 5 after 60 min on the trachea). The receptor reserve was calculated to be 416.4 in the ileum and 4.66 in the trachea. In the presence of dibenamine, cetirizine showed a mixed antagonism on the ileum (pA_2 = 6.93 ± 0.85, n = 29 and apparent pD'_2 = 6.75 ± 0.28, n=25).

In theory, the competitive nature of an antagonist can switch to a mixed profile if the drug has a slow dissociation rate and if the receptor reserve is small (Zhu, 1993). Our results lend support to this theory and to our initial hypothesis that the smaller H_1 receptor reserve in the guinea pig trachea compared to the ileum is responsible for the apparent non-competitive behaviour of cetirizine on this tissue.

Abe, T., Omata, T., Yoshida, K. *et al.* (1994) *Jpn. J. Pharmacol.* 66, 87-94.
Furchgott, R.F. (1966) *Adv. Drug Res.* 3, 21-55.
Kalher, C.P. & Du Plooy, W.J. (1994) *Med. Sci. Res.* 22, 743-745.
Motulsky, H.F. & Mahan, L.C. (1984) *Mol. Pharmacol.*,25, 1-9
Moguilevsky, N., Varsalona, F., Guillaume, J.P. *et al.* (1995) *J. Recept. & signal transd. Res.* 15, 91-102.
Van Rossum, J.M., (1963) *Arch. int. Pharmacodyn. Ther.* 143, 299-330.
Zhu, B.T. (1993) *J. Pharmacol. Toxicol. Method.* 29, 85-91.

233P STIMULATION OF CHLORIDE SECRETION IN MURINE COLONIC AND NASAL EPITHELIA BY CHLORZOXAZONE

J. Keogh and A. W. Cuthbert*. School Pharmacy, De Montfort University, Leicester LE1 9BH, *Department of Medicine, University of Cambridge, Cambridge, CB1 8QQ.

Stimulation of transepithelial Cl^- secretion requires the activation of both apical Cl^--channels and basolateral K^+-channels. Therefore basolateral K^+-channel openers, specifically targeted to airway epithelium could make other forms of cystic fibrosis treatment more effective. Chlorzoxazone (5-chloro-2 (3H)-benzoxazolone) (Cz) is an approved drug used in the treatment of muscle spasm that has also been reported to stimulate transepithelial Cl^- secretion in the human colonic T84 cell line, human airway Calu-3 monolayers and in primary cultures of human airway cells by activating an inwardly rectifying K^+-channel that is blocked by charybdotoxin (ChTX) (Schultz *et al.*, 1999). Here the effects of Cz on electrogenic Cl^- secretion in murine colonic and nasal epithelium have been investigated using short circuit current (SCC) methods.

The tissues used in all experiments were taken from CD1 mice either male or female, killed by cervical dislocation. The colons and nasal epithelia were immediately removed and placed in cold Krebs Henseleit Solution (KHS). The distal end of the colon was opened up and the muscle layers dissected away from the epithelium. The nasal epithelia had no further preparation. both types of tissue were short circuited by conventional methods as described previously (MacVinish *et al.*, 1998). Amiloride (100μM) was present in the apical bathing solution in all experiments to block electrogenic sodium absorbtion and Cz was applied both apically and basolaterally. An unpaired t-test was used for statistical comparisons with $P<0.05$ being considered significant.

Cumulative concentration-response curves indicate maximal responses to Cz occurred at 600μM (producing a current of 72.4±10.4 μAcm^{-2}, n=6) and 250μM (producing a current of 28.0±11.9 μAcm^{-2}, n=6) in the colon and nasal epithelium respectively. At higher concentrations the responses in both tissues were depressed. Approximate EC_{50}s were 300μM and 25μM for the colonic and nasal tissues respectively. In the colon Cz (300μM) caused a sustained increase in current of 36.8±4.1 μAcm^{-2} (n=23). Addition of furosemide (1mM) basolaterally reduced the response to Cz from 40.7±7.9 μAcm^{-2} to 17.5±4.8 μAcm^{-2} (n=7, $P<0.03$). Similarly basolateral addition of ChTX (50nM) reduced the response to Cz (300μM) from 45.5±6.4 μAcm^{-2} to 26.5±2.7 μAcm^{-2} (n=8, $P<0.02$). In a concurrent set of experiments where ChTX was added before Cz, the responses to the latter were reduced compared to the experiments in which ChTX was added second (23.4±6.0 μAcm^{-2} (n=7) versus 45.5±6.4 μAcm^{-2} (n=8), $P<0.03$) The results suggests that Cz causes an increase in chloride secretion in the colon by an effect on a basolateral, ChTX-sensitive K^+-channel. In nasal epithelia Cz (100μM) produced a sustained increase in SCC of 17.1±1.8 μAcm^{-2} (n=20). However, neither furosemide or ChTX significantly affected the responses (furosemide reduced the response from 15.0±3.8 μAcm^{-2} to 9.3±2.3 μAcm^{-2}, n=6, NS and ChTX increased the response from 18.0±3.0 μAcm^{-2} to 19.8±3.4 μAcm^{-2}, n=7, NS). Nevertheless Ba^{2+}, 5mM, applied basolaterally reduced the Cz current from 18.5±3.2 μAcm^{-2} by 37.9±9.8 μAcm^{-2} (n=6, $P< 0.001$). Thus Ba^{2+} may inhibit K^+-channels opened by Cz, as well as block already patent K^+-channels. The results suggest that different K^+-channels are activated by Cz in the colonic and nasal epithelium, but more definitive evidence is needed to confirm that the current represents electrogenic chloride secretion. Finally in the colon, when the basolateral bathing solution was replaced by a potassium depolarising solution containing impermeant anions, Cz (300μM) caused a reduction in SCC of 16.4±4.1 μAcm^{-2} (n=4). The inwardly directed chloride current in these conditions suggests that Cz has additional effects on apical CFTR Cl^--channels.

MacVinish, L.J., Hickman, M. E., Mufti, D.A., *et al.* (1998) *J. Physiol.* 510, 237-247.
Schultz, B.D., Singh, A.K., Devor, D.C. *et al.* (1999) *Physiol. Rev.* 79, S109-S144.

234P ENHANCEMENT OF THIOL AND DISULPHIDE-MEDIATED PEROXYNITRITE -DEPENDENT α_1-ANTIPROTEINASE INACTIVATION BY BICARBONATE

*Whiteman, M., *Ketsawatsakul, U. & **Halliwell, B. (Introduced by S. D. Brain). *International Antioxidant Research Centre, Guy's, King's & St. Thomas' School of Biomedical Sciences, St. Thomas Street, London SE1 9RT. **Dept. Biochemistry, National University of Singapore, 10 Kent Ridge Crescent, Singapore 119260.

Peroxynitrite ($ONOO^-$) is a cytotoxic species formed from the rapid reaction between nitrogen monoxide ($NO^\bullet$) and superoxide ($O_2^{\bullet-}$). Its formation *in vivo* is implicated in numerous diseases. Part of its toxicity involves the oxidation and nitration of biological substrates. Recently (Whiteman & Halliwell, 1997) it has been shown that at physiological concentrations certain thiols and disulphide compounds may increase oxidative damage to biomolecules. Interestingly, the one and two electron oxidations by $ONOO^-$ are modified by the presence of physiological concentrations of HCO_3^- (in equilibrium with CO_2) *via* the formation of nitrosoperoxycarbonate anion ($ONOOCO_2^-$). Considering the interest in the development of therapeutic $ONOO^-$ scavengers and the role thiol compounds may play, we investigated the effect of HCO_3^- on the reactivity of $ONOO^-$ towards thiols and disulphides using 2 model systems of $ONOO^-$ toxicity; α_1-antiproteinase (α_1-AP) inactivation and tyrosine nitration.

$ONOO^-$ was prepared as described (Whiteman & Halliwell, 1997). 1mM tyrosine was incubated in 100mM K_2HPO_4-KH_2PO_4 buffer, pH 7.4 ± 25mM $NaHCO_3$ ± test compounds for 15 min at 37°C and $ONOO^-$ (1mM) added. 3-Nitrotyrosine formed was measured by HPLC. To examine $ONOO^-$ -mediated inactivation of α_1-AP, 40μl of α_1-AP (4mg/ml) was incubated in 100mM K_2HPO_4-KH_2PO_4 buffer, pH 7.4 containing 25mM $NaHCO_3$ ± test compounds for 15 min at 37°C and $ONOO^-$ (500μM) added. Residual elastase activity was measured after the addition of 100μl elastase substrate (4mg/ml) and the change in absorbance at 410nm measured for 30 sec (Whiteman *et al.*, 1999). Data was analysed by an independent t-test (Students; 2 populations)

Bicarbonate (25mM) had little effect on the ability of thiols / disluphides to inhibit tyrosine nitration. However, low concentrations (1-30μM) significantly increased $ONOO^-$ -mediated inactivation of α_1-AP and inclusion of bicarbonate (25mM) significantly enhanced this (Figure 1). Control experiments showed this phenomenon to be short lived (< 5 secs).

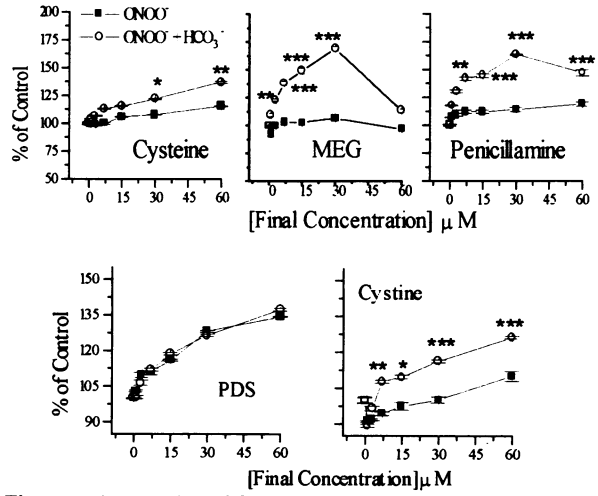

Figure 1. Aggravation of $ONOO^-$ -mediated inactivation of α_1-AP by thiols / disulphides by bicarbonate. Data are Mean ± sem (n=6). MEG, mercaptoethylguanidine; PDS, penicillamine disulphide. * $p< 0.05$, ** $p < 0.01$, *** $p < 0.001$

These results suggest that HCO_3^- enhances $ONOO^-$ -mediated oxidation of thiols / disulphides probably by catalysing the one electron oxidation of thiols / disulphides to short lived sulphur or oxysulphur-centred radicals capable of inactivating α_1-AP.

We are grateful to the Arthritis Research Campaign (ARC) for their generous support

Whiteman, M. & Halliwell, B. (1997). *FEBS Letts.* **379**, 74-76
Whiteman, M., Szabó, C. & Halliwell, B. (1999).. *Br. J. Pharmacol.* **126**, 1646-4652

235P EFFECTS OF BICARBONATE ON THE PEROXYNITRITE SCAVENGING ACTIVITY OF POLYPHENOLS

*Ketsawatsakul , U., *Whiteman, M., & **Halliwell, B. (Introduced by S. D. Brain).*International Antioxidant Research Centre, Guy's, King's & St. Thomas' School of Biomedical Sciences, St. Thomas Street, London SE1 9RT. **Dept. Biochemistry, National University of Singapore, 10 Kent Ridge Crescent, Singapore 119260.

The Reactive Nitrogen Species (RNS) oxoperoxonitrate (1-) [peroxynitrite, $ONOO^-$], formed from the rapid reaction of nitrogen monoxide ($NO^\bullet$) with superoxide ($O_2^{\bullet-}$) is implicated in numerous inflammatory and neurodegenerative diseases. Therefore, there is considerable interest in the development of potential *in vivo* $ONOO^-$ scavengers; dietary polyphenols have been suggested to fulfil this role (Pannala *et al.*, 1998). $ONOO^-$ reacts rapidly with CO_2 (in equilibrium with HCO_3^-) to form the nitrosoperoxycarbonate anion ($ONOOCO_2^-$). This reaction catalyses the nitration of aromatic substrates and substantially modifies the oxidative reactions of $ONOO^-$. Therefore, in assessing potential $ONOO^-$ scavengers, the effects of bicarbonate were assessed using 2 model systems of $ONOO^-$ toxicity; α_1-antiproteinase (α_1-AP) inactivation and tyrosine nitration.

$ONOO^-$ was synthesised as described and stock concentrations calculated immediately before use (Whiteman & Halliwell, 1997). 1mM tyrosine was incubated in 100mM K_2HPO_4-KH_2PO_4 buffer, pH 7.4 ± 25mM $NaHCO_3$ ± test compounds for 15 min at 37°C and $ONOO^-$ (1mM) added. 3-Nitrotyrosine formed was measured by HPLC. To examine $ONOO^-$ -mediated inactivation of α_1-AP, 40µl of α_1-AP (4mg/ml) was incubated in 100mM K_2HPO_4-KH_2PO_4 buffer, pH 7.4 containing 25mM $NaHCO_3$ ± test compounds for 15 min at 37°C and $ONOO^-$ (500µM) added. Residual elastase activity was measured after the addition of 100µl elastase substrate (4mg/ml) and the change in absorbance at 410nm measured for 30 sec (Whiteman *et al.*, 1999). Data was analysed by an independent t-test (Students; 2 populations)

Bicarbonate (25mM) significantly decreased the ability of caffeic acid, chlorogenic acid, coumaric acid and ferulic acid but not gallic acid, catechin and epicatechin to inhibit $ONOO^-$ -mediated tyrosine nitration (Table 1). Substantially higher concentrations of the antioxidants were required to achieve 50% inhibition of 3-nitrotyrosine formation in the presence of HCO_3^-. Bicarbonate also decreased the ability of all the polyphenols tested to protect α_1-AP from $ONOO^-$ -mediated inactivation. Table 2 shows the concentrations needed to inhibit $ONOO^-$ -mediated α_1-AP inactivation by 30%.

	IC_{50} (µM)	
Polyphenol	- Bicarbonate	+ Bicarbonate
Caffeic Acid	20.5 ± 0.8	138.5 ± 2.2***
Catechin	46.2 ± 1.3	51.3 ± 1.5
Chlorogenic acid	56.4 ± 1.8	102.6 ± 1.5***
o-coumaric acid	41.0 ± 1.6	87.18 ± 1.2**
p-coumaric acid	102.5 ± 1.1	184.6 ± 1.3**
Epicatechin	51.3 ± 1.1	51.3 ± 1.3
Ferulic acid	46.2 ± 0.9	66.7 ± 0.8***
Gallic acid	28.2 ± 0.5	28.2 ± 0.6
Quercetin	35.9 ± 0.5	56.4 ± 1.0*

Table 1. Inhibition of $ONOO^-$ -mediated tyrosine nitration by polyphenols: Modulation by Bicarbonate (25mM). Data are expressed and Mean ± sem (n=6). * $p < 0.05$, ** $p < 0.01$, *** $p < 0.001$.

	IC_{30} (µM)	
Polyphenol	- Bicarbonate	+ Bicarbonate
Caffeic Acid	42.4 ± 0.8	72.7 ± 1.0 **
Catechin	54.5 ± 0.9	>1000
Chlorogenic acid	48.5 ± 1.0	66.7 ± 0.2**
o-coumaric acid	751.0 ± 4.6	751.0 ± 5.2
p-coumaric acid	66.7 ± 1.2	133.3 ± 2.3***
Epicatechin	54.5 ± 0.6	667.0 ± 4.8***
Ferulic acid	115.1 ± 1.0	363.0 ± 6.4***
Gallic acid	60.1 ± 0.2	80.4 ± 2.2*
Quercetin	42.4 ± 1.0	158 ± 3.0***

Table 2. Inhibition of $ONOO^-$ -mediated α_1-AP inactivation by polyphenols: Modulation by Bicarbonate (25mM). Data are expressed and Mean ± sem (n=6). * $p < 0.05$, ** $p < 0.01$, *** $p < 0.001$.

The effectiveness of peroxynitrite scavengers may be severely modified by the physiological concentrations of bicarbonate. Therefore, experiments in the presence and absence of bicarbonate should be conducted to avoid obtaining misleading data.

Pannala, A. S., *et al.*, (1998). *Biochem. Biophys. Res.Commun.* **232**, 164-168
Whiteman, M. & Halliwell, B. (1997). *FEBS Letts.* **379**, 74-76
Whiteman, M., Szabó, C. & Halliwell, B. (1999).. *Br. J. Pharmacol.* **126**, 1646-4652

236P MODULATION OF PEROXYNITRITE SCAVENGING ACTIVITY OF ANTIOXIDANTS BY BICARBONATE

*Whiteman, M., *Ketsawakatsul, U. & **Halliwell, B. (Introduced by S. D. Brain).*International Antioxidant Research Centre, Guy's, King's & St. Thomas' School of Biomedical Sciences, St. Thomas Street, London SE1 9RT. **Dept. Biochemistry, National University of Singapore, 10 Kent Ridge Crescent, Singapore 119260.

Peroxynitrite ($ONOO^-$) is a reactive nitrogen species (RNS) formed from the reaction between nitrogen monoxide ($NO^\bullet$) and superoxide ($O_2^{\bullet-}$). $ONOO^-$ formation *in vivo*, as assessed by the measurement of its suggested bio-marker 3-nitrotyrosine is implicated in numerous inflammatory and neurodegenerative diseases. Recently, physiological concentrations of HCO_3^- (in equilibrium with CO_2) have been shown to alter the reactivity of $ONOO^-$ towards substrate molecules via the formation of the nitrosoperoxycarbonate anion ($ONOOCO_2^-$). Therefore, we investigated the effect of HCO_3^- on the reactivity of $ONOO^-$ towards antioxidants using 2 model systems of $ONOO^-$ toxicity; α_1-antiproteinase (α_1-AP) inactivation and tyrosine nitration.

$ONOO^-$ was synthesised as described and stock concentrations calculated immediately before use (Whiteman & Halliwell, 1997). 1mM tyrosine was incubated in 100mM K_2HPO_4-KH_2PO_4 buffer, pH 7.4 ± 25mM $NaHCO_3$ ± test compounds for 15 min at 37°C and $ONOO^-$ (1mM) added. 3-Nitrotyrosine formed was measured by HPLC. To examine $ONOO^-$ -mediated inactivation of α_1-AP, 40µl of α_1-AP (4mg/ml) was incubated in 100mM K_2HPO_4-KH_2PO_4 buffer, pH 7.4 containing 25mM $NaHCO_3$ ± test compounds for 15 min at 37°C and $ONOO^-$ (500µM) added. Residual elastase activity was measured after the addition of 100µl elastase substrate (4mg/ml) and the change in absorbance at 410nm measured for 30 sec (Whiteman & Halliwell, 1997). Data was analysed by an independent t-test (Students; 2 populations)

Bicarbonate (25mM) significantly decreased the ability of ascorbate, reduced glutathione (GSH), the vitamin E analogue Trolox and urate to inhibit $ONOO^-$ -mediated tyrosine nitration (Table 1). Substantially higher concentrations of the antioxidants were required to achieve 50% inhibition of 3-nitrotyrosine formation in the presence of HCO_3^-. In contrast, HCO_3^- had little effect on ascorbate, GSH and Trolox at protecting α_1-AP from $ONOO^-$, except at high (>500µM) concentrations (Figure 1). Urate was unable to prevent $ONOO^-$ -mediated inactivation of α_1- AP in the absence of HCO_3^- and when HCO_3^- (25mM) was added some protection was observed (Figure 1).

	IC_{50} (µM)	
Antioxidant	**- Bicarbonate**	**+ Bicarbonate**
Ascorbate	161.9 ± 3.0	217 ± 4.1***
GSH	120 ± 2.8	175.9 ± 2.6**
Urate	54.8 ± 3.1	169.5 ± 3.1***
Trolox	88.6 ± 2.6	137.4 ± 3.0***

Table 1. Inhibition of $ONOO^-$ -mediated tyrosine nitration by antioxidants: modulation by bicarbonate (25mM). Data are expressed as mean ± sem (n=6). * $p < 0.05$, ** $p < 0.01$, *** $p < 0.001$.

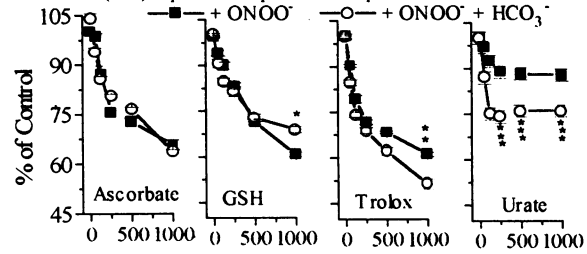

Figure 1. Effect of bicarbonate (25mM) on $ONOO^-$ scavenging activity of antioxidants: Inactivation of α_1-AP. Data are expressed as mean ± sem (n=6). * $p < 0.05$, ** $p < 0.01$, *** $p < 0.001$.

Nitration of tyrosine by $ONOO^-$ is catalysed by CO_2, *via* the formation of $ONOOCO_2^-$. $ONOOCO_2^-$ undergoes homolytic fission to produce $NO_2^\bullet$ and $CO_3^{\bullet-}$ radicals providing additional radicals for nitration and oxidation. The results presented here suggest that the antioxidants tested are less effective at preventing $ONOO^-$ -mediated toxicity in the presence of bicarbonate. Due to the high HCO_3^- concentration *in vivo* and the rapid reaction of HCO_3^- with $ONOO^-$, the testing of potential $ONOO^-$ scavengers for therapeutic use should be examine both in the presence and absence of HCO_3^- to eliminate the possiblilty of misleading results.

Whiteman, M. & Halliwell, B. (1997). *Free Rad. Biol. Med.* **22**, 1309-1312

237P PHARMACOLOGICAL CHARACTERISTICS OF [^{32}P] cADPR BINDING TO SEA URCHIN EGG HOMOGENATE

J. M. Thomas, G. C. Churchill, C. J. Lad, A. Galione. Department of Pharmacology, Oxford University, Mansfield Road, Oxford, OX1 3QT.

Cyclic ADP-ribose (cADPR), a metabolite of NAD^+, has been shown to mobilise Ca^{2+} from sea urchin eggs in a manner as potent as IP_3. Considerable evidence suggests that cADPR activates the ryanodine receptor/Ca^{2+} release channel. Indeed, cADPR activated Ca^{2+} release is subject to modulation by ryanodine receptor modulators including caffeine, divalent cations and calmodulin. The aim of the present study was to investigate the influence of such agents on [^{32}P]cADPR binding to sea urchin egg homogenate.

Sea urchin egg homogenate was made up to a final concentration of 0.5 mg/ml protein in an intracellular buffer. Approximately 22.5 fmol of [^{32}P]cADPR together with varying concentrations of unlabelled test compound was incubated with homogenate at a total volume of 250 µl for 10 minutes at room temperature. Non-specific binding was assessed by the addition of 10 µM unlabelled cADPR. The binding reaction was terminated by rapid filtration through GF/C filters.

[^{32}P]cADPR bound to sea urchin egg homogenate with a K_d of 2.6 ± 1.3 nM (mean ± s.e.mean, n=5), a B_{max} of 12 fmol/mg protein and a Hill coefficient of 1. Specific binding represented >60 % of total binding. In agreement with Lee (1991), the specificity of binding was illustrated by the fact that neither NAD^+ (2 µM) or ADPR (2 µM) was effective in competing for the [^{32}P]cADPR binding site, whereby specific [^{32}P]cADPR binding was 87.6 ± 5.5 % (n=3) and 72.1 ± 3.9 % (n=3) of control, respectively. Moreover, specific binding was also insensitive to IP_3 (2 µM) and NAADP (100 nM). Specific binding, however, was eliminated by incubation with the specific cADPR antagonist 8-amino-cADPR (500 nM). Binding was found to be relatively insensitive to caffeine, ryanodine and Mg^{2+}. In the presence of 10 mM caffeine, 600 µM ryanodine and 10 mM Mg^{2+}, specific cADPR binding represented 69.5 ± 3.3 % (n=6), 83.8 ± 2.0 % (n=6) and 92.2 ± 4.7 % (n=6) of control, respectively. The influence of calmodulin on specific [^{32}P]cADPR binding was examined using the calmodulin antagonists calmidazolium, W7 and suramin. Calmidazolium inhibited specific cADPR binding in a concentration dependent manner (IC_{50}= 33.7 ± 7.3 µM, n=6) whereby maximal inhibition (200 µM calmidazolium) reduced specific binding to 15.0 ± 2.1 % (n=6) of control. Similarly, W7 (1 mM) and suramin (30 µM) were found to reduce specific binding to 32.9 ± 6.5 % (n=6) and 11.0 ± 0.8 % (n=6) of control, respectively.

Here we show a marked sensitivity of [^{32}P]cADPR binding to inhibitors of calmodulin. This data correlates with the requirement of calmodulin for cADPR activated calcium release (Lee *et al.*, 1994) and suggests that at least one of the effects of calmodulin is at the level of direct cADPR binding or assembly of a cADPR-binding accessory protein with the ryanodine receptor release channel complex.

Supported by the Wellcome Trust.

Lee, H.C. (1991) *J. Biol. Chem.*, **268**, 293-299.
Lee, H.C. *et al.* (1994) *Nature*, **370**, 307-309.

238P CHARACTERIZATION OF AN INOSITOL 1,4,5,-TRISPHOSPHATE-SENSITIVE CALCIUM STORE IN *XENOPUS TROPICALIS* OOCYTES

Jonathan S. Marchant, Nick Callamaras and Ian Parker, Department of Neurobiology & Behavior, University of California Irvine, CA 92697-4550, USA.

The diploid frog *Xenopus tropicalis* is currently the focus of research efforts committed at establishing a genetic model system, which would combine the feasibility of transgenic approaches with the more familiar advantages of the allotetraploid *Xenopus laevis* for experimental embryology (Amaya *et al.*, 1998). Here, we have investigated the pharmacological properties of the endoplasmic reticulum Ca^{2+} store within the *Xenopus tropicalis* oocyte, with a view to assessing its potential as an expression system for proteins involved in intracellular Ca^{2+} homeostasis.

Nuclear injection of a plasmid encoding an endoplasmic reticulum (ER) targetted-yellow fluorescent protein (YFP) chimera led to the visualisation of ER morphology within 24 hours and peak expression, as judged by fluorescence intensity, was maximal by 36 hours. A polarised distribution of ER was evident across the oocyte, with greater peak fluorescent signals in the animal compared to the vegetal pole (313±13%, n=3 discrete donors) and a larger apparent depth of subcortical ER in the animal hemisphere (~20µm animal cf ~5µm vegetal, respectively). Confocal linescan images recorded within animal hemisphere of *Xenopus tropicalis* oocytes previously injected with caged inositol trisphosphate (IP_3) and the fluorescent calcium indicator Oregon Green 488 BAPTA-1 (final intracellular concentrations ~40µM and 5µM respectively), showed that photorelease of IP_3 evoked a dose-dependent liberation of Ca^{2+} from the subcortical ER, with saturating flashes evoking Ca^{2+} waves (pseudo-ratio F/F_0=2.73±0.59, n=46 cells from 3 donors) across the entire 100µm scan line within a latency of less than 100ms. Maximal responses were larger in the animal compared to the vegetal hemisphere (149±14%, n=25 cells from 3 donors), measured using the low affinity calcium indicator Oregon Green-5N. Neither the application of caffeine (10mM) or ryanodine (<5µM), or photorelease of either cyclic ADP-ribose or nicotinic acid adenine dinucleotide phosphate under identical conditions of photostimulation, evoked a rise in intracellular Ca^{2+}.

We conclude that *Xenopus tropicalis* oocytes contain a functional IP_3-sensitive Ca^{2+} store with similar properties to that described in *Xenopus laevis* oocytes, and that the *Xenopus tropicalis* oocyte can similarly function as an expression system for heterologus proteins.

Supported by the NIH (GM 48071) and a Wellcome Trust Fellowship (053102) to JSM.

Amaya, E., Offield, M.F., Grainger, R.M. (1998) *Trends in Genetics*, 14, 253-255.

239P POTENT ANALOGUES OF ADENOPHOSTIN A THAT RELEASE THE INTRACELLULAR Ca^{2+} STORES OF HEPATOCYTES

V. Correa[1], R.D. Marwood[2], S. Shuto[2], A.M. Riley[2], D.J. Jenkins[2], B.V.L. Potter[2], and C.W. Taylor[1]. [1]Department of Pharmacology, Cambridge, CB2 1QJ, and [2]Department of Pharmacy and Pharmacology, Bath, BA2 7AY.

Adenophostin A (**1**, Fig. 1) is the most potent known agonist of inositol 1,4,5-trisphosphate (IP_3) receptors. Removal of the adenine moiety from adenophostin A produces an agonist, RibP_3 (**2**), with similar potency to IP_3 (Marchant *et al.*, 1997). Here we compare the activities of adenophostin analogues with modified base (**2-5**) or glucose moieties (**6,7**). The novel analogues (**3-7**) were prepared by total synthesis.

Figure 1: Structures of adenophostin analogues.

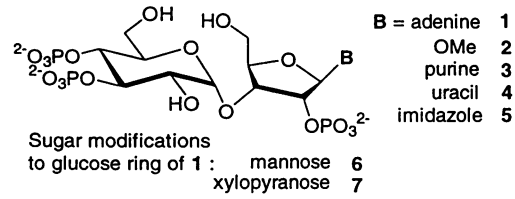

The intracellular stores of saponin-permeabilized hepatocytes were loaded with $^{45}Ca^{2+}$ at 37°C in cytosol-like medium, thapsigargin (1.25µM) was then added to inhibit further Ca^{2+} uptake. After 30s IP_3 or the analogues were added, and after a further 2min, the $^{45}Ca^{2+}$ contents of the stores were determined using a filtration assay (Marchant *et al.*, 1997).

Maximally effective concentrations of each of the analogues (Fig. 1) stimulated release of the entire IP_3-sensitive Ca^{2+} pool, which amounts to ~50% of the actively accumulated $^{45}Ca^{2+}$ content of the intracellular stores (Table 1). Responses to IP_3 and each of the analogues were positively cooperative (Hill coefficients, h ~2).

Table 1: Results (means±s.e.means of n independent determinations) show the EC_{50}, h and maximal response (% IP_3-sensitive stores) for each of the analogues.

	EC_{50} nM	h	Maximal release %	n
IP_3	119±8	2.69±0.55	55±3	15
Adenophostin **1**	14±2	1.99±0.18	51±6	6
Purinophostin **3**	18±1	2.04±0.24	52±3	10
Uridophostin **4**	34±2	2.55±0.40	48±4	6
Imidophostin **5**	108±20	2.51±0.64	57±3	7
Mannophostin **6**	180±16	2.85±0.55	49±3	8
Xylophostin **7**	28±8	2.50±0.77	52±4	8

We conclude that both the base and glucose moieties contribute to the activity adenophostin A, but that even substantial modifications can be made without loss of activity.

Supported by the Wellcome Trust (CWT 039662; BVLP, 045491)

Marchant, J.S. *et al.* (1997) *Biochemistry* **36**, 12780-12790.

240P IDENTIFICATION OF CALMODULIN-BINDING SITES IN TYPE 1 INOSITOL 1,4,5-TRISPHOSPHATE RECEPTORS

S.A. Morris[1], C.E Adkins[1], H. De Smedt[2], I. Sienaert[2], K. Török[3] and C.W. Taylor[1]. [1]Department of Pharmacology, Cambridge. CB2 1QJ, [2]Laboratorium voor Fysiologie, Leuven, Belgium, and [3]School of Biological Sciences, Queen Mary and Westfield College, London. E1 4NS.

Calmodulin binds to purified cerebellar (Patel *et al.*, 1997) and recombinant type 1 inositol 1,4,5-trisphosphate (IP_3) receptors (Cardy & Taylor 1998) in both the presence and absence of Ca^{2+}. Furthermore, calmodulin inhibits IP_3 binding to both full-length (Cardy & Taylor, 1998) and N-terminal (Sipma *et al.*, 1999) constructs of type 1 IP_3 receptors in a Ca^{2+}-independent manner. A short sequence within the modulatory domain of type 1 IP_3 receptors binds Ca^{2+}-calmodulin (Yamada *et al.*, 1995), but the binding sites for apo-calmodulin have not been defined. Here we use scintillation proximity assays (SPA) and photoaffinity labelling to identify other calmodulin-binding sites in type 1 IP_3 receptors.

GST-fusion proteins of type 1 IP_3 receptor domains (Sienaert *et al.*, 1997) were coupled to protein A-coated SPA beads via an anti-GST antibody. Coupling was quantifed by SDS-PAGE and Western blot analysis using a monoclonal anti-GST antibody. Binding of [^{125}I]-calmodulin (0.4nM) to the beads was determined in 5mM KH_2PO_4, 20mM Hepes, 100µM BAPTA, 10mg/ml BSA, 0.1% surfact-Amps X-100, pH 7.2, with or without 300µM $CaCl_2$ (Patel *et al.*, 1997). For photoaffinity labelling, GST-fusion proteins were incubated with 235nM N-hydroxysuccinimidyl-4-azidobenzoate (HSAB)-calmodulin (Bredt *et al.*, 1992) in 50mM Tris (pH 7.4) and either 7mM EGTA or 700µM Ca^{2+}, irradiated with ultraviolet light, and the crosslinked adducts detected by Western Blotting using an anti-calmodulin antibody. All results are reported as means±sem of ≥3 experiments.

From analyses of [^{125}I]-calmodulin binding to GST-fusion proteins covering the full length of the type 1 IP_3 receptor, [^{125}I]-calmodulin bound to only two IP_3 receptor domains. Cyt1 (residues 6-159) and cyt 11 (residues 1499-1649) bound [^{125}I]-calmodulin in both the presence (K_d = 1.42±0.72µM and 172±37nM, respectively) and absence (K_d = 0.76±0.18µM and 48±11nM) of Ca^{2+}. There was no detectable specific binding to beads coated with GST-syncollin, an 18kDa protein that lacks calmodulin-binding sites. Photoaffinity labelling of the same GST-fusion proteins identified HSAB-calmodulin binding to cyt11 in both the absence and presence of Ca^{2+}, but failed to detect binding to the lower affinity sites in cyt1. Cyt11 contains the previously identified Ca^{2+}-dependent calmodulin-binding site which was shown to be abolished by a mutation of Trp^{1576} to Ala. The analogous mutation in cyt11 reduced specific [^{125}I]-calmodulin binding by 63±9% in the presence of Ca^{2+} and by 67±18% in the absence of Ca^{2+}.

These experiments have identified two intrinsic calmodulin-binding sites in sequences derived from type 1 IP_3 receptors. While the effects of calmodulin binding to the sites present in the modulatory region (cyt11) are unknown, calmodulin-binding to a site within the first 159 amino acids is likely to mediate Ca^{2+}-independent inhibition of IP_3 binding by calmodulin

Supported by the Wellcome Trust (039662) and BBSRC.

Bredt, D.S., Ferris, C.D. & Snyder, S.H. (1992) *J. Biol. Chem.* 267,10976-10981.
Cardy, T.J.A. & Taylor, CW. (1998) *Biochem. J.* 334, 447-455.
Patel, S. *et al.* (1997) *Proc. Nat. Acad. Sci. USA.* 94,11627-11632.
Sienaert, I.*et al.* (1997) *J. Biol. Chem.* 272,25899-25906.
Sipma, H. *et al.* (1999) *J. Biol. Chem.* 274,12157-12162.
Yamada, M. *et al.* (1995) *Biochem. J.* 308, 83-88

241P TYPES 1, 2 AND 3 INOSITOL 1,4,5-TRISPHOSPHATE RECEPTORS ARE INHIBITED BY Ca^{2+}-CALMODULIN

C.E. Adkins and C.W. Taylor. Department of Pharmacology, Tennis Court Road, Cambridge. CB2 1QJ.

Calmodulin inhibits binding of inositol 1,4,5-trisphosphate (IP_3) to type 1, but not type 3, IP_3 receptors in a Ca^{2+}-independent manner (Cardy & Taylor ,1998), and it also inhibits IP_3-evoked Ca^{2+} release from cerebellar microsomes (Patel *et al*, 1997). Here we examine whether inhibition of IP_3-evoked Ca^{2+} release is, like calmodulin-inhibition of IP_3 binding, Ca^{2+}-independent and specific to type 1 IP_3 receptors.

The intracellular stores of saponin-permeabilized cells were loaded with $^{45}Ca^{2+}$ in cytosol-like medium (CLM) (Marchant *et al.*, 1997) and their $^{45}Ca^{2+}$ contents determined after stimulation with IP_3. Calmodulin was usually included during the loading period and subsequent exposure to IP_3, but to examine the Ca^{2+}-dependence of the calmodulin effect, cells loaded with $^{45}Ca^{2+}$ were diluted into media with or without calmodulin and with the free [Ca^{2+}] buffered by BAPTA (5mM) to 200nM or ~4nM. After 5min IP_3 was added and 2min later, the $^{45}Ca^{2+}$ contents of the stores were determined. The same method was used to test the calmodulin antagonists, calmidazolium (50μM) and a peptide from Ca^{2+}-calmodulin-dependent protein kinase II (Pep-3, 20μM), (Cardy & Taylor 1998). Results are means±s.e.means of 3 experiments.

Calmodulin inhibited IP_3-evoked $^{45}Ca^{2+}$ release from cells expressing largely type 1, 2 or 3 IP_3 receptors. In the presence of calmodulin (10μM), the EC_{50} for IP_3-evoked $^{45}Ca^{2+}$ release increased from 90±6nM to 191±6nM in SH-SY5Y cells (type 1), from 167±1nM to 260±15nM in rat hepatocytes (type 2), and from 84±4nM to 174±27nM in RINm5F cells (type 3). In SH-SY5Y cells, calmodulin (IC_{50}~15μM) inhibited IP_3-evoked $^{45}Ca^{2+}$ release only in the presence of Ca^{2+}: in 200nM free [Ca^{2+}],10μM calmodulin reduced the $^{45}Ca^{2+}$ release evoked by a submaximal concentration of IP_3 from 70±4% to 56±1%, but in nominally Ca^{2+}-free, the $^{45}Ca^{2+}$ release was unaffected by 10μM calmodulin (release of 81±3% and 78±2% of the stores in the absence and presence of calmodulin, respectively). Calmodulin antagonists abolished the inhibitory effect of calmodulin; the $^{45}Ca^{2+}$ release evoked by a submaximal concentration of IP_3 was reduced from 84±7% to 47±2% by 10μM calmodulin in control experiments, but unaffected by calmodulin in the presence of either 50 μM calmidazolium (68±8% and 68±9% release, with and without calmodulin, respectively) or 20μM Pep-3 (82±1% and 73±11% release). The inhibition did not result from enhanced metabolism of IP_3 because calmodulin also reduced the sensitivity of the stores to adenophostin A, a stable agonist of IP_3 receptors: 10μM calmodulin increased the EC_{50} for adenophostin A from 5±3nM to 17±2nM. The effect of calmodulin persisted after inhibition of calcineurin:10μM calmodulin reduced the $^{45}Ca^{2+}$ release evoked by a submaximal concentration of IP_3 from 89±16% to 22±18% in control experiments, from 63±26% to 27±14 % in the presence of 300nM FK506, and from 96±21% to 27±12% in the presence of 1μM cyclosporin A.

We conclude that there are two effects of calmodulin on IP_3 receptors. Ca^{2+}-calmodulin inhibits IP_3-evoked Ca^{2+} release mediated by all three receptor subtypes. Ca^{2+}-independent calmodulin binding to type 1 IP_3 receptors inhibits IP_3 binding, but the functional consequences are presently unclear.

Supported by the Wellcome Trust (039662)

Cardy, T. J. A. & Taylor, C.W. (1998) *Biochem. J.* **334**, 447-455.
Marchant, J.S. *et al.* (1997) *Biochemistry* **36**, 12780-12790.
Patel, S. *et al.* (1997) *Proc. Nat. Acad. Sci.* **94**, 11627-11632.

242P THE RELATIVE BINDING AFFINITIES OF A SERIES OF 2-(DIPROPYLAMINO)TETRALINS AT THE HUMAN 5-HT_{1A} RECEPTOR EXPRESSED IN CHO CELLS

J. T.Alder, A. M. Johansson[1] & P. G. Strange. School of Animal and Microbial Sciences, University of Reading, P.O. Box 228, Whiteknights, Reading, RG6 6AJ. [1]Organic Pharmaceutical Chemistry, Upsala University, Sweden.

The compound 8-hydroxy-2-(dipropylamino)tetralin (8-OH-DPAT) is a high affinity agonist at the 5-hydroxytryptamine$_{1A}$ (5-HT; serotonin) receptor. 8-OH-DPAT in common with many catecholamine receptor and other serotonergic receptor ligands, has an amino group which is believed to interact with an aspartate residue (transmembrane 3) which is conserved in cationic amine receptors. Many of these ligands also have hydroxyl groups which may form hydrogen bonds with other conserved residues within the transmembrane domains, (Hibert, *et al.*, 1991).

In the present study, the relative binding affinities and stereoselectivity of a series of 2-(dipropylamino)tetralins (see Fig 1) were determined. Competition binding studies were carried out against [^{3}H] 8-OH-DPAT which labels the high affinity state of the receptor, *i.e.* receptor coupled to G-protein, (Wreggett and De Léan, 1984).

Figure 1. Chemical structure of *R*-DPAT, showing position of hydroxyl group for compounds studied.

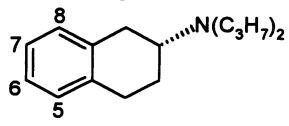

Membranes prepared from CHO cells stably expressing the human 5-HT_{1A} receptor (Newman-Tancredi *et al.*, 1992) were incubated with [^{3}H] 8-OH-DPAT (0.25 nM) in 20 mM HEPES, 5 mM $MgSO_4$ pH 7.4 in the presence of competing ligand, for 2.5h at 25°C, followed by vacuum filtration. Inhibition of [^{3}H] 8-OH-DPAT binding was analysed using Graphpad Prism software.

The hydroxyl group in the 8- position gave the most favourable binding, with a 23-fold higher affinity than *R*-DPAT. *R* and *S* enantiomers of 7-OH-DPAT, 6-OH-DPAT and 5-OH-DPAT bound with significantly lower affinity than *R*-DPAT (students *t*-test, $p < 0.05$). No significant difference in binding affinity was observed between the *R* and *S* enantiomers of 8-OH-DPAT, or 5-OH-DPAT. Significant stereoselectivity was observed for DPAT, 7-OH-DPAT and 6-OH-DPAT, with the *R* enantiomer binding with higher affinity (Table 1).

These data suggest that a hydroxyl group is not necessary for stereoselectivity of 2-dipropylaminotetralins at the 5-HT_{1A} receptor and that hydroxyl groups at position 7-, 6- or 5- are detrimental to binding. Indeed only position 8- improved binding over the non-hydroxylated *R*-enantiomer.

This work was supported by the BBSRC.

Hibert, M.F. *et al.*, (1991) *Mol. Pharm.* 40, 8-15.
Newman-Tancredi, A. *et al.*, (1992) *Biochem. J.* 285, 933-938.
Wreggett, K.A. and De Léan, A. (1984) *Mol. Pharm.* 26, 214-227.

Table 1. Relative binding affinities (pKi) of 2-(dipropylamino)tetralins at the human 5-HT_{1A} receptor expressed in CHO cells.

8-OH-DPAT		7-OH-DPAT		6-OH-DPAT		5-OH-DPAT		DPAT	
R-	*S*-	*R*-	*S*-	*R*-	*S*-	*R*-	*S*-	*R*-	*S*-
9.51 ± 0.05	9.41 ± 0.05	7.23 ± 0.08	6.58 ± 0.04	5.98 ± 0.09	5.69 ± 0.07	6.39 ± 0.11	6.74 ± 0.15	8.08 ± 0.11	7.22 ± 0.18
		*** p = 0.0003		* p = 0.042				* p = 0.016	

Data are pKi values ± s.e.mean from at least three experiments performed in triplicate. p values indicate significant stereoselectivity (students *t*-test).

243P CHARACTERISATION OF RECOMBINANT HUMAN 5-HT_{2C} EDITED (VSV) AND UNEDITED (INI) RECEPTORS

Porter R.H.P., Allen N.H., Lamb H., Revell D. and Malcolm C.S
Cerebrus, 613 Reading Road, Winnersh, Wokingham, RG41 5UA

The 5-HT_{2C} receptor has been demonstrated to undergo RNA editing at various sites which is thought to decrease the efficiency of G protein coupling (Burns *et al.*, 1997). The agonist responses of 5-HT, mCPP (m-chlorophenylpiperazine) and DOI (2,5-dimethoxy-4-iodoamphetamine hydrobromide) were characterised at the native unedited human 5-HT_{2C} receptor (5-$HT_{2C\text{-}INI}$) and the most abundantly expressed edited variant (5-$HT_{2C\text{-}VSV}$) in human brain (Niswender *et al.*, 1999). Both receptors were expressed at similar low densities in CHO-K1 cells and the compounds were characterised with respect to potency, efficacy and both homologous and heterologous desensitisation profiles following pre-incubation with a supramaximal concentration of the compounds (10μM).

Agonist responses were measured using a fluorometric imaging plate reader (FLIPR). Cells were seeded at a density of 30,000 cells/well in black walled clear bottomed 96 well plates and incubated overnight before use. The cells were dye loaded with 4μM Fluo-3-AM and the maximum increase in fluorescence that occurs as a result of calcium mobilisation was recorded. In order to measure desensitisation, the cells were pre-incubated for 0-24 hours with the compound of interest, prior to wash out and the addition of 10μM 5-HT on FLIPR. Pre-incubation times of 2 hours or less were performed during the dye loading procedure.

The agonists were more potent at unedited, than at edited receptors, (e.g. mCPP EC_{50}'s = 26.9nM and 74.6nM respectively), but edited receptors typically elicited approximately 3 times greater fluorescence increases than unedited receptors.

5-$HT_{2C\text{-}INI}$ receptors were more sensitive to desensitisation by all 3 agonists, which elicited similar time profiles with $T_{1/2}$'s of 5-10 min reducing the subsequent 5-HT response to approximately 15% control levels after 24 h. 5-$HT_{2C\text{-}VSV}$ receptors exhibited a differential compound specific desensitisation time profile with mCPP and DOI eliciting a more rapid desensitisation profile than 5-HT. Additionally, the mCPP and DOI induced desensitisation appeared to partially recover (Figure 1). Preincubation with the 3 agonists for 24 h reduced subsequent responses to 50-60% control levels.

Figure 1 Desensitisation of 5-HT_2 receptor isoforms

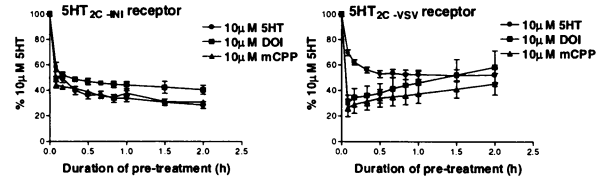

CHO-K1 cells have previously been demonstrated to express an endogenous P2 receptor (Iredale and Hill, 1993). Pre-incubation with 10μM 5-HT for 60 min followed by addition of ATP (adenosine triphosphate) resulted in a greater degree of desensitisation (decrease in potency and maximal response) after stimulation of 5-$HT_{2C\text{-}VSV}$ receptors than 5-$HT_{2C\text{-}INI}$ receptors.

These results suggest a divergence in terms of functional and regulatory profiles of the edited and unedited 5-HT_{2C} receptors.

Burns, C.M. *et al.*, (1997) *Nature* **387,** 303-308.
Iredale, P.A. & Hill, S.J.(1993) *Br. J. Pharmacol.* **110,** 1305-1310
Niswender, C.M. *et al.*, (1999) *J.Biol. Chem.* **274,** 9472-9478.

244P ANTISENSE OLIGODEOXYNUCLEOTIDE TO RAT GLUCOCORTICOID RECEPTOR, GIVEN ICV IN POLYMER MICROSPHERES, REDUCES GLUCOCORTICOID- AND INCREASES 5-HT_{2A}-RECEPTOR BINDING

A. Islam, K.S.J. Thompson[1], S. Akhtar and S.L. Handley. Pharmaceutical Sciences Institute, Aston University, Aston Triangle, Birmingham B4 7ET, UK. [1]BASF Pharma, Research and Development, Nottingham, NG1 1GF, UK.

Adrenal steroids and 5-HT show extensive functional inter-relationships (Meijer & de Kloet, 1998), and both have been implicated in the pathophysiology of depression and schizophrenia (Hrdina et al., 1993). In certain cell lines, the 5-HT_{2A} receptor gene is under transcriptional control by the glucocorticoid receptor (GR) (Garlow and Ciaranello, 1995). We therefore used RNase H accessibility mapping to design an antisense oligodeoxynucleotide (AS-ODN) targeted against the rat GR to reveal whether such regulation occurs *in vivo*. Because glucocorticoids are important in stress responses, we minimised the stress of the procedure by administering the AS-ODN as a single ICV injection in a slow-release polymer microsphere vehicle.

The AS-ODN (21-mer phosphorothioate, antisense to residues 1162-1182 of rat GR, accession number M14053) was formulated in polylactide-co-glycolide (PL-GA) polymer microspheres using a solvent evaporation double emulsion method (Akhtar & Lewis, 1997). Four groups of male Wistar rats (n = 8/group; 270-310g, anaesthetised with N_2O/isofluorane) received 2μL of the microsphere suspension ICV in saline during stereotaxic surgery using a pseudo-randomised design. Groups received: sham injections (SH), saline-loaded polymer microspheres (PL). antisense (AS), or mismatch (MM) ODN-loaded polymer microspheres. The animals were killed after 5 days and frontal cortex removed for radioligand binding. GR binding was determined using 10nM [^{3}H]-dexamethasone, with 2μM mifepristone to define non-specific binding. 5-HT_{2A} binding was determined with 0.5-50nM [^{3}H]-ketanserin, and 5μM methysergide for non-specific binding. Statistical analysis was by ANOVA/Tukey-HSD.

AS treatment markedly reduced GR binding, by 66.8% compared to SH (AS c.f. all other groups, $^{**}p<0.01$, Fig. 1), whereas PL and MM treatments altered binding by 7.4% and 6.2% respectively (not significant). In the same animals, 5-HT_{2A} receptor density increased to 121.4% after AS treatment, compared with SH ($^{*}p<0.05$, AS c.f. all other groups, Fig. 1), whereas PL (92.5%) and MM (88.6%) treatments had no significant effect.

Figure 1. GR and 5-HT_{2A} receptor binding in rat frontal cortex.

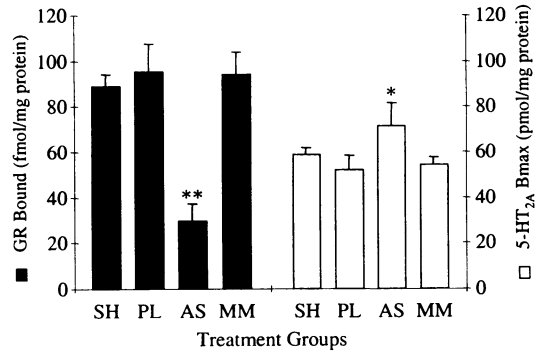

These data demonstrate that the AS-ODN to the rat GR suppresses GR expression over 5 days *in vivo*. The correlated increase in 5-HT_{2A} receptor density suggests these receptors are under tonic inhibitory control by GR. Furthermore, a single PL-GA microsphere injection ICV proved to be an effective means of delivering the AS-ODN.

Akhtar S. & Lewis K.J. (1997) *Int. J. Pharmaceutics* 151:57-67.
Garlow S.J. & Ciaranello R.D. (1995) *Mol. Brain Res.* 31:201-209.
Hrdina P.D., Demeter E., Vu T.B., *et al.* (1993) *Brain Res.* 614:34-37.
Meijer O.C. & de Kloet E.R. (1998) *Crit. Rev. Neurobiol.* 12:1-20.

245P AUTORADIOGRAPHIC LOCALISATION OF THE 5-HT$_7$ RECEPTOR IN THE GUINEA-PIG BRAIN USING [^{3}H]SB-269970

J.C. Roberts, D.R. Thomas, J.J. Hagan and R.A. Leslie.
Neuroscience Research Department, SmithKline Beecham Pharmaceuticals, New Frontiers Science Park (North), Third Avenue, Harlow, Essex CM19 5AW, UK.

We have used tritiated SB-269970, (*R*)-3-(2-(2-(4-Methyl-piperidin-1-yl)ethyl)-pyrrolidine-1-sulfonyl)-phenol, to define the distribution of 5-HT$_7$ receptors in the brains of Dunkin-Hartley (adult male, 250-350g) guinea pigs. The binding of [^{3}H]SB-269970 to guinea pig cerebral cortex homogenates has been previously characterised (Thomas *et al.*, 1999) and compared with the non-selective 5-HT$_7$ receptor agonist 5-carboxamidotryptamine ([^{3}H]5-CT). Since 5-CT also has affinity for 5-HT$_{1A/B/D}$ receptors, masking ligands were used to inhibit binding to non-5-HT$_7$ binding sites. [^{3}H]5-CT and [^{3}H]SB-269970 displayed similar affinity for the 5-HT$_7$ receptor in the guinea pig cortex (pKi 8.80 ± 0.17 and 8.79 ± 0.15, respectively).

Autoradiographic radioligand binding was used to define the density and distribution of 5-HT$_7$ receptors using [^{3}H]SB-269970 (3nM) and [^{3}H]5-CT (1nM) in the presence of masking ligands. Unlabelled GR127935 (10μM) and WAY 100635 (1μM) were used to block binding to 5-HT$_{1B/1D}$ and 5-HT$_{1A}$ receptors, respectively. Unlabelled SB-269970 (10μM) and unlabelled 5-CT (10μM) were added to define nonspecific binding. Selective binding of [^{3}H]5-CT to 5-HT$_7$ receptors, compared with binding of [^{3}H] SB-269970 is shown in Table 1. Essentially, specific binding with [^{3}H]SB-269970 gave an identical distribution pattern to that seen with [^{3}H]5-CT in the presence of masking ligands, with binding particulary noticeable in the superficial layers of the cerebral cortex, the hippocampus and the thalamus. Very low binding was seen in the caudate nucleus, putamen or cerebellum. Our results are in agreement with the 5-CT binding study reported by Waeber *et al.* (1995) and illustrate that [^{3}H]SB-269970 is a suitable ligand to investigate the localisation of 5-HT$_7$ receptors in guinea pig brain.

Table 1 Distribution of [^{3}H]5-CT and [^{3}H]SB-269970 specific binding in guinea pig brain

Brain area	**[^{3}H]5-CT**	**[^{3}H]SB-269970**
Cingulate ctx.	10.20 ± 0.41	11.06 ± 1.16
Somatosensory ctx.	9.31 ± 0.13	10.01 ± 1.52
Auditory ctx.	9.34 ± 0.06	9.67 ± 0.56
Ectorhinal ctx.	9.46 ± 0.12	9.21 ± 1.02
Perirhinal ctx.	9.27 ± 1.46	10.17 ± 1.12
Entorhinal ctx.	9.28 ± 0.04	9.89 ± 0.97
Hippocampus	8.24 ± 0.03	7.31 ± 2.7
Thalamus	7.24 ± 0.06	6.97 ± 1.6
Caudate nucleus	1.67 ± 0.07	0.98 ± 0.1
Cerebellum	1.31 ± 0.17	1.27 ± 0.41

Data (nCi.mg^{-1} tissue) are expressed as means of 3 sections from 3 separate brains (±SEM). ctx = cerebral cortex.

Waeber, C. *et al.* (1995) Eur.J.of Pharmacology 283,31-46
Thomas, D.R. *et al.* (1999) Br .J.Pharmacology 128 232P

246P HUMAN MUSCARINIC M$_5$ AND M$_3$ CHOLINOCEPTOR COUPLING TO G-PROTEIN AND PHOSPHOLIPASE C ACTIVATION

P. Smith, R.M. Eglen[1] and S.R. Nahorski
Department of Cell Physiology and Pharmacology, University of Leicester, Leicester, LE1 9HN, UK
[1] Center for Biological Research, Neurobiology Unit, Roche Bioscience, Palo Alto, CA 94304,USA.

Evidence from molecular cloning indicates that there are five separate human genes that encode muscarinic receptor proteins (Caulfield, 1993). However, the relative inability to pharmacologically distinguish between M$_3$ and M$_5$ mucscarinic receptors has hampered investigations, particularly of the latter subtype (Reever et al, 1997).

In this study we have investigated the ability of different agonists to activate M$_3$ and M$_5$ cholinoceptors in an attempt to identify functional coupling differences at the level of G$\alpha_{q/11}$ and phospholipase C. Clones of CHO cells were chosen to match expression of M$_3$ and M$_5$ receptors ([^{3}H]-N-methylscopolomine binding: fmol mg^{-1} protein 178± 27.2 and 221± 36.8 respectively). Agonist-stimulated [^{3}H]-InsPx accumulation was determined following [^{3}H]-myo-inositol labelling (2.5μCi ml^{-1} for 48hrs) and [35S]GTPγS binding immunoprecipitation of G$\alpha_{q/11}$ was performed according to Akam et. al. (1998).

The ability of several agonists to stimulate M$_3$ and M$_5$ cholinoceptor-mediated [^{3}H]-InsPx accumulation revealed that whereas both methacholine and arecoline were equally effective at M$_3$ and M$_5$ receptors, oxotremorine M and pilocarpine more effectively activated M$_5$ receptors. This was apparent in the greater potency of the full agonist oxotremorine M and the larger maximal stimulation of the partial agonists oxotremorine and pilocarpine (refer to Table 1).

Table 1.
Agonist Activation of Phospholipase C Activity.

Agonist	M3	M5	M3	M5
	(-log EC$_{50}$)		Maximal stimulation	
Methacholine	5.6 ± 0.16	5.8 ± 0.05	100%	100%
Oxotremorine M	5.6 ± 0.03	6.4 ± 0.05	100%	100%
Arecoline	5.2 ± 0.14	5.0 ± 0.25	72%	70%
Oxotremorine	5.5 ± 0.45	5.8 ± 0.25	24%	62%
Pilocarpine	5.6 ± 0.07	5.3 ± 0.19	25%	36%

The ability of oxotremorine M (100μM) to stimulate [^{35}S]GTPγS binding to G$\alpha_{q/11}$ (membranes prepared from CHO M$_3$ and M$_5$ cells were incubated with agonist, 1nM [^{35}S]GTPγS, 1μM GDP in 10 mM $MgCl_2$, 100mM NaCl and 10 mM HEPES, pH 7.4, buffer for 2 minutes) following solubilisation and immunoprecipitation also revealed a greater maximal coupling of M$_5$ cholinoceptors at this level (378 % over basal for M$_3$ and 820 % over basal for M$_5$).

These data suggest that certain muscarinic agonists more effectively activate M$_5$ receptors than M$_3$ and this may reflect, in part, selective agonist-mediated coupling to G$\alpha_{q/11}$. Such agonist specific coupling suggest that different active conformations of the M$_5$ receptor could lead to differential coupling to G$\alpha_{q/11}$ and subsequent activation of phospholipase C. The nature of such differences may provide an opportunity to distinguish M$_3$ and M$_5$ cholinoceptor signalling in native tissues.

References.

Akam E.C., Challiss R.A.J. & Nahorski S.R. (1998) Br.J. Pharmacol., **125**, 24P.
Caulfield M.P. (1993) Pharmac.Ther., **58**, 319-179.
Reever C.M., Ferrari-Di-Leo G & Flynn D.D. (1997) Life Sci, **60**, 1105-1112.

247P CARBACHOL AND ACETYLCHOLINE MAY HAVE DIFFERENT MODES OF INTERACTION WITH MUTANT M_1 MUSCARINIC ACETYLCHOLINE RECEPTORS

S.D.C. Ward & E.C. Hulme, Division of Physical Biochemistry, National Institute for Medical Research, Mill Hill, London NW7 1AA

Carbamylcholine (carbachol) is frequently used as a 'non-hydrolysable' agonist to investigate the function of muscarinic acetylcholine receptors (mAChRs). Compared to acetylcholine (ACh), it has an amino group instead of a methyl group at the end of the side chain attached to the quaternary nitrogen.

A study on the M_5 mAChR suggested that carbachol interacted strongly with an asparagine residue which is conserved in all mAChRs (Spalding, *et al.*, 1998). However, a recent study in the M_1 mAChR which looked at the interactions made by ACh showed that the homologous asparagine was less important than the adjacent tyrosine residue, which is also conserved in all mAChRs (Ward, *et al.*, 1999). Therefore, it was decided to probe the interactions made by carbachol further to determine whether there are differences in the binding interactions made by ACh and carbachol.

All the experimental methods used are identical to those described by Ward, *et al.* (1999). The data obtained from radioligand binding studies and phosphoinositide turnover experiments are summarised in Table 1.

The results show: 1) Carbachol has reduced affinity and signalling efficacy at the wild-type M_1 mAChR, when compared to ACh. 2) Both removal of the Tyr381 hydroxyl group and the benzene ring gave reduced signalling efficacy and ligand affinity. 3) Mutation of Asn382 has a smaller effect on carbachol binding and signalling efficacy than removing the Tyr381 side chain.

The Asn382Ala mutation does not discriminate carbachol from ACh. However, Tyr381Phe produces a significant reduction in efficacy, that was not seen with ACh. This may indicate a significant occupancy of an unproductive binding mode by carbachol in the Tyr381Phe mutant, resulting from weakened binding of the side chain.

This work was funded by the Medical Research Council.

Lu, Z.-L., Curtis, C.A.M., Jones, P.G., *et al.* (1997) *Mol. Pharmacol.* 51, 234-241.

Spalding, T.A., Burstein, E.S., Henderson, S.C., *et al.* (1998) *J. Biol. Chem.* 273, 21563-21568.

Ward, S.D.C., Curtis, C.A.M. & Hulme, E.C. (1999) *Mol. Pharmacol.* 56, 1031-1041.

Table 1: Summary of data obtained from radioligand binding studies, phosphoinositide turnover experiments and efficacy calculations.

	Carbachol binding affinity			Carbachol induced phosphoinositide turnover				% Signalling
	pIC50	nH	n	pEC50	nH	% Response ‡	n	Efficacy
Wild-type	3.87 ± 0.03 †	0.85 ± 0.02	4	5.88 ± 0.10	0.61 ± 0.09	103 ± 5	6	63
Tyr381Phe	3.06 ± 0.07 *** †	1.06 ± 0.05	3	4.17 ± 0.03 ***	1.28 ± 0.26 *	77 ± 5 **	4	15
Tyr381Ala	3.11 ± 0.07 *** †§	1.03 ± 0.12	4	2.73 ± 0.12 *** §	0.84 ± 0.12	72 ± 2 **	4	4
Asn382Ala	Not measured			4.46 ± 0.06 ***	0.78 ± 0.13	116 ± 3	3	73 ††
dLoop	3.82 ± 0.15	0.86 ± 0.03	3	5.21 ± 0.09 **	1.15 ± 0.15 *	51 ± 2 ***	3	9
Asn382Ala-dLoop	3.44 ± 0.08 **	1.09 ± 0.19	4	4.13 ± 0.03 ***	1.10 ± 0.13 *	93 ± 13	3	2

The binding and functional data are shown as mean ± s.e.mean. t-test: *p<0.05, **p<0.01, ***p<0.001 vs. Wild-Type. † Data are from Ward, *et al.* (1999). Radioligand binding studies could not be performed on Asn382Ala (Ward, *et al.*, 1999) and thus Asn382Ala-dLoop binding data was used (††); the dLoop mutation enhances expression with little effect on ligand binding affinities (Lu, *et al.*, 1997). ‡ Phosphoinositide response is shown as % of the fold basal response produced by ACh at Wild-Type (4.4 ± 0.4). § The potency of the carbachol induced phosphoinositide response is not significantly different to the binding affinity. Signalling efficacy is shown as % of ACh efficacy at the wild-type (Ward, *et al.*, 1999).

248P A FILTRATION ASSAY FOR THE ROUTINE MEASUREMENT OF THE BINDING OF A RADIOLABELLED ALLOSTERIC LIGAND TO THE ALLOSTERIC SITE ON M_2 MUSCARINIC RECEPTORS

C. Tränkle, A. Mynett, O. Weyand[1], A. Popham[2], S. Lazareno[2], K. Mohr[1] & N.J.M. Birdsall, Division of Physical Biochemistry, National Institute for Medical Research, Mill Hill, London, NW7 1AA, UK, [1]Dept of Pharmacology & Toxicology, Institute of Pharmacy, University of Bonn, 53121 Bonn, Germany, and MRC Collaborative Centre, Mill Hill, London NW7 1AD.

[^{3}H]Dimethyl-W84 (N,N′-bis[3-(1,3-dihydro-1,3-dioxo-4-methyl-2H-isoindol-2-yl)propyl]- N,N,N′, N′-tetramethyl-1,6-hexanediaminium diiodide) is the first radioligand demonstrated to label the allosteric site on M_2 muscarinic receptors (Tränkle *et al.*, 1998). Under the ionic conditions used (4 mM Na_2HPO_4, 1 mM KH_2PO_4, pH 7.4, 23°C) the radioligand bound strongly to glass fibre filters. Consequently a centrifugation assay was developed but this exhibited high nonspecific binding for 0.3 nM [^{3}H]dimethyl-W84 [a non-saturable component (20%) and a saturable low affinity component (50-60%)]. Here we report a filtration assay procedure, using membranes from Chinese hamster ovary cells expressing M_2 receptors, in which the nonspecific binding is reduced considerably. [^{3}H]dimethyl-W84 (specific activity 154 Ci/mmol) was handled in 20 mM NaCl plus 0.01% bovine serum albumin (BSA) and the binding experiments (0,3 ml volume) were performed with 1.5 nM [^{3}H]dimethyl-W84 in 10 mM Hepes, 20 mM NaCl, and 0.01% BSA, pH 7.4 at 23°C for 2h. The glass fibre filtermats were pretreated with 0.2% polyethyleneimine. Filtration on a Tomtech 96-well Harvester (Wallac®) was followed by a single washing step (0.8 ml 100 mM NaCl). This protocol minimised adsorption of the radioligand during the handling, incubation and filtration, allowing a relatively high ratio of specific: nonspecific binding (up to 3:1). Inhibition of [^{3}H]dimethyl-W84 binding by non-labelled dimethyl-W84 (0.3 nM - 100 μM) was compatible with an interaction at a single site (pK_D = 8.3 ± 0.1, mean ± s.e.m, n=3). No saturable component of nonspecific [^{3}H]dimethyl-W84 binding was observed. The receptor specificity of [^{3}H]dimethyl-W84 binding was confirmed in inhibition studies using several allosteric modulators. The Hill slopes were not different from unity (F-test, P>0.05) and all ligands, at high concentrations, inhibited the same asymptotic fraction of total radioligand binding. The pK_I values were 7.3 ± 0.1 (n=2) for W84 (hexane-1,6-bis(dimethyl-3'-phthalimido-propyl-ammonium bromide)), 7.3 ± 0.03 (n=5) for gallamine, 6.9 ± 0.3 (n=2) for alcuronium and 5.1 ± 0.2 (n=2) for strychnine which were compatible with the expected potencies. Gallamine (10 μM) was selected to define nonspecific [^{3}H]dimethyl-W84 binding. Saturation experiments with [^{3}H]dimethyl-W84 (pK_D = 8.7 ± 0.1) gave a B_{max} of 901 ± 74 (n=3) fmol/mg protein which matched the B_{max} = 795 ± 36 fmol/mg protein (n=3) found for the muscarinic antagonist [^{3}H]N-methylscopolamine (pK_D = 9.8 ± 0.1), confirming the 1:1 stoichiometry of the binding sites.

In conclusion, a filtration assay for measuring radioligand binding at the allosteric site of M_2 receptors is described that should allow more direct insight into the kinetic and equilibrium interactions of ligands binding to the allosteric site.

Tränkle, C., Mies-Klomfaß, E., Botero Cid, H.M. *et al.*, (1998) *Mol. Pharmacol.* 54, 139-145.

249P THE VOLTAGE-GATED SODIUM CHANNEL β3 SUBUNIT MODULATES αIII CHANNEL GATING IN *XENOPUS* OOCYTES

E.B Stevens, R.D. Pinnock & K. Lee
Parke Davis Neuroscience Research Centre, Cambridge University Forvie Site, Cambridge, CB2 2QB, U.K.

The type III sodium channel α subunit is highly expressed during development of the CNS and is down-regulated postnatally. The sodium channel β1 subunit has been shown to functionally couple to αIII in *Xenopus* oocytes, but is absent from the developing embryo (Patton *et al.*, 1994). Accessory proteins with different molecular weights to β1 have been immunprecipitated from embryonic brain using polyclonal anti-β1 antibodies (Sutkowski & Catterall, 1990), suggesting that other β subunits may associate with αIII. Recently we have isolated a novel β subunit, β3, from PC12 cells using subtractive cloning (Morgan *et al.*, *submitted*). In contrast to β1, β3 is highly expressed during development (Shah *et al.*, *this meeting*). The present study investigates whether β3 can functionally couple to αIII in *Xenopus* oocytes.

Xenopus laevis were anaesthetized by immersion in 0.3% (w/v) 3-amino benzoic acid solution before surgical removal of ovarian lobes. Oocytes were injected with αIII, β1 and β3 cRNAs and Na^+ currents were measured 4-7 days later. Currents were recorded using two-electrode voltage clamp in an external solution containing 96 mM NaCl, 2 mM KCl, 1.8 mM $CaCl_2$, 1 mM $MgCl_2$, 5 mM Hepes, pH 7.6.

Na^+ currents recorded from oocytes expressing αIII subunit had slow rates of inactivation which were described by two exponential components (τ_1 = 1.1 ± 0.1 ms and τ_2 = 60 ± 4.8 ms at −10 mV, n = 4, mean ± S.E.M.). Co-expression of β1 or β3 with αIII subunit altered the inactivation time course. β1 and β3 had no effect on the time constants of decay of αIII, however the relative amplitudes of the exponential components were significantly different ($p<0.01$, Student t test). The percentage of current described by the fast time constant of inactivation at −10 mV were 6.5 ± 1.6%, 71 ± 3.5% and 29 ± 1.2% (n = 4-5) for αIII, αIII+β1 and αIII+β3, respectively. The rate of recovery from inactivation of αIII was also significantly ($p<0.01$) altered by co-expression of β1 or β3. Time course of recovery from inactivation of αIII, αIII+β1 and αIII+β3 were described by similar time constants (for αIII, τ_1 = 5.4 ± 0.2 ms, τ_2 = 112 ± 9 ms, n = 4). However recovery of αIII+β1 and αIII+β3 were described predominantly by the fast time constant (72.5 ± 1.3% and 70.2 ± 2.6% of total current, respectively, n = 4) compared with αIII expressed alone (29 ± 1.2% of total current, n = 4). Coexpression of αIII with β1 or β3 caused a significant ($p<0.01$) change in the voltage-dependence of inactivation. The voltage of half-maximal inactivation (V½) for αIII, αIII+β1 and αIII+β3 were −26 ± 0.8 mV, -41.7 ± 0.3 mV and −37.8 ± 0.3 mV, respectively, while the corresponding slope factors were 7 ± 0.5 mV, 5.5 ± 0.2 mV and 7.5 ± 0.3 mV (n = 4).

In conclusion this study demonstrates that αIII couples to both β1 and β3 in *Xenopus* oocytes. β1 and β3 have significantly different effects on inactivation kinetics and voltage-dependence of inactivation of αIII. The present study contrasts with a previous report which shows little effect of β1 on αIII inactivation time constants (Patton *et al.*, 1994). Given that the time course of expression of αIII and β3 overlap during development of the rat CNS (Shah *et al.*, *this meeting*), it is possible that β3 may form a multimeric complex with αIII during development.

Patton, D. E., Isom, L. L., Catterall, W.A. *et al.* (1994) *J. Biol. Chem.* **269**: 17649-55
Morgan, K., Stevens, E. B., Shah, B. *et al. Submitted to PNAS*
Shah, B., Pinnock, R. D., Lee, K. *et al. This meeting*
Sutkowski, E. M. & Catterall, W.A. (1990) *J. Biol. Chem.* **265**: 12393-9.

250P THE VOLTAGE-DEPENDENT SODIUM CHANNEL SUBUNIT B3 IS THE PREDOMINANT β SUBUNIT EXPRESSED DURING DEVELOPMENT IN RAT CNS

B.S. Shah, R.D. Pinnock, K. Lee, & A.K. Dixon.

Parke Davis Neuroscience Research Centre, Cambridge University Forvie Site, Robinson Way, Cambridge, CB2 2QB.

Rat brain voltage gated sodium channels are thought to be composed of three glycoprotein subunits; a pore-forming alpha subunit and two auxiliary subunits, β1 and β2 (Catterall, 1992). Alpha subunits form a heterogenous group, whilst at present only two beta subunits have been identified. Recently we have identified a novel beta subunit, β3, which is related to β1 exhibiting 50% homology. β1 and β3 show a complimentary pattern of distribution in adult rat (Morgan *et al. submitted*). No expression of β1 has been detected in the embryo (Sutkowski and Catterall 1990). Therefore, in this study we have examined the distribution of β3, and compared it to the distribution of β1 and the embryonic alpha subunit α3, during rat development by semi-quantitative *in situ* hybridisation histochemistry.

Adjacent 5μm thick sections of whole rat embryo at stages E10, E15, E17 and E19 and brain at postnatal stages P1, P3, P9, P14 and adult were cut on a cryostat and mounted on poly-l-lysine slides. Mounted tissue was fixed in 4% paraformaldehyde. Hybridisation buffer containing 45bp long radio-labelled oligoprobes diluted to a concentration of 3000cpm/μl, was added onto each slide and hybridised at 42°C overnight. Slides were subjected to stringency washes and apposed to X-ray film. Slides were also coated with liquid emulsion, developed, and stained in cresyl violet. Quantification of autoradiographs for relative optical density (ROD) in arbitrary units was carried out using an MCID image analyser.

In situ hybridisation analysis showed α3 and β3 mRNAs to be absent at embryonic stage E10. However, the expression of α3 and β3 appeared to steadily increase in all areas of the CNS following this time point, being most abundant by stage E19. In contrast, no signal was observed for β1 mRNA during any of the embryonic stages examined. Thus high levels of β3 mRNA was observed throughout the brain in regions such as the hippocampus, thalamus, colliculi, and to a lower extent in the developing cerebellum. High levels of β3 were also found extending down to the spinal cord. α3 showed a similar pattern of distribution to β3, although its expression in the cerebellum was slightly higher. Postnatally in the thalamus, expression of α3 and β3 decreased from P1 (18.4 ± 1.4 and 20.8 ± 0.8 ROD units respectively) to adult (0.01 ± 0.04 and 2.7 ± 0.05 units respectively), while β1 mRNA expression increased to maximum at P14 (29.2 ± 2.4 units). The cortex showed decrease in α3 and β3 expression from P1 (14.1±0.61 and 25.7±1.9 units respectively) to adult (0.5±0.3 and 9.8 ± 1.9 units respectively). β1 expression peaked at P14 (12.1 ± 1.7 units) in the cortex. In the striatum, α3 and β3 expression decreased from P1 (12.9±0.58 and 25.4±1.9 units respectively) to adult (1.0±0.05 and 12.8±0.5 units respectively) while β1 expression remained low (2.1±0.36units). Within the hippocampus, α3 expression remained constant throughout development (18.2±1.1units) whilst β1 and β3 expression increased to a maximum level at P14 (51.3±4.0 and 146.8±15.1units respectively)

In conclusion, we have performed a detailed distribution analysis of the voltage gated sodium channel auxiliary subunits β1 and β3 during rat development. The data indicates that β3 is the predominant β subunit during development, and its embryonic distribution closely matches that of α3.

Catterall W.A. (1992). *Physiol. Rev.* **72**: S15-48
Morgan K. *et al.* (1999). *submitted to P.N.A.S.*
Sutkowski E.M. and Catterall W.A. (1990) *J. Biol. Chem.* **265** : 12393-12399

251P PERTUSSIS TOXIN-SENSITIVE ACTIVATION OF MAP KINASE BY THE HISTAMINE H_1 RECEPTOR IN DDT$_1$MF-2 CELLS

A.J. Robinson and J.M. Dickenson, Department of Life Sciences, Nottingham Trent University, Clifton Lane, Nottingham NG11 8NS.

Histamine H_1-receptors are $G_{q/11}$-protein linked and stimulate phospholipase C activation leading to inositol 1,4,5-trisphosphate (IP_3)-induced Ca^{2+} release and protein kinase C (PKC) activation (Hill *et al*, 1997). Recent studies have shown that $G_{q/11}$-protein coupled receptors also activate the mitogen-activated protein kinase (MAPK) signalling pathway (Sudgen & Clerk, 1997). The aim of this study was to investigate whether the endogenous histamine H_1 receptor in hamster vas deferens DDT$_1$MF-2 smooth muscle cells activates the MAPK signalling pathway.

DDT$_1$MF-2 cells were grown in 6-well plate cluster dishes and serum starved for 16 h, in DMEM containing 0.1% bovine serum albumin, prior to determining MAPK activation. After agonist stimulation (5 min unless otherwise stated) cells were solubilised in lysis buffer as described previously (Dickenson *et al*, 1998). Protein samples (25 μg) were then separated using 10% SDS-PAGE and transferred to nitrocellulose membranes. MAPK activation was determined by immunoblotting using an anti-phospho-MAPK antibody, which detects activated p42-kDa (ERK1) and p44-kDa (ERK2) MAPK isoforms. Data are expressed as mean ± s.e.m. and statistical significance was determined by Student's *t* test.

Stimulation of DDT$_1$MF-2 cells with histamine produced a rapid and transient activation of MAPK with dominant activation of p42-kDa MAPK. The MAPK response to histamine was concentration-dependent ($p[EC_{50}]$ = 6.1 ± 0.3; n=4) and time-dependent (peak activation occurring at 5 min). MAPK responses to histamine (100 μM) were antagonised by the histamine H_1 receptor antagonist, mepyramine, yielding an apparent K_D value of 3.1 ± 0.8 nM (n=3). Responses to histamine (100 μM) were inhibited by pre-treatment (30 min) with the MAP kinase kinase 1 (MEK1) inhibitor, PD 98059 (50 μM; 89 ± 5% inhibition; n=3; $P<0.05$) and the tyrosine kinase inhibitor, genistein (100 μM; 87 ± 8% inhibition; n=4; $P<0.05$). G_i/G_o-protein coupled receptors are known to activate MAPK via a pathway involving phosphatidylinositol 3-kinase (PI-3K; Sudgen & Clerk, 1997). Pre-treatment (30 min) of cells with the selective PI-3K inhibitor, wortmannin (100 nM), inhibited the MAPK response to 100 μM histamine by 92 ± 3% (n=3). The role of Ca^{2+} and PKC in MAPK activation by the histamine H_1 receptor was investigated using Ca^{2+}-free Hanks/HEPES buffer containing 0.1 mM EGTA (to prevent Ca^{2+} influx) and the selective PKC inhibitor Ro 31-8220. Pre-treatment (30 min) of DDT$_1$MF-2 cells with Ro 31-8220 (10 μM) inhibited 100 μM histamine-induced MAPK activation by 41 ± 7% (n=6; $P<0.05$). No significant reduction in 100 μM histamine-induced MAPK activity was observed in the absence of extracellular Ca^{2+} (72 ± 11% of control response; n=3). Finally, pre-treatment (16 h) of DDT$_1$MF-2 cells with pertussis toxin (PTX, 100 ng ml^{-1}) reduced responses to 100 μM histamine (75 ± 13% inhibition; n=6; $P<0.05$), suggesting that the histamine H_1 receptor couples to MAPK via G_i/G_o proteins.

In summary, we have shown that stimulation of the endogenous histamine H_1 receptor in DDT$_1$MF-2 cells induces MAPK activation via MEK1, PI-3K, PKC, and tyrosine kinases. Furthermore, it is notable, that histamine H_1 receptor-mediated MAPK activation was PTX-sensitive, indicating this receptor is also coupled to G_i/G_o proteins in DDT$_1$MF-2 cells.

Dickenson, J.M., Blank, J.L., & Hill, S.J. (1998) Br. J. Pharmacol. **124**, 1491-1499.
Hill, S.J., *et al*, (1997) Pharmacol. Rev. **49**, 253-278.
Sugden, P.H. & Clerk, A. (1997) Cell. Signal. **9**, 337-351.

252P CHARACTERISATION OF NEUROPEPTIDE NPY$_1$ AND NPY$_2$ RECEPTOR-MEDIATED STIMULATION OF A MITOGEN-ACTIVATED PROTEIN KINASE REPORTER GENE IN CHO CELLS

J. Camacho and S. Rees, Biological Chemistry Unit, Glaxo Wellcome Medicines Research Centre, Stevenage, Hertfordshire, England, SG1 2NY (Introduced by Alan Wise).

Neuropeptide Y (NPY) is an abundant brain peptide which modulates a number of physiological processes such as the regulation of the cardiovascular system. Agonist activity at these receptors leads to an activation of $G\alpha_i$-family G-proteins to increase cytoplasmic calcium concentration and to inhibit adenylyl cyclase activity (Nie and Selbie 1998). The NPY$_1$ receptor has also been shown to activate MAP kinase (Mannon and Raymond, 1998)

CHO cell lines stably expressing one of the human NPY$_1$ and NPY$_2$ receptors together with a MAP kinase reporter gene were used to develop a reporter gene assay to study ligand efficacy at these receptors. The reporter gene system consists of the chimeric transcription factor Gal4/Elk-1 together with a second plasmid containing the firefly luciferase gene under the transcriptional control of a Gal4 responsive promoter (Bevan *et al.*, 1998). For assay, cells were seeded at $1x10^4$ cells/well into black 96 well plates, and grown overnight at 37°C. The growth media was removed and replaced with medium without phenol red or serum and cells were incubated for a further 24 hours. MAPK Reporter Assays were performed in a final volume of 100μl to which NPY peptide (10μM-1nM) was added. The plates were incubated at 37°C for 4 hours and luciferase was measured using the Luclite kit and plates were counted on a Packard Top Count microplate luminometer.

NPY activity at the NPY$_1$ and NPY$_2$ receptors resulted in a dose dependent increase in the activity of the MAP kinase reporter gene with EC_{50} values of 33 (14-74)nM (confidence interval, n=4) at the NPY$_1$ receptor and 9.5(4.9-19)nM (n=6) at the NPY$_2$ receptor. These values are similar to those reported in other cell based assays (Nie and Selbie, 1998). To assess the suitability of these cell lines for compound screening the stability of the reporter read-out was followed over 22 passages in culture. It was found that the EC_{50} was unchanged and there was no change in the fold response to NPY. The stability of this response to DMSO was also studied and it was found that the response to NPY at either receptor was unaffected by DMSO concentrations of up to 1%.

In conclusion the NPY$_1$ and NPY$_2$ receptors have been stably expressed in CHO cells where they can activate a MAPK reporter construct. These studies indicate that these cell lines would be suitable for automated high throughput compound screening.

Bevan, N., Scott, S., Shaw P., *et al.*, (1998) Neuroreport 9, 2703-2708.
Nie, M. & Selbie, L. A. (1998) Reg. Peptides 75-76, 207-213.
Mannon, P. J. & Raymond, J. R. (1998). Biochem. Biophysi. Res. Comm. 246, 91-94.

253P PURINERGIC RECEPTOR REGULATION OF MAP KINASE REPORTER GENES

S Scott, K.Patel*, J. Camacho, D. Cousens*, F.H. Marshall* and E.S. Rees, Biological Chemistry Unit *Molecular Pharmacology. Glaxo Wellcome Medicines Research Centre, Stevenage, Hertfordshire, England, SG1 2NY.

It has previously been shown that the P2Y Purinergic receptors couple to $G\alpha_{q/11}$ G-proteins to cause an increase in intracellular calcium and the activation of the MAPK cascade via ERK and JNK. In the present study we have investigated the use of MAP kinase reporter genes to study agonist activity at these receptors.

The human $P2Y_1$, $P2Y_4$ and $P2Y_6$ receptors were stabley expressed in rat 1321N1 astrocytoma cells. A Fluorometric Light Imaging Plate Reader (FLIPR) assay of agonist stimulated Ca^{2+} mobilisation was used to demonstrate receptor expression and function. Cells were grown for 3 days prior to assay in black 96 well plates and then incubated with 4μM FLUO-3AM, at 37°C in 5%CO_2 for 90mins and washed once in Tyrodes buffer (145mM NaCl, 10mM glucose, 2.5mM KCl, 1.5mM $CaCl_2$, 10mM HEPES, pH7.4) containing 2.5mM probenicid. Basal fluorescence (11,000 – 15,000 FIU) was determined prior to drug additions. Cell fluorescence was monitored (λ_{Ex} =488nm, λ_{Em}=540nm) in the FLIPR following exposure of increasing concentration of agonist (20μl). Receptor activation of the MAP kinase cascade was studied using a series of reporter gene constructs which were made up of one of the chimeric transcription factors Gal4/Elk-1 or Gal4/Sap1a together with a second plasmid containing luciferase reporter gene under the transcriptional control of a Gal4 responsive promoter, Bevan *et al.*, 1998.

Transient transfections were performed using LipofectAMINE reagent. The transfection cocktail containing 5μg of either pSG/Gal4/Elk-1 or pSG/Gal4/Sap1a together with 5μg p5Xgal4/luicferase. This was replaced with 100μl/well of growth medium and cells were maintained for 24 h at 37°C. Following transfection cells were serum starved for 24h in phenol red free and serum free quiescence media. When assayed cells were stimulated with appropriate agonist in a final volume of 100μl for 15min. The drug solution was replaced with fresh quiescence medium (100μl/well) and cells left for 5h. Luciferase activity was assayed using the Luclite reagent and the luminescence measured on Packard Top Count using a 1s/well count.

Table 1

	DRUG	REPORTER	pEC_{50} FLIPR ±SEM	pEC_{50} REPORTER
P2Y1	ADP	Gal4/Elk-1	7.7± 0.08 (n=3)	7.2 ± 0.02 (n=3)
P2Y4	UTP	Gal4/Sap1a	6.9 ± 0.16(n=3)	7.5±0.23 (n=3)
P2Y6	UDP	Gal4/Sap1a	6.5± 0.08(n =3)	6.2±0.09(n=4)

All agonist profiles were in good agreement with EC_{50} data generated on the FLIPR as shown in Table 1. This raises the possibility of using MAP kinase reporter genes as tools for the pharmacological characterisation of members of the P2Y purinergic receptor family.

Bevan, N., Scott, S., Shaw P., *et al.*, (1998) Neuroreport 9, 2703-2708

254P COMPARISON OF THE ABILITIES OF PARTIAL AGONISTS TO MEDIATE PHOSPHORYLATION AND DESENSITISATION OF A G_q-COUPLED RECEPTOR

A. Rae & A.B. Tobin, (Introduced by S.R. Nahorski), Dept of Cell Physiology & Pharmacology, University of Leicester, University Road, Leicester, LE1 9HN.

A number of studies have demonstrated a correlation between the efficacy of an agonist and it's ability to produce G protein-coupled receptor (GPCR) phosphorylation and desensitisation (Reviewed by Clark *et al.* 1999). However these studies have focused mainly on adenylyl cyclase-coupled GPCRs, such as the β_2-adrenoceptor (January *et al.* 1997).

The aim of this study was to examine the relationship between agonist efficacy and receptor phosphorylation and desensitisation for the phospholipase C-coupled muscarinic M3 receptor.

This was performed using Chinese hamster ovary cells transfected with cDNA for the m3 receptor (CHO-m3 cells). Agonists used were the full muscarinic agonist carbachol and the partial muscarinic agonists arecoline, oxotremorine and pilocarpine. Inositol (1,4,5)-trisphosphate (IP_3) concentrations were determined by a radioligand receptor assay (Challiss *et al.*). Maximal IP_3 production was seen at 10 seconds of agonist stimulation, and desensitisation was achieved by a 5 min prestimulation of the cells, followed by a 5 min rest period before subsequent stimulation. Receptor phosphorylation was assessed using ^{32}P-orthophosphate incorporation into the receptors.

It was found that the ability to desensitise carbachol-mediated IP_3 production was similar for both full and partial agonists. Prestimulation of a carbachol response by carbachol itself resulted in an average desensitisation of IP_3 production by 47.9 ± 5.9 % (all experiments n=3). Prestimulation using arecoline, oxotremorine or pilocarpine desensitised carbachol-mediated IP_3 production by 44.3 ± 6.8 %, 44.4 ± 10.2 % and 50.8 ± 5.0 %, respectively.

Arecoline, oxotremorine and pilocarpine induced m3 receptor phosphorylation to a similar extent (approximately 4-8 fold over basal) and rate (maximal phosphorylation complete within 5 seconds) as the full agonist carbachol. Furthermore, initial analysis of the concentration-response curve for receptor phosphorylation indicates that they are similar for both carbachol and arecoline.

These data suggest that, a) the muscarinic partial agonists used here are just as effective at desensitising m3 receptor-mediated IP_3 production as is the full agonist carbachol, and b) the partial agonists act as full agonists with regard to receptor phosphorylation.

Challiss, R.A.J. *et al.* (1988) Biochem Biophys Res Commun. 157, 684-691.
Clark, R.B. *et al.* (1999) *Trends Pharm Sci.* 20, 279-286.
January, B. *et al.* (1997) *J Biol Chem.* 272, 23871-23879.

This work was supported by the Wellcome Trust.

255P EFFECT OF A POINT MUTATION IN THE THIRD INTRACELLULAR LOOP OF THE HUMAN DOPAMINE D_{2short} RECEPTOR ON AGONIST AFFINITY, POTENCY AND EFFICACY

J. Wilson, [1]J. A. Javitch & P. G. Strange. School of Animal and Microbial Sciences, University of Reading, P. O. Box 228, Whiteknights, Reading, RG6 6AJ. [1]Centre for Molecular Recognition, Columbia University, New York 10032, USA.

Mutations in the C-terminal portion of the third intracellular loop of many G protein-coupled receptors have led to the observation of constitutive (agonist-independent) activity. The Extended Ternary Complex Model (Samama *et al.*, 1993) predicted that constitutively active receptors would demonstrate several properties, including increased agonist affinity and potency and an enhanced basal activity. In the absence of an agonist, receptors spontaneously isomerise between an inactive (R) and a partially activated (R*) conformational state, with only the R* conformation being able to couple to G proteins. Agonists display a preferentially higher affinity for R* and R*G states and stabilise the active (R*G) conformation of the receptor. In the present study, a threonine in the third intracellular loop (residue 343) of the human D_{2short} dopamine (D_{2S}) receptor was mutated to an arginine residue. In order to determine if this mutated (T343R) receptor displayed characteristics of constitutive activity, a selection of structurally-related dopamine agonists was used to determine any changes in binding affinity or functional potency, the latter using an adenosine 3',5'-cyclic monophosphate (cAMP) accumulation assay.

Membrane preparations of Chinese hamster ovary (CHO) cell lines stably expressing wild-type (WT) and T343R D_{2S} receptors were used to determine binding affinities of dopamine agonists by competition versus [^{3}H]spiperone (0.25 nM). Agonist inhibition of cAMP accumulation was performed on whole CHO cells following addition of forskolin (10 μM), as previously described (Hall & Strange, 1997). All competition experiments for dopamine agonists were best described by a two site model. The affinities of dopamine and *meta*- tyramine for the high (K_h) and low (K_l) affinity binding sites were all increased for the T343R receptor compared with the WT. In contrast, binding affinities of *para*-tyramine and *beta*-phenylethylamine were not significantly different between the two receptors (Table 1). Furthermore, all agonists displayed an increased (4 - 9 fold) potency at T343R receptors at inhibiting forskolin-stimulated cAMP levels. However, there were no significant differences in the maximal inhibition of cAMP accumulation between WT and T343R receptors for each agonist (Table 1).

Previous work has shown that substitution of a threonine residue with an arginine in the human D_{2S} receptor resulted in an increased affinity for dopamine and NPA in both the absence and presence of GTP (Wilson *et al.*, 1999). This present study extends these findings, but demonstrates that this increased affinity is not observed for all ligands investigated. However, all agonists had an increased potency to inhibit cAMP accumulation in the T343R receptor, suggesting that this mutated receptor may have an increased tendency to adopt the R* conformation.

This work was supported by the BBSRC and AstraZeneca (Charnwood).

Hall, D.A. & Strange, P.G. (1997) *Br. J. Pharmacol.*, 121, 731-736.
Samama, P., Cotecchia, S., Costa, T. & Lefkowitz, R.J. (1993) *J. Biol. Chem.*, 268, 4625-4636.
Wilson, J., Javitch, J.A. & Strange, P.G. (1999) *Br. J. Pharmacol.*, 126, 109P.

Table 1. Binding affinity, potency and efficacy of dopamine and dopamine analogues at WT and T343R receptors

	pK_h		pK_l		pIC_{50}		% dopamine inhibition	
	WT	T343R	WT	T343R	WT	T343R	WT	T343R
Dopamine	6.81 ± 0.05	7.79 ± 0.07*	5.05 ± 0.07	6.07 ± 0.19*	7.54 ± 0.15	8.46 ± 0.28*	100	100
meta-tyramine	6.33 ± 0.09	7.61 ± 0.02*	4.62 ± 0.11	5.61 ± 0.18*	6.33 ± 0.06	6.98 ± 0.11*	96.3 ± 1.8	93.5 ± 6.5
para-tyramine	5.12 ± 0.10	5.01 ± 0.32	3.02 ± 0.20	3.07 ± 0.47	4.42 ± 0.28	5.32 ± 0.27*	88.7 ± 4.2	82.6 ± 6.2
beta-phenylethylamine	5.24 ± 0.19	5.63 ± 0.22	3.29 ± 0.23	3.79 ± 0.46	5.40 ± 0.14	6.27 ± 0.12*	86.5 ± 7.3	90.7 ± 3.6

Data are mean ± s.e.mean of 3 - 6 experiments. *, $p < 0.05$ compared with corresponding WT value (Student's *t* test).

256P ADENOSINE A_1 RECEPTOR-MEDIATED ACTIVATION OF PROTEIN KINASE B IN DDT_1MF-2 CELLS

John M. Dickenson, Department of Life Sciences, Nottingham Trent University, Clifton Lane, Nottingham NG11 8NS.

The serine/threonine protein kinase B (PKB, also called Akt) is an important regulator of various physiological processes including glucose metabolism and apoptosis (for review see Downward, 1998). Furthermore, it is now well established that PKB is a major downstream target of phosphatidylinositol 3-kinase (PI-3K) activation in response to insulin and other growth factors (Coffer *et al.*, 1998). Several recent reports have demonstrated that G protein-coupled receptors including M_1 and M_2 muscarinic receptors activate PKB (Murga *et al.*, 1998). The aim of the present study was to investigate whether the endogenous adenosine A_1 receptor in hamster vas deferens DDT_1MF-2 smooth muscle cells activates the PKB signalling pathway.

DDT_1MF-2 cells were grown in 6-well plate cluster dishes and serum starved for 16 h, in DMEM containing 0.1% bovine serum albumin, prior to determining PKB activation. After agonist stimulation (10 min unless otherwise stated) cells were solubilised in lysis buffer as described previously (Dickenson & Hill, 1998). Protein samples (25 μg) were then separated using 10% SDS-PAGE and transferred to nitrocellulose membranes. PKB activation was determined by immunoblotting with an antibody (anti-phospho-PKB) that detects only activated PKB. Statistical significance was determined by Student's *t* test ($P<0.05$ was considered statistically significant). Data are expressed as mean ± s.e.m.

Initial experiments using serum-deprived DDT_1MF-2 cells revealed that insulin (100 nM) and the selective adenosine A_1 receptor agonist N^6-cyclopentyladenosine (CPA; 1 μM) induced increases in PKB phosphorylation of 210 ± 15% (n=3; $P<0.05$) and 207 ± 9% (n=3; $P<0.05$) above basal, respectively. The PKB response to CPA was concentration-dependent ($p[EC_{50}]$ = 9.03 ± 0.14; n=5) and time-dependent (peak activation occurring at 10 min; 221 ± 34% increase above basal PKB activity; n=4). Responses to CPA (10 nM) were antagonised by the adenosine A_1 receptor antagonist, 1,3, dipropylcyclopentylxanthine (DPCPX) yielding an apparent K_D value of 2.5 ± 0.2 nM (n=3). Pertussis toxin pre-treatment (PTX; 100 ng ml^{-1} for 16 h) completely inhibited the response to 1 μM CPA, demonstrating that G_i/G_o protein(s) couple the adenosine A_1 receptor to PKB in DDT_1MF-2 cells. In contrast, PTX pre-treatment had no significant effect on insulin-induced PKB activation (PKB phosphorylation increased 225 ± 24% above basal in control cells and 217 ± 17% above basal in PTX-treated cells; n=4). Pre-treatment (30 min) of DDT_1MF-2 cells with the selective PI-3K inhibitor, wortmannin (100 nM) completely blocked the activation of PKB elicited by CPA (1 μM) and insulin (100 nM). Basal PKB activity was also abolished following 30 min exposure to wortmannin.

In summary, we have shown that stimulation of the endogenous adenosine A_1 receptor in DDT_1MF-2 cells induces PKB activation via PTX-sensitive G_i/G_o protein(s) and PI-3K. These observations extend our knowledge of known signal transduction pathways that are activated following adenosine A_1 receptor stimulation. However, further studies are required in order to determine whether PKB activation by the adenosine A_1 receptor contributes to the physiological functions of adenosine.

Dickenson, J.M. & Hill, S.J. (1998) Eur. J. Pharmacol. **355,** 85-93.
Downward, J. (1998) Curr. Opin. Cell Biol., **10,** 262-267.
Coffer, P.J., Jin, J. & Woodgett, J.R. (1998) Biochem. J. **335,** 1-13.
Murga, C., Laguinge, L., Wetzker, R., Cuadrado, A. & Gutkind, J.S. (1998) J. Biol. Chem., **273,** 19080-19085.

257P [^{3}H]-ZM 241385 BINDING TO ENDOGENOUS A_{2A} ADENOSINE RECEPTORS IS REGULATED BY AGONIST PRETREATMENT AND GRK2

J.M.Willets, A.-L. Matharu and E.Kelly, Department of Pharmacology, School of Medical Sciences, University of Bristol, Bristol BS8 1TD

We have previously shown that NG108-15 mouse neuroblastoma x rat glioma cells express functional A_{2A} adenosine receptors (Mundell *et al.*1998). In the present study, we used the selective A_{2A} adenosine ligand [^{3}H]-ZM 241385 ([2-^{3}H] 4-(2-(7-amino-2-(2-furyl)[1,2,4]triazolo[2,3-a][1,3,5]triazin-5-ylamino) ethyl)phenol) to label these receptors. NG108-15 cells were cultured, and the binding assay was performed on a crude membrane fraction of cells, exactly as previously described (Willets et al., 1999). Non-specific binding was determined with the adenosine receptor agonist R-PIA (R(-)N^6-(2-phenylisopropyl) adenosine, 100 μM).

In NG108-15 cell membranes [^{3}H]-ZM 241385 bound to a single site with a K_D of 5.6 ± 0.4 nM and a B_{max} of 172.2 ± 14.0 fmol mg^{-1} protein (means ± s.e. mean of 4 separate experiments). Specific binding accounted for 50-60% of total binding at concentrations of [^{3}H]-ZM 241385 of 3nM or less. Adenosine receptor agonists displaced 3 nM [^{3}H]-ZM 241385 binding with the following IC_{50} values: CGS 21680 (2-p-(2-carboxyethyl) phenethylamino-5'-N-ethylcarboxamidoadenosine), 0.17 ± 0.04 μM; NECA (5'-(N-ethylcarboxamido)-adenosine), 0.23 ± 0.02 μM; R-PIA, 18 ± 2 μM; values are means ± s.e. mean from 3-4 separate experiments in each case. Pretreatment of cells with NECA (10 μM) led to a time-dependent reduction in the binding of 3 nM [^{3}H]-ZM 241385 to NG108-15 cell membranes (Table 1).

Agonist-induced desensitization of the A_{2A} adenosine receptor response (cAMP accumulation) preceded the loss of binding. After 30 min pretreatment with NECA (10 μM), the ability of CGS 21680 (10 μM) to stimulate adenylyl cyclase activity in cell homogenates (Willets et al., 1999) was reduced from 18.3 ± 2.6 to 12.4 ± 1.7 pmol cAMP min^{-1} mg^{-1} protein (means ± s.e. mean from 6 independent experiments; $p<0.05$, Student's t test).

Table 1. NECA-induced loss of 3 nM [^{3}H]-ZM 241385 binding to NG108-15 cell membranes. Specific binding is expressed as fmol mg^{-1} protein. Values are means ± s.e. mean of 4 separate experiments. NECA pretreatment reduced binding at 1, 4 and 24 h ($p<0.05$; repeated measures ANOVA with Bonferroni post test).

Time of NECA pretreatment (h)	Control (Water)	10 μM NECA pretreated
0.5	51.2 ± 2.8	48.5 ± 5.9
1	55.0 ± 2.0	30.8 ± 1.9*
4	53.5 ± 5.0	30.6 ± 6.1*
24	47.1 ± 2.5	15.9 ± 1.7*

In NG108-15 cells overexpressing GRK2 (G protein-coupled receptor kinase 2) by around 30-fold (termed B7 cells; Mundell et al., 1998), 3 nM [^{3}H]-ZM 241385 binding was less than in plasmid-transfected controls (termed P1 cells). In P1 cells, specific binding of 3 nM [^{3}H]-ZM 241385 was 163.2 ± 20.3 and in B7 cells 85.0 ± 11.6 fmol mg^{-1} protein (means ± s.e. mean of 4 independent experiments; $p<0.05$, Student's t test). This difference was absent in cells pretreated for 48 h with 0.25 units ml^{-1} adenosine deaminase; in P1 cells 180.8 ± 24.0 and in B7 cells 140.7 ± 14.6 fmol mg^{-1} protein. Together, these experiments indicate that [^{3}H]-ZM 241385 can be used to label endogenous A_{2A} adenosine receptors, and that membrane expression of this receptor is regulated by both agonist and changes in cellular GRK2 expression.

Mundell, S.J. *et al.* (1998) Brit. J. Pharmacol., 125, 347-356.
Willets, J.M. *et al.* (1999) J. Neurochem. 73, 1781-1789.

258P PROLONGED PHASE OF VASODILATATION TO ATP IN RAT MESENTERIC BED IS ATTENUATED BY P2X RECEPTOR DESENSITIZATION BUT DOES NOT INVOLVE CAPSAICIN-SENSITIVE SENSORY NERVES

V. Ralevic, School of Biomedical Sciences, University of Nottingham Medical School, Queen's Medical Centre, Nottingham NG7 2UH

Primary afferent nerves in rat mesenteric arteries, when activated by a variety of stimuli, release calcitonin gene-related peptide to mediate slow vasodilatation (Kawasaki *et al.*, 1988). It is known that ATP can excite primary afferents, via actions at ionotropic P2X receptors, indicating a role in nociception (Burnstock & Wood, 1996). However, it is not known if P2X receptors are present on the peripheral terminals of primary afferent nerves in blood vessels, and whether or not they can mediate a local change in blood vessel tone. Therefore, the present study investigated the possible involvement of primary afferent nerves and P2X receptors in vasodilatation to ATP of the rat mesenteric arterial bed.

Male Wistar rats (250-300g) were killed by exposure to CO_2 and decapitation. Mesenteric beds were isolated and perfused via the superior mesenteric artery with oxygenated Krebs' solution at 5 ml min^{-1} (Ralevic *et al.*, 1995). After 30min equilibration, preparations were preconstricted with methoxamine (10-50μM) and relaxant responses to ATP (0.005-5000nmol) were investigated. A group of mesenteries was pre-treated with capsaicin (10μM for 1h) in order to cause desensitization and/or neurotransmitter depletion of sensory nerves. Data are expressed as mean ± s.e.m. and analysed by Student's t test or ANOVA with Tukey's post test.

ATP elicited dose-dependent vasodilatation of the mesenteric beds that was biphasic at doses of 50nmol and greater, as described previously (Stanford & Mitchell, 1998). The pED_{50} (negative logarithm of the dose that elicits 50% relaxation) value for the first, rapid, phase of the response was 9.2±0.2 (n=8). The second phase of relaxation to 50nmol ATP was 55.9±3.0% of methoxamine-raised tone (n=8). The non-selective P2 receptor antagonist suramin (100μM), attenuated the first phase of relaxation to ATP; the pED_{50} value was 7.8±0.1 (n=5; $P<0.001$). The prolonged response to 50 and 500 nmol ATP was also significantly blocked by suramin; relaxation to 50nmol ATP was 15.2±3.2% (n=5; $P<0.001$). Capsaicin pre-treatment had no significant effect on either phase of vasorelaxation to ATP (n=6). Neither phase of relaxation was affected by the P1 receptor antagonist 8-sulfophenyltheophylline (1μM; n=6) or indomethacin (10μM, n=4). Desensitization of P2X receptors with α,β-methylene ATP (10μM) had no significant effect on the transient first phase of relaxation to ATP, but attenuated the second phase of relaxation to 50 and 500 nmol ATP; relaxation to 50 nmol ATP was 24.9±8.3% (n=8; $P<0.01$).

These data show that both the rapid and the prolonged phases of vasodilatation to ATP of the rat mesenteric arterial bed are mediated by P2 receptors, but neither phase involves capsaicin-sensitive afferents. This suggests that P2 receptors are either not expressed on capsaicin-sensitive afferent nerves in the rat mesentery, or that they do not mediate a vasomotor response. Adenosine P1 receptors and prostanoids do not contribute significantly to either phase of ATP-mediated vasorelaxation. Attenuation of the prolonged phase of the vasodilator response to ATP by desensitization of P2X receptors implicates smooth muscle P2X receptors in this response, and the mechanism underlying this is under investigation.

I thank the Royal Society for financial support.

Burnstock, G. & Wood, J.N. (1996) *Curr. Op. Neurobiol.*, **6**, 526-532.
Kawasaki, H. *et al.* (1988) *Nature* **335**, 165-167.
Ralevic, V. *et al.* (1995) *J. Pharmacol. Exp. Ther.* **274**, 64-71.
Stanford, S.J. & Mitchell, J.A. (1998) *Br. J. Pharmacol.*, **125**, 94P.

259P SLOW CLOSURE OF THE P2X$_7$ RECEPTOR ION CHANNEL AND ITS ASSOCIATION WITH AGONIST POTENCY

A.D. Hibell, A.D. Michel, Xing, M and P.P.A. Humphrey, Glaxo Institute of Applied Pharmacology, Dept of Pharmacology, University of Cambridge, Cambridge CB2 1QJ

The P2X receptors are a family of ligand-gated cation channels. The most recently identified member of this family, the P2X$_7$ receptor, exhibits several unusual properties including channel dilation and, at the rat orthologue, an increase in the time for responses to decay after agonist removal (Surprenant et al., 1996). This prolonged decay time, presumably represents slow closure of the channel, and is not observed at the mouse receptor (Chessell et al., 1998). In this study we have investigated further these species differences.

Whole cell patch clamp studies were performed using HEK293 cells expressing recombinant P2X$_7$ receptors (Chessell et al., 1998). ATP or 2'&3'-O-benzoylbenzoyl-ATP (BzATP) was repeatedly applied for 2s every 30s and the decay time calculated as the time taken for each response to decay from 95 to 5% of its maximum. In some studies ethidium accumulation was monitored (Michel et al., this meeting). Data are the mean±s.e.mean of at least 3 experiments.

Repeated applications of 100μM BzATP to the rat P2X$_7$ receptor increased the decay time (4.3±1.5 and 18±8s after the 1st and 5th applications; P<0.05; 1 way ANOVA) but did not change the decay time at the mouse or human P2X$_7$ receptors. There were species differences in BzATP potency (pEC$_{50}$ 5.2±0.1, 4.1±0.1 <4 at rat, human and mouse P2X$_7$ receptors, respectively). However, increases in decay time were also observed when using lower concentrations of BzATP at the rat receptor (significant increases achieved with 10 or 6 applications of 3 or 10μM BzATP, respectively).

ATP possessed >10 fold lower potency than BzATP at the three species orthologues and no changes in decay time occurred after applying 1mM ATP, suggesting that increased decay time was related to agonist potency. To test this hypothesis, studies were performed in NaCl-free, sucrose buffer since agonist potency at P2X$_7$ receptors is increased in this buffer (Michel et al., 1999). Patch-clamp studies could not be performed in sucrose buffer, however, BzATP (pEC$_{50}$ 6.6±0.1) and ATP (pEC$_{50}$ 5.5±0.2) stimulated ethidium accumulation in cells expressing rat P2X$_7$ receptors. Furthermore, it was possible to demonstrate slow closure of the P2X$_7$ channel after agonist removal by measuring ethidium accumulation. Thus, if cells were exposed to 4μM BzATP or 30μM ATP for 30s and washed, they remained permeable to ethidium for approximately 60 and 1-2 min, respectively. The pEC$_{50}$ of BzATP for rat P2X$_7$ receptors was reduced to 5.4±0.3 by 10mM $MgCl_2$ and in its presence, cells previously exposed to 4μM BzATP and washed, only remained permeable to ethidium for approximately 2-4min. BzATP and ATP possessed low affinity (pEC$_{50}$ <5) for mouse P2X$_7$ receptors and no sustained changes in ethidium permeability were detected after agonist removal.

In summary, prolonged decay times were only observed at rat P2X$_7$ receptors, for which agonists have highest affinity, and only with the high affinity agonist, BzATP. The duration of the persistent increase in ethidium permeability observed after agonist washout was also related to agonist potency. Given this association with potency, it is possible they both phenomena reflect slow dissociation of agonist from the P2X$_7$ receptor since differences in agonist affinity could be reflected in differences in agonist dissociation rates. Finally, the increase in decay time after repeated agonist application at the rat P2X$_7$ receptor may be due to the increase in agonist potency which occurs at P2X$_7$ receptors after agonist exposure (Michel et al., 2000).

Chessell, I.P. *et al.*, (1998). FEBS letts., 439, 26-30
Michel, A.D. *et al.*, (2000), Br.J.Pharmacol. This meeting.
Michel, A.D., Chessell, I.P. & Humphrey, P.P.A. (1999). Naunyn Schmiedebergs Arch. Pharmacol.,359,102-109
Surprenant, A. *et al.*, (1996). Science, 272, 735-738.

260P RUNDOWN OF ATP-INDUCED RESPONSE IN RECOMBINANT P2X$_4$ RECEPTORS IS NOT CALCIUM- OR ATP-DEPENDENT

C.A. Jones, I.P. Chessell, J. Simon, P.A. Smith & P.P.A. Humphrey. Glaxo Institute of Applied Pharmacology, University of Cambridge, Tennis Court Rd, Cambridge, CB2 1QJ

Previous studies have demonstrated that ionotropic, agonist-mediated responses of P2X$_4$ receptors are subject to a rundown phenomenon which appears to be distinct from straightforward desensitisation (Miller *et al.*, 1998; Jones *et al.*, 2000). This can be circumvented by patching rafts of 4 or more electrically coupled HEK-293 cells, but the reason for this has not been investigated. The aim of this study was therefore to further investigate the rundown of P2X$_4$ receptor-mediated responses.

Electrophysiological recordings were made from single cells or cell rafts of HEK-293 cells stably expressing rat, human or mouse recombinant P2X$_4$ receptors using a HEPES-buffered extracellular solution. Unless otherwise specified, all experiments were carried out using the whole cell patch clamp technique with a Cs-aspartate containing intracellular solution, with varying levels of ATP and free calcium. Perforated patch experiments were carried out by inclusion of amphotericin (100μg/ml), in the internal solution. Unless otherwise specified, ATP applications were separated by 5 min wash periods. Cells were voltage clamped at –90mV. Responses (mean±SEM) are expressed as a percentage of the maximum response to 10μM ATP in each experiment.

Magnitude of ATP-induced response in single cells expressing P2X$_4$ orthologues was significantly smaller after the 5th (human), 4th (rat) and 3rd (mouse) agonist application and declined to 38±14% (human), 36±10% (rat) and 27±5% (mouse) after 8 applications (n=6-9). When the same experiments were carried out on cell rafts, no significant variation in response was observed at any species orthologue with 8 ATP applications over a 35 min period, indicating that the changes in single-cell responses were not attributable to desensitisation.

Experiments using consecutive 2s ATP applications with 5, 10, 15 or 30 min wash periods indicated that response rundown was time- rather than application-dependent. For example, after 30min, mean responses declined to 33±5% of the initial response with 5min wash times (i.e. the 7th ATP application) and declined to 35±5% with 30min wash times (i.e. the 2nd ATP application).

When the perforated patch method was used to record from single cells expressing P2X$_4$ receptors, no significant rundown was observed, with the 8th response being 82±10% of the maximum, giving similar results to those obtained using cell rafts with the whole cell configuration. It thus appeared that response rundown was eliminated by preventing whole cell dialysis, as has been described for kainate channels (Wang *et al.*, 1991). To investigate this possibility, the effect of varying concentrations of calcium and ATP in the dialysing solution, on rundown of ATP-induced response at the mouse P2X$_4$ receptor was studied. Rundown was not prevented when free intracellular calcium levels of 0 (in the presence of 5mM BAPTA), 1nM or 1μM were used, with the 8th response to ATP being 5±3%, 9±2% and 7±1% (n=6-7) that of the 1st, for zero calcium, low calcium and high calcium concentrations respectively. Addition of MgATP (5mM) to the internal solution also had no significant effect on rundown; responses declined to 44±7% on the 3rd application, and to 17±3% (n=6) by the 8th application.

In summary, we have found that rundown of responses in HEK-293 cells expressing recombinant P2X$_4$ receptors is time-dependent and can be circumvented by making whole cell recordings from cell rafts, or by using the perforated patch clamp technique, confirming the validity of the use of cell rafts in the characterisation of the mouse P2X$_4$ receptors (Jones *et al.*, 2000). We suggest that rundown is due to an alteration of the intracellular environment caused by whole cell dialysis, but that changes in free calcium concentration or removal of ATP are not critical in its development.

Jones *et al.* (2000) *Br. J. Pharmacol. (in press)*
Miller *et al.* (1998) *Neuropharmacol.* **37:** 1579-1586
Wang *et al.* (1991) *Science* **253:** 1132-1135

261P IMMUNOHISTOCHEMICAL LOCALISATION OF THE SOMATOSTATIN SST_4 RECEPTOR IN RAT AND HUMAN BRAIN

I.-S. Selmer[1,2], M. Schindler[2], P. P. A. Humphrey[2], H. Waldvogel[3], R. L. M. Faull[3], P. C. Emson[1].
[1]Department of Neurobiology, Babraham Institute, Cambridge UK; [2]Glaxo Institute of Applied Pharmacology, University of Cambridge, Cambridge, UK; [3]Faculty of Medicine and Health Science, University of Auckland, Auckland, NZ.

The biological actions of the neuropeptide somatostatin are mediated through a family of G-protein coupled receptors of which five members, sst_{1-5}, have been identified [Hoyer *et al.*, 1995]. Although the mRNA distribution of the sst_4 receptor has been reported [Harrington *et al.*, 1995], no information about the localisation of the receptor protein in the CNS is available. We have therefore raised a polyclonal anti-peptide antibody against the carboxy-terminus of the sst_4 receptor and used this to identify the receptor localisation in the rat and human brain.

Human post-mortem material (n=9) and rat brains (n=7) were used in this study. For the human material, post-mortem delay varied between 8 and 20 hours. To produce specific receptor antibodies, a peptide with the sequence LETTGGAEEEPLYDYYA (corresponding to the predicted amino acids 328-345 of the rat sst_4 receptor) was coupled to Tuberculin PPD and injected into two rabbits following standard protocols. Affinity purification of the sst_4 receptor antibody, immunohistochemistry and Western analysis was carried out according to [Schindler *et al.*, 1997].

The selectivity of the sst_4 receptor antibody was demonstrated by Western blotting of membrane proteins isolated from CHO-K1 cells expressing the human recombinant sst_4 receptor. This and the Western analysis of membranes from the rat hippocampus resulted in the identification of a single band of approximately 42 kDA. No cross-reactivity was observed with the other recombinant sst_{1-5} receptor subtypes.

Immunohistochemistry in the human and rat brain showed the sst_4 receptor to have a widespread distribution. The most prominent staining was observed in the hippocampus and the medulla. Immunoreactive pyramidal cells were identified in the cerebral cortex, however, their abundance varied between different cortical regions. In the hippocampal formation, there was a widespread labelling of pyramidal cells in all the hippocampal subfields. A species specific difference was seen in the Purkinje cells in the cerebellar cortex where sst_4 receptor labelling was identified in the human but this signal was absent in the rat. Strong fibre and neuropil staining was observed in the medulla. All signals where absent when preadsorbed antibody (100 μM) was used.

This study presents for the first time the localisation of the sst_4 receptor in the human and rat brain. Overall, our data indicate a good regional correlation between the two species. Detailed knowledge of the sst_4 receptor localisation is essential in understanding its role in mediating somatostatin neurotransmission in the brain.

Harrington, K. A., Schindler, M., Humphrey, P. P. A. *et al.*, (1995), *Neurosci. Lett.* 188, 17-20
Hoyer, D., Bell, G. I., Berelowitz, M. *et al.*, (1995), TIPS. 16, 86-88
Schindler M., Sellers, L. A., Humphrey, P. P. A. *et al.*, (1997), *Neuroscience* 76, 225-240

262P PROLIFERATION OF PANCREATIC B CELLS IS INHIBITED BY SOMATOSTATIN SST_2 RECEPTORS VIA A MECHANISM INVOLVING SAPK ACTIVATION AND THE DEPHOSPHORYLATION OF ERK1/2

P.A. Smith, L.A. Sellers and P.P.A. Humphrey. Glaxo Institute of Applied Pharmacology, University of Cambridge, Tennis Court Road, Cambridge, CB2 1QJ.

We have investigated the ability of somatostatin receptor-selective agonists to inhibit the proliferation of the mouse pancreatic β cell line, MIN6. To correlate the effects observed on proliferation with the activation of a particular MAP kinase cascade, whole cell protein extract was analysed by Western blotting using antibodies specific for the phosphorylated and hence active forms of extracellular signal-regulated kinases (ERKs), stress-activated protein kinases (SAPKs) and p38. Whereas ERKs are universally activated by mitogens, SAPKs and p38 induce apoptosis (Widmann *et al.*, 1999) and thus may play an important role in the well documented antiproliferative function of somatostatin.

MIN6 cells in log phase of growth on plastic coverslips, were serum-starved for 4h. The coverslips were transferred to fresh wells containing somatostatin or a selective agonist (Humphrey *et al.*, 1998) for sst_1 (CH275), sst_2 (BIM23027), sst_4 (NNC-226900) or sst_5 (L-362,855) receptor types, in the presence and absence of 10% serum. Viable cells were counted 24h later (Table 1). Somatostatin (100nM) inhibited the increase in basal cell number, in the absence of serum whereas none of the receptor-selective agonists (100nM) had any significant effect. The increased cell count induced by serum was abolished by somatostatin or BIM23027 and partially inhibited by L-362,855. The other ligands were without effect. This data suggests that serum-induced proliferation is inhibited by the sst_2 receptor type, as L-362,855 has agonist activity at the sst_5 receptor. An involvement of the sst_3 receptor was ruled out as the sst_3 receptor antagonist, BIM23056 (1μM), had no significant effect (130 ± 5) on the somatostatin-induced inhibition (136 ± 8) of serum-stimulated proliferation. The observation that somatostatin, but non of the receptor-selective agonists inhibited cell proliferation in the absence of serum, suggests that this function is mediated either by the co-operative effects of multiple receptor types or possibly through the sst_3 receptor.

Table 1. The mean number of MIN6 cells harvested from a single coverslip following incubation for 24h with somatostatin analogues (100nM) in the absence (basal) and presence of serum (10%) ($x10^3$ ± SEM, $n = 3$). The mean number of cells at time 0 was 96 ± 6 $x10^3$.

	Basal	SRIF	BIM23027	NNC	L-362855	CH275	BIM23056
Basal	130 ± 5	[a]106 ± 4	127 ± 5	135 ± 2	134 ± 6	141 ± 7	134 ± 4
+FCS	[a]218 ± 9	[b]138 ± 7	[b]141 ± 2	230 ± 9	[b]158 ± 6	217 ± 8	224 ± 8

[a]$P<0.01$ *versus* Basal; [b]$P<0.01$ *versus* FCS; NNC = NNC-226900.

Addition of serum (10%) to quiescent cells induced a biphasic activation of ERKs 1/2 with a marked transient response that peaked at 10 min followed by sustained activation (<4 h). Somatostatin (100nM) produced only a weak transient phosphorylation in the absence of serum, that declined to basal levels 30 min post-application. Somatostatin in the presence of serum had no detectable effect on the transient phosphorylation of ERK, but the sustained component was abolished. It is possible that the mechanism mediating the antiproliferative activity of somatostatin is via inhibition of the serum-induced ERK stimulation. Somatostatin also evoked a marked and sustained activation of SAPKs (but not of p38) whereas serum was without effect. The activation of this alternative MAP kinase cascade may have a significant role in the antiproliferative effect of somatostatin, and may be responsible for the inhibition of basal growth. It will be of interest to determine if the sst_2 receptor agonist exhibits differential regulation of these two kinase cascades. Both the antiproliferative function of somatostatin and the inhibition of the serum-induced sustained component of ERK activation were blocked following pre-treatment of MIN6 cells with pertussis toxin (100 $ngml^{-1}$ for 18h), suggesting the involvement of Gi/o proteins. Somatostatin and its analogues are currently used in the management of endocrine gastroentero-pancreatic (GEP) tumours and the identification of the specific somatostatin receptor type involved in inhibiting cell growth will enable the development of a more effective treatment.

Humphrey, P.P.A. *et al.* (1998) In: *The IUPHAR Compendium*, pp. 246-255, IUPHAR Media, London.
Widmann, C. *et al.* (1999) *Phys. Rev.* **79**, 143-180.

263P OPPOSING PROLIFERATIVE EFFECTS OF SOMATOSTATIN $sst_{2(A)}$ AND $sst_{2(B)}$ RECEPTOR ISOFORMS ARE MEDIATED BY DIFFERENTIAL ACTIVATION OF p38 OR Akt PATHWAYS

L.A. Sellers, F. Alderton, M. Schindler and P.P.A. Humphrey. Glaxo Institute of Applied Pharmacology, University of Cambridge, Tennis Court Road, Cambridge, CB2 1QJ.

Three major kinase cascades have been recently identified that culminate in the activation of the different sets of mitogen-activated protein kinases: extracellular signal-regulated kinases (ERKs), stress-activated protein kinases (SAPKs) and p38 (Widmann et al., 1999). ERKs are activated by mitogens, whereas a number of findings indicate that SAPKs and p38 may play a decisive role in the control of cell death. Phosphatidylinositol 3-kinase (PI 3-K), required for G_1 cell cycle progression, can also protect against apoptosis by activating Akt (PKB-α) (Dudek et al., 1997). In the present study, we have examined the ability of two G protein-coupled receptor isoforms to differentially activate these pathways to explain the contrasting effects that the receptors mediate on cell proliferation.

Somatostatin at the recombinant $sst_{2(b)}$ receptor expressed in CHO-K1 cells, induced an increase in cell number which was sensitive to MEK1 (PD 98059; 20μM) or PI 3-kinase (LY 294002; 100nM) inhibitors but unaffected by a p38 inhibitor (PD 169316; 10μM). In contrast, the $sst_{2(a)}$ receptor mediated an inhibition of cell proliferation induced by basic fibroblast growth factor which was blocked by PD 169316 (Table 1).

Table 1. The mean number of $CHOsst_{2(a)}$ and $CHOsst_{2(b)}$ cells harvested from a single coverslip following incubation with incomplete media (Basal), somatostatin (100nM; SRIF), bFGF (10ngml^{-1}) or in combination (S + F) in the presence and absence of the kinase inhibitors, 24 h after application to partially denuded cell monolayers (x10^3 ± SEM, n = 3).

	$sst_{2(a)}$				$sst_{2(b)}$	
Treatment	**Basal**	**SRIF**	**bFGF**	**S + F**	**Basal**	**SRIF**
Vehicle	176 ± 7	172 ± 3	[a]278 ± 1	[b]176 ± 4	149 ± 3	[d]267 ± 7
+PD98059	157 ± 6	156 ± 6	[b]206 ± 7	184 ± 6	135 ± 5	[e]165 ± 8
+LY294002	174 ± 3	165 ± 9	[b]211 ± 9	170 ± 8	165 ± 9	[e]141 ± 4
+PD169316	171 ± 2	166 ± 6	267 ± 9	[c]257 ± 9	140 ± 3	259 ± 6

$CHOsst_{2(a)}$; [a]P<0.001 *versus* Basal; [b]P<0.01 *versus* bFGF; [c]P<0.01 *versus* S + F.
$CHOsst_{2(b)}$; [d]P<0.001 *versus* Basal; [e]P<0.001 *versus* SRIF.

In order to correlate the effects observed on cell proliferation with the activation of a particular kinase cascade, we analysed whole cell protein extract by Western blotting using antibodies specific for the phosphorylated and hence active forms of MAP kinases and Akt. Somatostatin (100nM) at either receptor induced a sustained activation of ERK (<4 h) which became more marked in the presence of bFGF. Activation of $sst_{2(b)}$ receptors produced only a weak transient activation of p38 compared to a sustained phosphorylation by $sst_{2(a)}$ receptors, that was again enhanced by bFGF. Phosphorylation of p38 by bFGF alone was undetectable, in contrast to a biphasic stimulation of ERKs. None of the receptors induced any change in the activity of SAPKs and in contrast to the lack of effect by the $sst_{2(a)}$ receptor, somatostatin induced a marked phosphorylation of Akt following $sst_{2(b)}$ stimulation which was abolished following PI 3-kinase inhibition.

There is accumulating evidence that suggests high-intensity Ras stimulation can evoke prolonged ERK activation leading to the induction of the cell cycle inhibitor, $p21^{cip1}$. Our data also suggest that a strong and sustained activation of ERK, as observed in both $CHOsst_{2(a)}$ and $CHOsst_{2(b)}$ cells, cannot alone be responsible for the induction of such an effective antiproliferative activity. In $CHOsst_{2(a)}$, but not in $CHOsst_{2(b)}$ cells, $p21^{cip1}$ protein expression was elevated over basal following treatment for 24 h with somatostatin in the presence of bFGF. The increased expression of $p21^{cip1}$ was reduced in $CHOsst_{2(a)}$ cells by either the MEK1 or the p38 inhibitors. It would thus appear that an enhanced and sustained activation of both p38 and ERK are required for the induction of $p21^{cip1}$ that is provided in this system by the co-operative effects of both the growth factor and $sst_{2(a)}$ receptor activities. We conclude that the contrasting growth responses evoked by somatostatin at the $sst_{2(a)}$ and $sst_{2(b)}$ receptors can be accounted for in part by their differential ability, despite apparent coupling to identical Gα protein pools (Carruthers *et al.*, this meeting), to activate p38 or Akt pathways.

Carruthers, A.M. *et al.* (2000) this meeting.
Dudek, H. *et al.* (1997) *Science* **275**, 661-665.
Widmann, C. *et al.* (1999) *Phys. Rev.* **79**, 143-180.

264P AGONIST-SPECIFIC DESENSITISATION OF THE HUMAN SOMATOSTATIN sst_4 RECEPTOR MAY BE ACCOUNTED FOR BY RECEPTOR PHOSPHORYLATION AND NOT INTERNALISATION

K.S.M. Smalley, L.A. Sellers, J.A. Koenig, W. Feniuk and P.P.A. Humphrey. Glaxo Institute of Applied Pharmacology, University of Cambridge, Tennis Court Road, Cambridge, CB2 1QJ.

We have previously demonstrated prolonged desensitisation of the human sst_4 receptor in response to somatostatin, but not the synthetic analogue, L-362,855 (Smalley *et al.*, 1998). Receptor internalisation can often account for desensitisation and in this regard Chinese hamster ovary cells recombinantly expressing the sst_4 receptor ($CHOsst_4$) can internalise radiolabelled somatostatin in a time-dependent manner ($t_{½}$ = 19.0 ± 3.9 min^{-1}) (Smalley *et al.*, 1999). However, confocal microscopy of permeabilised cy-3-labelled heamagglutinin-tagged human sst_4 receptors revealed virtually no internal immunostaining after somatostatin treatment. The aim of the present study was to further investigate receptor internalisation and to examine the role of receptor phosphorylation in the mechanism of agonist-selective desensitisation.

A radioimmunoassay using ^{125}I-congugated IgG antibody fragment ($F(ab')_2$) was devised to estimate cell surface receptor expression in $CHOsst_4$-tagged cells. Binding of low concentrations of $F(ab')_2$ fragment (0.04 μgml^{-1}) had reached steady state by 4h at 37°C. Saturation curves constructed by incubation for 4h with increasing concentrations of $F(ab')_2$ gave estimates of cell surface receptor expression of 6.2 x10^5 and 3.9 x10^5 receptors per cell (n = 2, performed in duplicate). Maximal internalisation of [^{125}I-Tyr^{11}]-somatostatin was calculated at 1.8 ± 0.2 x10^4 molecules per cell (n = 3) and had a similar rate constant ($t_{½}$ = 15.8 ± 0.9 min^{-1}; k = 0.043 ± 0.03) to that for cells expressing the untagged receptor. It is thus estimated that only 3.5% of the surface sst_4-tagged receptor is internalised after 1h in the presence of somatostatin. The rapid recycling of the radioligand, coupled with the apparently low proportion of receptors being internalised, may explain the discrepancy between the difficulty in visualising internalisation and the intracellular accumulation of somatostatin. In addition, the poor internalisation efficiency of the human sst_4 receptor suggests that this process is unlikely to account for the marked desensitisation observed on application of somatostatin.

To investigate the involvement of receptor phosphorylation in desensitisation, CHO-K1 cells expressing the human tagged sst_4 receptor were incubated in the presence of radiolabelled inorganic phosphate (10 μCi per 200,000 cells) for 3h prior to stimulation with agonist. Immunoprecipitated receptor from whole cell lysates prepared in CHAPS buffer (10mM) containing AEBSF (1mM) and NaF (15μM) was resolved by SDS PAGE and transferred to nitrocellulose. Autoradiography showed time-dependent protein phosphorylation in response to somatostatin (10nM) but not L-362,855 (100nM). The onset of phosphorylation was rapid and although the peak response determined at 8 min had slightly diminished by 15 min, it was still elevated over basal. The apparent molecular weights of the phosphorylated products correlated with the electrophoretic mobilities of the main immunoreactive bands detected following Western analysis of the nitrocellulose with an anti-HA antibody. Phosphorylated proteins had molecular sizes of 35-37, 42 and 55-70 kDa. The anti-HA antibody detected a broad spread between 52-70 kDa as well as smaller molecular weight species of ~36 kDa, and consistent with the immunoreactive products obtained using an anti-sst_4 receptor antibody. The same electrophoretic mobilities of the phosphorylated products and the anti-HA immunoreactivity is strong evidence to support somatostatin-induced receptor phosphorylation, although it cannot be ruled out that changes in the phosphorylation of proteins non-covalently associated with the receptor and concomitantly immunoprecipitated are also being detected. In summary, somatostatin-induced desensitisation (Smalley *et al.*, 1998) may be a consequence of receptor phosphorylation. The lack of desensitisation and receptor phosphorylation observed with L-362,855, may be the result of its lower efficacy which has been observed in some functional studies (Sellers *et al.*, 1999).

Sellers, L.A. *et al.* (1999) *J. Biol. Chem.* **274**, 16423-16430.
Smalley, K.S.M. *et al.* (1998) *Br. J. Pharmacol.* **125**, 833-841.
Smalley, K.S.M. *et al.* (1999) *Br. J. Pharmacol.* **126**, 125P.

265P INVERSE AGONISM AT α_{1B}-ADRENOCEPTORS: QUINAZOLINES *VS* NON-QUINAZOLINES

P. Hein, S. Cotecchia*, M. Goepel, M.C. Michel, Depts. of Medicine and Urology, Univ. Essen, 45122 Essen, Germany and *Dept. of Pharmacology, Univ. Lausanne, Switzerland

Clinically quinazoline and non-quinazoline α_1-adrenoceptor antagonists differ in their cardiovascular effects but the underlying reasons are not fully understood (Djavan & Marberger 1999). Therefore, we have quantitatively compared the effects of several antagonists on basal and agonist-stimulated inositol phosphate formation.

[^{3}H]Inositol phosphate (IP) formation was determined during a 45 min incubation in the absence and presence of 10 µM phenylephrine as previously described (Taguchi et al. 1998) in [^{3}H]inositol-labelled Rat-1 fibroblasts which had been stably transfected with wild-type hamster α_{1B}-adrenoceptors (WT) and a constitutively active mutant thereof (CAM) at a density of 2729±104 and 1838±156 fmol/mg protein, respectively (Hein et al. 1999). Data are means ± s.e.m. of 4-9 experiments.

Phenylephrine concentration-dependently stimulated IP formation in WT and CAM cells (-log EC_{50} [M] 6.02±0.14 and 8.33±0.34, respectively). In WT cells the quinazolines alfuzosin, doxazosin, prazosin and terazosin and the non-quinazolines BE 2254 (2[ß-(4-hydroxyphenyl)-ethyl-aminomethyl]tetralone HCl), tamsulosin and SB 216,469 (N-[3-[4-(2-methoxyphenyl)-1-piperazinyl]propyl]-3-methyl-4-oxo-2-phenyl-4-H-1-benzopropyran-8-carboxamide monomethanesulfonate) concentration-dependently inhibited the response to 10 µM phenylephrine with potencies (-log K_i [M]) of 9.01±0.06, 9.53±0.21, 9.21±0.30, 9.23±0.21, 9.26±0.29, 7.28±0.18 and 9.41±0.18, respectively; very similar values were obtained in CAM cells.

In the absence of phenylephrine, all quinazolines concentration-dependently lowered basal IP formation in CAM cells (maximum lowering ≈55%). Maximal inhbition by the non-quinazolines was smaller (28±6% for BE 2254 and 13±2 for SB 216,469), and tamsulosin even enhanced basal IP formation by up to 69±10% (corresponding to ≈16% of maximal phenylephrine values). While drug potency (-log EC_{50}) for inverse agonism could not be calculated for SB 216,469 due to weak efficacy, it was similar to but significantly greater than antagonist potency for all drugs (≈0.5 log units, $P < 0.05$ in a paired t-test). The same was true for partial agonism by tamsulosin. In WT cells, however, none of the tested drugs caused caused detectable inverse agonism, and tamsulosin did not cause statistically significant partial agonism.

SB 216,469 (10 µM) abolished the inhibition by 10 nM alfuzosin, doxazosin, prazosin and terazosin and the stimulation by 10 nM tamsulosin.

We conclude that quinazolines may have greater inverse agonism than non-quinazolines at α_{1B}-adrenoceptors. SB 216,469 may be an almost neutral antagonist, and tamsulosin may be a very weak partial agonist.

Dajavan, B. & Marberger, M. (1999) *Eur. Urol.* 36: 1-13
Hein, P., et al. (1999) *Nottingham Meeting* P39
Taguchi, K., et al. (1998) *Naunyn-Schmiedeberg's Arch. Pharmacol.* 358: 100-110

266P CHARACTERISTICS OF REDUCED GLUTATHIONE EFFLUX FROM HUMAN LUNG TUMOUR CELLS CONTRAINING DIFFERENT AMOUNTS OF MULTIDRUG RESISTANCE-ASSOCIATED PROTEIN, MRP1

T. Bagrij and M.A. Barrand
Department of Pharmacology, University of Cambridge, Tennis Court Road, Cambridge, CB2 1QJ, U.K.

Efflux of reduced glutathione (GSH) occurs from many cell types and may play a role in control of tissue cysteine/GSH homeostasis. In the lungs at least it also provides important extracellular antioxidant protection in the airway surface fluid. Several different transporters have been implicated in mediating this efflux including the cystic fibrosis transmembrane conductance regulator (Linsdell & Hanrahan, 1998) and the multidrug resistance-associated proteins, MRP1 and cMOAT (Paulusma et al, 1999). In order to study the possible involvement of MRP1, we have compared GSH efflux from human large cell lung tumour L23R cells (Barrand et al, 1995) which overexpress MRP1 but not cMOAT at the cell surface and from parental L23P cells which contain low levels of cytoplasmic MRP1.

Cells were exposed to Hanks buffered salt solution containing γ-glutamyltranspeptidase inhibitor, acivicin for up to 3 h at 37°C and the content of GSH in the supernatant or in the cells then measured spectrophotometrically. Greater GSH efflux occurred from the high MRP1-expressing cells (values in nmoles/10^6 cells/h: 7.34±0.16, L23R v 3.86±0.69, L23P, n=8; differences between cell types significant, $p<0.05$ by unpaired t test) despite lower GSH content (values in nmoles/10^5cells; 0.65±0.05, L23R v 1.53±0.09, L23P, n=8; differences between cell types significant, $p<0.05$) and was more marked from trypsinised than attached cells (values for L23R in nmoles/10^6 cells/h: 7.34±0.16 attached v 21.6±1.69 trypsinised, n=8; differences significant, $p<0.01$). ATP depletion following 30 min exposure to 6 mM deoxyglucose and 10 mM sodium azide produced no significant change in GSH efflux although this treatment reduced ATP-dependent MRP1-mediated calcein efflux in these cells. This together with the observation of only a 2 fold decrease in GSH efflux in both cell types at 20°C compared to 37°C is suggestive of passive rather than active extrusion. How MRP1 affects GSH efflux is unclear though co-transport of GSH is said to accompany MRP1-mediated export of natural product drugs (Loe et al, 1998; Rappa et al, 1997). Of the MRP1 inhibitors tested at concentrations known to block MRP1 activity, 5 mM probenecid decreased GSH efflux from MRP1-expressing cells but increased it from parental cells (ratios, treated/untreated of 0.6±0.21, L23R v 1.6±0.3, L23P, n=8; values significantly different from 1, $p<0.05$) whereas 10 µM indomethacin caused significant increases in both cell types (ratios treated/untreated of 1.7±0.2, L23R and 2.0±0.4, L23P, n=8; values significantly different from 1, $p<0.05$) and with 25 µM MK571 the increases were insignificant (1.4±0.2, L23R and 1.3±0.3, L23P, n=8). There is thus no clear relation between MRP1 activity and GSH efflux.

It is concluded that GSH efflux from these lung tumour cells is probably not energy-dependent but there may be interactions with MRP1 at the cell surface. Intracellular GSH levels are high compared with the external medium so passive permeability pathways should be sufficient to allow release of GSH from cells. Nevertheless, the presence of MRP1 may well influence the extent of such GSH extrusion.

Barrand, M.A., Robertson, K.J., Neo, S-Y. et al. (1995) *Biochem. Pharmacol.* 50, 1725-1729.
Linsdell, P. & Hanrahan, J.W. (1998) *Am. J. Physiol.* 275, C323-C326.
Loe, D.W., Deeley, R.G. & Cole, S.P.C. (1998) *Cancer Research*, 58, 5130-5136.
Paulusma, C.C., van Geer, M.A., Evers, R. et al. (1999) *Biochem. J.* 338, 393-401.
Rappa, G., Lorico, A., Flavell, R.A. & Sartorelli, A.C. (1997) *Cancer Research*, 57, 5232-5237.

TB holds a MRC studentship.

267P INTRACELLULAR pH IN A MRP1 OVEREXPRESSING LUNG TUMOUR CELL LINE

S.B. Hladky, K. Patel & M.A. Barrand Department of Pharmacology, University of Cambridge, Tennis Court Road, Cambridge, CB2 1QJ, UK.

Use of the fluorescent pH indicator, BCECF, 2',7'-bis-(2-carboxyethyl)-5-(and-6)-carboxyfluorescein, to measure intracellular pH (pH_i) is complicated in certain cell types by transport of the indicator by the multidrug resistance-associated protein (MRP1), but this can be overcome by cooling cells to 15°C or applying MRP1 inhibitors (Hladky et al, 1997). Using the protocol indicated in Fig. 1 we now report results of quantitative comparison of pH_i in MRP1 containing human lung tumour COR-L23R cells and their drug sensitive parent cells, COR-L23P, and we demonstrate changes in pH_i that occur when the cells are transferred from HCO_3^- to HEPES buffered medium.

Cells grown on coverslips were equilibrated for one hour in CO_2/HCO_3^- buffered solution at 37°C and then loaded with

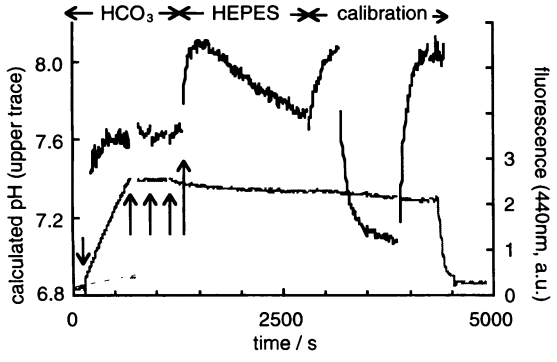

Figure 1 Fluorescence and calculated pH for COR-L23P cells.

indicator by exposure to CO_2/HCO_3^- medium containing the non-fluorescent precursor, BCECF-AM (0.5μM) at 15°C. Parent cells and a coverslip were inserted into the cuvette at the downward arrow. At the first upward arrow the coverslip was removed and the fluorescence of the medium measured. The medium was replaced three times with fresh HCO_3^- medium then with medium buffered with HEPES, all at 15°C without BCECF-AM. The rapid alkaline shift followed by recovery is expected from a rapid loss of CO_2 followed by slower loss of HCO_3^- from the cells. Traces from L23R cells were similar except for a progressive decrease in the 440nM fluorescence after removal of BCECF-AM. pH_i during loading, with BCECF-AM and BCECF in the medium, was calculated from the ratio of the increases of cell associated (total - medium) fluorescence at 502nm and 440nm (emission 526nm). pH after loading was calculated from the ratio of the fluorescences corrected for the background measured after addition of saponin at the end of the experiment. Fluorescence ratios for cell associated BCECF were converted to pH using values measured with potassium aspartate calibration solutions containing nigericin.

For cells cultured, incubated, and measured in medium equilibrated with 5% CO_2 (final external pH 7.4), pH_i during loading was 7.54±0.03 (mean±s.e.mean, n=10) for the L23P cells and 7.44±0.05 (n=5, difference $p>0.05$, unpaired t-test) for the L23R cells. After loading the values were 7.59±0.03 (n=5) and 7.35±0.1 (n=5, $p<0.05$). In cells grown, incubated and measured in medium equilibrated with (nominal) 10% CO_2 (final pH 7.1), the values during loading were L23P, 7.52±0.03 (n=6) and L23R, 7.28±0.06 (n=7, $p<0.01$) and after loading 7.53±0.03 (n=7) and 7.33±0.06 (n=9, $p<0.05$). These results suggest that, pH_i in resistant cells is 0.1-0.2 pH units less than in the parent cells.

Hladky, S.B., Gewert, C. & Barrand, M.A. (1997) *Br. J. Pharmacol.* 123, 338P.

268P EFFECTS OF CALMIDAZOLIUM AND 17 β-OESTRADIOL ON AMYLASE RELEASE AND PERMEABILISATION TO ETHIDIUM BROMIDE IN ATP-STIMULATED RAT PAROTID ACINI *IN VITRO*

S. Arkle & A. Douzenis, School of Pharmacy, University of Portsmouth, Portsmouth, UK. PO1 2DT

P2X7 receptor-mediated responses characteristically involve an initial increase in cell membrane cation permeability followed by formation of large pores permeable to compounds of molecular radii up to 600 Da (Suprenant *et al.*, 1996). Virginio *et al.* (1997) recently reported that calmidazolium (Cz) attenuates the cation permeability but not the pore-forming response to recombinant rat P2X7 receptor stimulation. Similarly, 17 β-oestradiol (OE_2) has a non-genomic action to inhibit human P2X7 receptor cation channels (Cario-Toumaniantz *et al.*, 1998). Here we report the effects of Cz and of OE_2 on P2X7-mediated responses to ATP in rat parotid acini.

To monitor cell permeabilisation, rat parotid acini were incubated in Krebs-Henseleit buffer (KHB) containing 20μM EthBr. EthBr fluorescence increases markedly when it interacts with nucleic acids following cell permeabilisation. EthBr fluorescence was monitored before and after addition of ATP or other agents to the acinar preparation. Amylase release was measured from parotid pieces that had been sequentially incubated for 10 min intervals in KHB in the presence or absence of ATP and other agents.

The results of our experiments are shown in table 1. ATP (3-300μM) caused a rapid, saturable and concentration-dependent increase in EthBr fluorescence that was antagonised by 30 min preincubation of acini with 300μM 5'-*p*-fluorosulphonylbenzoyladenosine (FSBA) ($P<0.01$, Student's *t*- test). Preincubation for 5 min with 5μM OE_2 or 50nM Cz did not alter the response to ATP ($P>0.05$) but after pretreatment for 30 min with 50nM Cz the response was diminished ($P<0.001$). 100μM ATP stimulated amylase release ($P>0.05$). This effect was antagonised ($P<0.01$) by 30 min preincubation with 50nM Cz but not by 10 min preincubation with 5μM OE_2 ($P>0.05$).

Table 1. Effects of agents on EthBr fluorescence in parotid acini and amylase release from parotid pieces (mean ± s.e.mean (n)).

treatment (preincubation (min))	EthBr fluorescence (% increase above basal)	amylase release (i.u./g tissue/min.)
basal	---	32.4 ± 4.7 (5)
3μM ATP	6.1 ± 1.6 (4)	---
10μM ATP	17.0 ± 2.2 (4)	---
30μM ATP	40.0 ± 5.4 (4)	---
100μM ATP	61.1 ± 6.1 (4)	56.3 ± 3.5 (4)
300μM ATP	59.6 ± 8.3 (4)	---
50nM FSBA (30) + 100μM ATP	21.0 ± 2.4 (3)	39.1 ± 3.9 (5)
50nM Cz (5) + 100μM ATP	48.3 ± 8.9 (4)	---
50nM Cz (30) + 100μM ATP	17.5 ± 1.2 (4)	33.0 ± 4.7 (5)
5μM OE_2 (5) + 100μM ATP	51.1 ± 7.7 (4)	---
5μM OE_2 (10) + 100μM ATP	---	45.9 ± 6.7 (4)

These data support the notion that ATP stimulates P2X7 receptor-dependent permeability changes in parotid acini that are attenuated by Cz, but differ from previous findings in that they show attenuation of permeability to the high molecular weight compound EthBr. In contrast to the findings of Virginio, *et al.* (1997) with recombinant receptors, the time course of Cz's effect in parotid acini was slow and not consistent with a fast, extracellular action. The lack of effect of OE_2 in this study may reflect species variability as there are marked differences in P2X7 receptor structure and pharmacology between rats and humans (Rassendren *et al.*, 1997).

Cario-Toumaniantz, C., *et al.* (1998). *J. Physiol.* **508**, 659-666.
Rassendren, F., *et al.* (1997). *J. biol. Chem* **272**, 5482-5486.
Suprenant, A., *et al.* (1996). *Science* **272**, 735-738.
Virginio, C., *et al.* (1997). *Neuropharmacol.* **36**, 1285-1294.

269P CHARACTERISATION USING FLIPR OF A BOMBESIN RECEPTOR ENDOGENOUSLY EXPRESSED IN CHO-DG44 CELLS

S. J. Brough, F. Jewitt, J. C. Jerman and D. Smart
Department of Neuroscience Research, SmithKline Beecham, New Frontiers Science Park, Harlow. CM19 5AW

Bombesin (BN), a tetradecapeptide isolated from the skin of the frog *Bombina bombina* (Anastasi *et al.*, 1971), is one of a family of peptides which have been used to characterise three BN receptor subtypes (Fathi *et al.*, 1993; Benya *et al.*, 1994). Initial studies showed CHO/DG44 cells to express an endogenous BN receptor. Therefore a range of these BN-like peptides were used to characterise the BN receptor endogenously expressed by CHO/DG44 cells.

CHO/DG44 cells (seeded at 30,000 cells per well) were incubated with the Ca^{2+} sensitive dye Fluo-3AM (4μM) at 37C.5%CO_2 in air for 60 min and washed with Tyrodes buffer containing 2.5 mM probenecid. Antagonists were pre-incubated at 37C.5%CO_2 in air for 30 min. Basal fluorescence was determined prior to agonist addition at 37C by FLIPR. For each response the peak increase in fluorescence was calculated and iteratively curve-fitted using a four parameter logistic model (Bowen & Jerman 1995).

Table 1: Potencies of BN-like peptides in CHO/DG44 cells

Ligand	pEC50
Bombesin	7.79 + 0.05
Neuromedin B	7.48 + 0.03
Neuromedin C	7.77 + 0.06
Ranatensin	8.28 + 0.05
PG-L	8.18 + 0.05
[D-Phe^{6},βAla^{11},Phe^{13},N-leu^{14}] Bombesin (6-14)	7.81 + 0.07
[D-Tyr^{6},βAla^{11},Phe^{13},N-leu^{14}] Bombesin (6-14)	7.88 + 0.04
Acetyl Neuromedin B (3-10)	7.99 + 0.03
[D-Phe^{6}, Phe^{13}] Bombesin (6-13) propylamide	7.61 + 0.03

Data are mean ± s.e.mean, n= 4-11

All the agonists caused a large, rapid (peak at 8 – 10 sec), transient increase in the levels of fluorescence which returned to baseline over 1 to 2 minutes. All nine BN-like peptides tested were full agonists. The non-selective antagonist (D-Arg^{1},D-Pro^{2},D-Trp^{7,9},Leu^{11})-Substance P inhibited the BN induced response with a pK_B of 6.33±0.06, whilst the Bombesin type 2 (BB2) receptor selective antagonist Bombesin (6-13) methyl ester inhibited the response with a pK_B of 9.47±0.04. The signal transduction mechanism was examined using a range of inhibitors. Thapsigargin, chelethyrine chloride and wortmannin inhibited the BN-induced response, with pK_B values of 7.68±0.04, 6.04±0.01 and 6.01±0.07 respectively. Ro-31-8220 (10 uM) also inhibited the BN-induced response by 17.5±2.5%, whilst H-89, LY294002 and U73122 were without effect. In the absence of extracellular calcium, the agonist potencies were reduced approximately five-fold and the maximum signal produced was reduced to 53.0±1.4% of control.

In conclusion, the rank order of the three main family members (BN=NMC>NMB) and activity of BN (6-13) methyl ester suggests CHO/DG44 cells express an endogenous BB2 receptor, which activates protein kinase C, mobilises calcium from intracellular stores and results in calcium influx. Thus CHO/DG44 cells are a useful model for assessing the pharmacology of bombesin ligands at the hamster BB2 receptor

Anastasi, A., Erspamer, V., Bucci, M., (1971) *Experimentia* **27**, 166-167
Bowen, W.P. & Jerman, J. (1995) *Trends Pharmacol. Sci.* **16**, 413 -417
Benya, R., Kusui, T., Shikado, F., *et al.*, (1994) *J. Biol. Chem.* **269**, 11721-11728
Fathi, Z., Corjay, M., Shapira, H., *et al.*,(1993) *J. Biol. Chem.* **268**, 5979-5984

270P PROTEASE-MEDIATED INHIBITION OF CHLORIDE SECRETION IN T84 HUMAN COLONIC CELLS

H. Danahay[1], R.J. Bridges[2] & C.T. Poll[1]. (Introduced by J. Fozard)
[1]Novartis Horsham Research Centre, Horsham. UK. [2]Dept. Cell Biology & Physiology, University of Pittsburgh, Pittsburgh, PA. USA

Evidence is growing that in addition to its role in digestion, trypsin plays a role in cell signalling through activation of protease activated receptors (PAR) and particularly PAR2 (Déry *et al.* 1998). PAR2 has been identified on epithelial membranes from a variety of tissues (Cocks *et al.* 1999; Nguyen *et al.* 1999), thus we have investigated the effects of trypsin on the human colonic cell-line T84, a model chloride secreting epithelium (Singh *et al.* 1998).

T84 monolayers on inserts were mounted into Ussing Chambers perfused with Ringer solution containing (mM): 120 NaCl, 25 $NaHCO_3$, 3.3 KH_2PO_4, 0.8 K_2HPO_4, 1.2 $CaCl_2$, 1.2 $MgCl_2$, 10 glucose (37°C, 5%CO_2:O_2) and voltage clamped to 0V. *Study 1*: Forskolin (2μM) was added apically (AP) and basolaterally (BL) to induce a Cl^- secretory current, followed by porcine trypsin (0.01-1.0μM,BL) and the change in short circuit current (I_{sc}) and the unidirectional fluxes of ^{36}Cl were measured. *Study 2*: Forskolin (2μM) was added to the cells 15min after trypsin (1μM,BL) or vehicle and the ΔI_{sc} was recorded. *Study 3*: Impedance analysis was used to monitor the effect of trypsin (1μM,BL) or human thrombin (10UmL^{-1},BL) on AP and BL resistance as described by Margineanu & Van Driessche (1990). The viability of all preparations was confirmed prior to termination of each experiment by checking transepithelial resistance (Rt) and by the addition of 1-EBIO (1-ethyl-2-benzimidazolinone) an activator of the basolateral Ca^{2+} regulated K^+ channel (Devor *et al.* 1996). T84 cell lysates were assayed by western blotting using antibodies specific for PAR1 and 2. Results are expressed as mean values ±s.e.mean. Statistical significance was assumed when $P<0.05$ using a paired Student's t-test.

Forskolin induced an increase in I_{sc} of 82±2.6 μAcm^{-2} (n=24). The subsequent addition of trypsin (0.01-1μM,BL, n=16) induced a further dose-dependent transient increase in I_{sc} followed by a sustained decrease in I_{sc} of 54±1.4% and an increase in Rt of 23±9.4%. The addition of trypsin (1μM,BL) before forskolin induced only a small increase in I_{sc} (2.3±0.4μAcm^{-2}) but significantly attenuated the subsequent forskolin-induced I_{sc} by 65.6±2.7% (n=5, $P<0.05$). Forskolin induced a serosal to mucosal flux of Cl^- (4.4±0.1μEqcm^{-2}h^{-1}, n=6) that was inhibited by trypsin (2.4±0.4μEqcm^{-2}h^{-1}) and a net Cl^- secretion (2.9±0.3μEqcm^{-2}h^{-1}) that was also trypsin sensitive (0.5±0.5μEqcm^{-2}h^{-1}) and consistent with the decrease in I_{sc}. Impedence analysis demonstrated that trypsin (1μM,BL) induced an initial fall in BL resistance from 479±45 to 132±24Ωcm^{-2} (n=4) coinciding with the increase in I_{sc}. BL resistance then slowly increased to a maximum of 1130±33Ωcm^2, which was mirrored by the sustained decrease in I_{sc} and increase in Rt. In forskolin stimulated, trypsin untreated cells the BL resistance increased from 413±50 to 506±56Ωcm^{-2} (n=3) over the same time period. There were no significant trypsin-induced changes in AP resistance. There was no effect of thrombin on I_{sc} or membrane resistances (n=3). Western analysis demonstrated the presence of PAR1 and PAR2 receptors in T84 cell lysates.

The results demonstrate trypsin causes an inhibition of forskolin stimulated Cl^- secretion. The effects of trypsin appear to be mediated at the BL membrane where trypsin causes an initial activation followed by an inactivation of the K^+ conductance. These effects are mirrored by a transient increase and subsequent decrease in I_{sc}. Trypsin's mechanism of action remains to be established but could be through an activation of PAR2 demonstrated to be present in these cells.

Margineanu & Van Driessche (1990) *J. Physiol.* **427**: 567-581
Devor DC, Singh AK, Frizzell RA *et al.* (1996) *Am. J. Physiol.* **271**: L775-L784
Dery O, Corvera CU, Steinhoff M *et al.* (1998) *Am. J. Physiol.* **274**:C1429-C1452
Singh AK, Tasken K, Walker W *et al.* (1998) *Am. J. Physiol.* **275**: C562-C570
Cocks TM, Fong B, Chow JM *et al.* (1999) *Nature* **398**: 156-160
Nguyen TD, Moody MW, Steinhoff M *et al.* (1999) *J. Clin. Invest.* **103**(2): 261-269

271P RETINOIC ACID INCREASES NO PRODUCTION IN ENDOTHELIAL CELLS AND INDUCES DDAH II GENE EXPRESSION: POSSIBLE MECHANISM FOR NO REGULATION DURING DEVELOPMENT

Cam Tran, Vinod Achan, Graeme Birdsey, Jo Santa Maria, James Leiper and Patrick Vallance. Centre for Clinical Pharmacology, University College London, The Rayne Institute, 5 University Street, London WC1E 6JJ

Asymmetric dimethylarginine (ADMA) is an endogenous compound that inhibits nitric oxide synthase (NOS) isozymes. It is metabolised to citrulline by dimethylarginine dimethylaminohydrolase (DDAH). We have recently identified a second isoform (DDAH II) and shown that DDAH I and II have distinct tissue distributions (Leiper *et al.*, 1999). Furthermore, DDAH II appears to be highly expressed in the foetus and may have a role in cellular differentiation, a process that also involves NO (Poluha *et al.*, 1997; Gouge *et al.*, 1998). To explore possible regulation of DDAH and NO during development and differentiation of endothelium we undertook studies with all-trans retinoic acid (RA).

Northern blot analysis. Cells of the murine endothelial cell line sEnd.1 were exposed to RA (1μM). Total cell RNA was extracted for northern blotting after 24h. *Reporter gene assay.* The DDAH II promoter region was cloned upstream of a luciferase reporter gene and transfected into ECV304 human umbilical vein endothelial cells. Transfected cells were exposed to RA (1μM) for 48h prior to determination of luciferase activity. *Dot blot analysis.* Labelled probes complimentary to human DDAH II and ubiquitin were sequentially hybridised to a commercially available human multiple-tissue mRNA dot blot. DDAH signals were corrected for RNA loading estimated from the ubiquitin signal. Data were analysed by two-way analysis of variance and Student's *t* test.

Northern blot analysis. Treatment of sEnd.1 cells with 1μM RA increased DDAH II mRNA by 73±0.85% (mean±s.e.mean; n=2). Coincident with the increase in DDAH II expression NO generation from the cells increased by 39.7±2.2% (n=9; $p<0.001$) although there was no detectable increase in eNOS mRNA and no induction of either nNOS or iNOS. Incubation of cells with the DDAH-specific inhibitor S-2-amino-4(3-methylguanidino)butanoic acid (4124W) reduced the RA-induced increase in NO production by 46.1±7.7% (n=3; $p<0.05$). *Reporter gene assay.* Sequencing of 1.4kb of DNA immediately upstream of the DDAH II coding region revealed the presence of a PPAR/RXR consensus binding site at -960bp. RA treatment of cells transfected with the DDAH II promoter/reporter construct produced a 52.3±6.8% (n=3, $p<0.05$) increase in promoter activity. *Dot blot analysis.* Northern dot blot analysis of DDAH II expression levels in a number of foetal and adult tissues indicated that DDAH II transcription is developmentally regulated (Table 1).

Table 1. *Dot blot analysis.* Figures represent percentage of maximal expression (foetal brain) as quantitated by phosphorimaging.

	brain	heart	kidney	liver	spleen	thymus	lung
Foetal	100	34	60	15	29	39	66
Adult	9	30	75	14	37	57	23

These data indicate that DDAH II is transcriptionally activated by RA, a factor known to induce differentiation in a number of cell types. This upregulation is paralleled by an increase in NO production. DDAH II might therefore regulate development by regulating NOS activity. This is supported by the observation that DDAH II expression levels differ in foetal and adult tissues.

Gouge, R.C., Marshburn, P., Gordon, B.E. *et al.* (1998) Biol. Repro. 58:875-879

Leiper, J.M., Santa Maria, J., Chubb, A. *et al.* (1999) Biochem. J. 343(1):209-214

Poluha, W., Schonhoff, C.M., Harrington, K.S. *et al.* (1997) J. Biol. Chem. 272(38):24002-24007

272P DIFFERENTIAL PROLIFERATIVE RESPONSE TO PROTEASE ACTIVATED RECEPTOR (PAR) AGONISTS ON GUINEA-PIG TRACHEAL CULTURED SMOOTH MUSCLE CELLS

...Randolph Corteling & Alexandre Trifilieff. (Alan Steward) Novartis Horsham Research Centre, Horsham, U.K.

Protease activated receptors (PARs) have been isolated on numerous cell types. The thrombin or PAR-1 like receptors consist of PAR-1, -3 and -4. Their main agonist is thrombin. PAR-2 is activated by trypsin and tryptase. Both thrombin (Brown *et al.*, 1995) and tryptase (Stewart *et al.*, 1995) have been shown to induce proliferation of human and dog tracheal smooth muscle cells, respectively. The aim of this work was to compare the proliferative response of both thrombin (PAR-1 like) and tryptase (PAR-2) in the same cell type.

The tracheas from 5 male Hartley guinea-pigs (300-350g) were used to isolate each batch of smooth muscle cells. The animals were anaesthetised with sodium pentabarbitone (30mg kg^{-1}). The trachea removed, the muscle band dissected free of any other tissue type and chopped finely, before being incubated at 37°C for 2 hours in an enzymic solution (0.1% Elastase, 0.2% collagenase type IV in Dulbecco's Modified Eagle Medium, DMEM). After filtration through a 70μm cell strainer, the cell suspension was washed with DMEM containing 10% Fetal Calf Serum (FCS) and seeded in a 25cm^2 flask. Once confluent, the cells were seeded on 96-well plate (60% confluency) for 24 hours in DMEM 10% FCS, then placed in DMEM 0% FCS for 48 hours. The growth factors were then added for a further 20 hours, followed by [H^3]-thymidine (0.5 μCi per well) for 4 hours. Thymidine incorporation was then measured.

At all the passages studied (P1 to P4) cells showed positive staining for α-actin and the doubling time ranged between 30-40 hrs. Tryptase induced cellular proliferation at P1 and P2 only, and the maximal effect was comparable to 10% FCS. This response was reduced by P3, and had completely disappeared by P4. The reverse was true for the proliferative response to thrombin. The first significant responses appeared at P4. Thrombin was not as potent a mitogen as tryptase. Figure 1 illustrates this differential response.

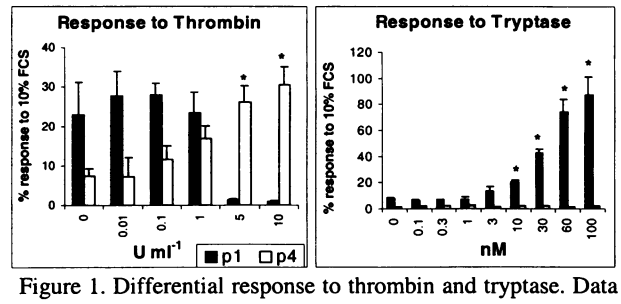

Figure 1. Differential response to thrombin and tryptase. Data are expressed as mean ± s.e.mean from 2 different experiments, each performed in triplicate. Significance versus non stimulated cells, (*, $p < 0.05$) was determined by paired Student's *t*-test.

The results suggest that through the passage, the proliferative response changes from a predominantly a PAR-2 to a PAR-1 like. Cultured guinea-pig tracheal smooth muscle cells can provide an *in vitro* system in order to study the sequential effect of the PARs in the same cell type.

Brown, J.K.,C.L.Tyler.,C.A.Jones *et al.* 1995. Am. J. Respir. Cell Mol. Biol. 13:227-236.

Stewart, A.G., D.J. Fernades, and P.R. Tomlinson. 1995. Br. J. Pharmacol. 116:3219-3226.

273P INCREASE IN DOPAMINE D_{2S} RECEPTOR AND G PROTEIN LEVELS FOLLOWING SODIUM BUTYRATE TREATMENT OF A RECOMBINANT CHO CELL LINE

D. L. Marston & P. G. Strange. School of Animal and Microbial Sciences, University of Reading, P. O. Box 228, Whiteknights, Reading, RG6 6AJ.

Variation in receptor expression levels in recombinant systems may alter the responsiveness of the receptor system (Hoyer & Boddeke, 1993). Sodium butyrate treatment results in increased receptor expression levels in cells and it has therefore been possible to examine agonist and antagonist properties in systems with varying receptor density (Lesage *et al.*, 1998). This compound is however a pleiotropic agent (Kruh, 1982) and may also alter G protein levels. The receptor to G protein ratio may affect the potency and efficacy of agonists and inverse agonists, thus in the present study the receptor:G protein stoichiometry following sodium butyrate treatment has been examined.

Human dopamine D_{2S} receptors were stably expressed in Chinese hamster ovary (CHO) cells and incubated with 5mM sodium butyrate for 18 hours before preparation of the cell membranes. Dopamine D_{2S} receptors were determined by saturation analysis with [^{3}H]spiperone as described by Sartania & Strange (1999). The number of dopamine-activated G proteins in untreated and sodium butyrate treated CHO-D_{2S} membranes was determined by [^{35}S]GTPγS isotopic dilution saturation binding as described by Newman-Tancredi *et al.*, (1997). The increase in B_{max} values was determined in parallel studies with untreated and sodium butyrate treated cells.

Receptor expression was increased 2.5 fold by treatment with sodium butyrate (Table 1). The binding affinity of [^{3}H]spiperone was unaffected ($p>0.05$, paired t-test). A parallel increase in receptor stimulated G protein binding was observed with no change in the binding affinity of [^{35}S]GTPγS ($p>0.05$, paired t-test) (Table 2).

Table 1. D_{2S} receptor levels following sodium butyrate treatment.

	Fold increase in B_{max}	pK_d K_d (pM)
Untreated	-	10.51 ± 0.06 31
+ Sodium Butyrate	2.50 ± 0.51	10.57 ± 0.05 27

B_{max} values ranged from 1.5-2.3pmol/mg (untreated) to 3.9-5.4 pmol/mg (treated). Values are mean ± s.e.mean, n=3.

Table 2. G protein binding following sodium butyrate treatment.

	Fold increase in B_{max}	pK_d K_d (nM)
Untreated	-	8.52 ± 0.17 3.0
+ Sodium Butyrate	1.94 ± 0.38	8.56 ± 0.19 2.8

B_{max} values ranged from 575.8 -1382 fmol/mg (untreated) to 871.9-2639 fmol/mg (treated). Values are mean ± s.e.mean, n=4.

These data indicate that sodium butyrate treatment of a CHO cell line expressing D_{2S} receptors does result in an increase in receptor levels. There is also an increase in the receptor stimulated G protein binding. This may be a reflection of increased G protein levels and should be considered when determining pharmacological properties of ligands.

This work was supported by the BBSRC.

Hoyer, D. & Boddeke, H. (1993). *Trends Pharmacol. Sci.* 14, 270-275.
Kruh, J. (1982). *Mol. Cell. Biochem.* 42, 65-82.
Lesage, A. S., Wouters, R., Van Gompel, P., *et al.* (1998). *Br. J. Pharmacol.* 123, 1655-1665.
Newman-Tancredi, A., Audinot, V., Chaput, C., *et al.* (1997). *J. Pharmacol. Exp. Ther.* 282, 181-191.
Sartania, N. & Strange, P. G. (1999). *J. Neurochem.* 72, 2621-2624.

274P POSSIBLE REGULATION OF CARDIAC ADP-RIBOSYL CYCLASE BY cGMP-DEPENDENT MECHANISMS

P. K. Solanki, S. Rakovic, A. Galione & D. A. Terrar, University Department of Pharmacology, Mansfield Road, Oxford OX1 3QT

Cyclic ADP-ribose (cADPR) has been demonstrated to promote calcium mobilisation from intracellular stores in a variety of cellular systems including the heart (Cui *et al*, 1999). The synthesis of cADPR from ß-NAD^+ is catalysed by the enzyme ADP-ribosyl cyclase. In the heart, the rate of ADP-ribosyl cyclase activity is enhanced by protein kinase A (Heath *et al*, 1999) and depressed by protein kinase C (Meszaros *et al*, 1997). The aim of this study was to investigate the regulation of ADP-ribosyl cyclase by cGMP-dependent mechanisms in a cardiac microsomal preparation.

Microsomes were prepared from the ventricles of male guinea-pig hearts using a method based on that of Sitsapesan & Williams (1990). ADP-ribosyl cyclase activity was assessed by measuring fluorimetrically the synthesis of cGDPR, an autofluorescent analogue of cADPR, from ß-NGD^+. cGDPR synthesis was monitored using a PTI fluorimeter (excitation 300 nm, emission 410 nm, 37°C). Experiments were performed in intracellular-mimicking solution (pH 7.2) containing 5 mM ATP, 20 mM phosphocreatine and 20 U/ml creatine phosphokinase as an ATP regenerating system.

As shown in Figure 1, cGMP, 8-bromo-cGMP and dibutyryl-cGMP (db-cGMP) were found to inhibit cGDPR synthesis in a concentration dependent manner (significant at all concentrations studied, $p<0.05$, unpaired 2-tail Student's t-test).

Figure 1

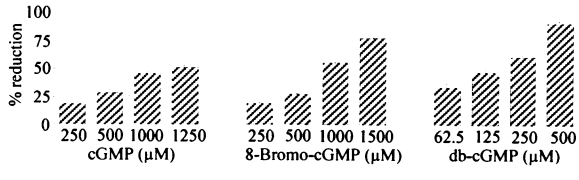

The inhibition of cGDPR synthesis by db-cGMP (75 μM) was reduced in the presence of a peptide inhibitor of protein kinase G (12±2% in its presence, 28±1% in its absence; $p<0.001$, n=5). Omission of ATP and its regenerating system also suppressed the extent of inhibition of cGDPR formation by db-cGMP (67±1% in the presence of ATP, 25±3% in its absence; $p<0.05$, n=6).

The ability of db-cGMP to inhibit cGDPR synthesis was enhanced if ADP-ribosyl cyclase was prestimulated with the catalytic subunit of PKA (50 U/ml). In the absence of PKA, 250 μM db-cGMP reduced the rate of cGDPR synthesis by 40±3% ($p<0.001$, n=5), compared to a 60±1% reduction in its presence ($p<0.001$, n=6). This is despite PKA itself increasing the rate of cGDPR production by 28±4% ($p<0.001$, n=5). This is illustrated in Figure 2.

Figure 2

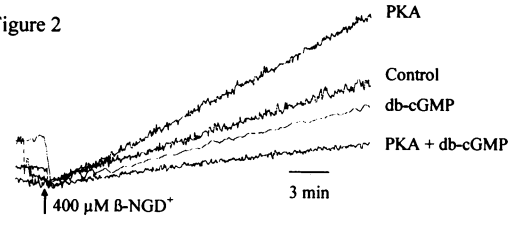

These data are consistent with an action of cGMP to inhibit the activity of ADP-ribosyl cyclase, particularly when the enzyme has been prestimulated by PKA. This may be mediated, at least in part, by a phosphorylatory mechanism involving protein kinase G.

Y. Cui, A. Galione & D. A. Terrar (1999) Biochem J 342, 269-73.
B. M. Heath, A. Galione & D. A. Terrar (1999) Br J Pharmac 126, 204P.
L. G. Meszaros, R. W. Wrenn & G. Varadi (1997) Biochem Biophys Res Commun. 234, 252-6.
R. Sitsapesan & A. J. Williams (1990) J Physiol Lond 423, 425-39.

275P IGF-1 MEDIATED INHIBITION OF APOPTOSIS IN RAT MESANGIAL CELLS

C.M. Ditchfield[1], T.S. Pillay[2], J. Savill[3], and I.P. Hall[1]. [1]Division of Therapeutics, [2]Molecular Endocrinology Group, Institute of Cell Signalling, University Hospital, Nottingham NG7 2UH. [3]Department of Internal Medicine, Royal Infirmary, Lauriston Place, Edinburgh, EH3 9YW.

Clearance of excess mesangial cells (MCs) by apoptosis mediates resolution of glomerulonephritis, but if allowed to proceed unchecked, promotes the formation of hypocellular scar tissue. Controlling the number of resident cells in the mesangium is therefore a balance between apoptosis, proliferation and survival signals. Work from our group has implicated the cytokine, IGF-1, as a survival factor for cultured rat MCs (Mooney *et al.*, 1997) but the mechanism by which this occurs has not been established.

Signalling through IGF-1 results primarily from the activation of the IGF-1 receptor. The phosphorylated receptor binds to the adapter proteins Shc and Insulin Receptor Substrate 1 and 2 (IRS-1/2) which recruit further downstream signalling molecules. We sought to define the intracellular signalling pathways by which IGF-1 signals MC survival and looked for expression of IRS-1 and IRS-2 in these cells.

A well characterised rat MC clone was used in all experiments (Baker *et al.*, 1994). Cells, washed with serum free media, were incubated in the presence or absence of cytokines for 24 h, then fixed with 4% formaldehyde. Apoptotic cells were counted by inverted fluorescence microscopy of propidium iodide stained cells.

Withdrawal of serum from the culture medium caused 8.7 ± 1.3% (mean ± SEM, $p<0.01$, n=8) of rat MCs to become apoptotic after 24 h. IGF-1 (100 $ngml^{-1}$) was able to rescue the cells from apoptosis induced by serum withdrawal (45.6 ± 6.2% reduction cf. control, $p<0.01$, n=8). No significant protection was provided by either Insulin (100$ngml^{-1}$) or PDGF (20$ngml^{-1}$) where the level of apoptosis was 11.9 ± 2.1 and 10.1 ± 2.2 % respectively, compared to 11.0 ± 1.8 % in the absence of serum (n=4).

RT PCR of DNase treated RNA isolated from rat MCs indicated the presence of both IRS-1 and IRS-2. This was confirmed by western blot analysis using specific antibodies against the C-terminus of IRS-1 (#06-248, UBI) and IRS-2 (A-19, Santa Cruz) (Zhou *et al.*, 1997). We looked to see whether the IRS proteins were phosphorylated following IGF-1 stimulation. An experiment, using a GST-fusion protein of the N-terminal SH2 domain of p85 to pull down IRS-1/2, showed that IRS-2 was phosphorylated after 5 min IGF-1 stimulation.

The results confirmed that IGF-1 is a survival factor in rat MCs. We have demonstrated the presence of IRS-1 and IRS-2 at the mRNA and protein level and shown that IRS-2 is phosphorylated after stimulation with IGF-1. These data suggest that the phosphorylation of IRS proteins may be important in IGF-1 mediated survival.

Baker, A.J., Mooney, A., Hughes, J., *et al.* (1994). *J. Clin. Invest.* 94 : 2105-2116

Mooney, A., Jobson, T., Bacon, R., *et al.* (1997). *J. Immunol.* 159 : 3949-3960

Zhou, L., Chen, H., Lin, C.H., *et al.* (1997). *J. Biol. Chem.* 272 : 29829-29833

This work was supported by a Welcome Prize Studentship (awarded to CD)

276P CHARACTERISATION OF BINDING OF [^{125}I] PROLACTIN-RELEASING PEPTIDE (PRRP-20) TO GPR10, A NOVEL G-PROTEIN COUPLED RECEPTOR

C.J. Langmead, *S.J. Ratcliffe, D.N.C. Jones & H.J. Herdon
Departments of Neuroscience Research and *Discovery Chemistry, SmithKline Beecham Pharmaceuticals, New Frontiers Science Park, Harlow, Essex, CM19 5AW.

GPR10 is a novel G protein coupled receptor (Marchese *et al.*, 1995) which is a human counterpart of rat UHR-1 (Welch *et al.*, 1995). Human prolactin-releasing peptide (PrRP) has been identified as an endogenous ligand for GPR10 (Hinuma *et al.*, 1998). The PrRP preproprotein can be cleaved at two different positions to give rise to two forms of 31or 20 amino acids: PrRP-31 and PrRP-20. Rat PrRP has also been identified and occurs as 31or 20 amino acid forms. In the present study the binding of [^{125}I]-PrRP-20 has been used to characterise GPR10 receptors in membranes from HEK293 cells stably transfected with the receptor. Radioligand binding assays to membranes from cells expressing GPR10 (Wilson *et al.*, 1998) were performed by a modification of the method of Miyamoto *et al.*, (1994).
[^{125}I]-PrRP-20 was used at a concentration of 0.2 nM in association, dissociation and competition studies; saturation analyses were carried out using a range of concentrations from 0.02 nM to 5 nM. Non-specific binding was measured in the presence of 0.1 µM rat PrRP-31. All results are the mean ± s.e.m. of at least 3 independent experiments. Specific binding of [^{125}I]-PrRP-20 was >90% of total binding and reached a maximum by 90 min of incubation. Membranes from untransfected cells displayed only non-specific binding. Saturation analysis suggested that the radioligand bound to both high and low affinity sites with K_D values of 0.026 ± 0.006 nM and 0.57 ± 0.14 nM and B_{max} values of 3.01 ± 0.40 and 8.57 ± 2.24 pmol mg $protein^{-1}$ respectively. [^{125}I]-PrRP-20 was shown to associate with a K_{obs} of 0.077 ± 0.008 min^{-1} and dissociate with a K_{off} of 0.0048 ± 0.0002 min^{-1}, giving a K_{on} value of 396 ± 54 min^{-1} μM^{-1}. Kinetic studies were unable to discern two distinct binding sites, though single site analysis of the data produced a K_D value of 0.012 nM which is close to the value for the higher affinity site revealed by the saturation studies.
Competition studies revealed that human PrRP-20 and PrRP-31 and rat PrRP-20 and PrRP-31 show similar potencies in competing for [^{125}I]-PrRP-20 binding to GPR10, with pK_i values of 9.4 ± 0.1, 9.0 ± 0.2, 9.4 ± 0.1 and 9.4 ± 0.1 respectively. Substance P, neurokinin-A, the neurokinin-B analogue $MePhe^7$ NK-B and neuropeptide-Y did not compete for binding at concentrations up to 1 µM. In conclusion, [^{125}I]-PrRP-20 binds to GPR10 and labels both high and low affinity binding sites. This radioligand should prove valuable for the further characterisation of the GPR10 receptor.

Hinuma, S., Habata, Y., Fujii, R. *et al.*, *Nature* **393**, 272-276 (1998)
Marchese, A., Heiber M., Nguyen, T. *et al.*, *Genomics* **29**, 335-344 (1995)
Miyamoto, Y., Habata, Y., Ohtaki, T. *et al.*, *Biochim. Biophys. Acta* **1218**, 297-307 (1994)
Welch, S., O'Hara B., Kilduff, T. *et al.*, *Biochem. Biophys. Res. Comm.* **209(2)**, 606-613 (1995)
Wilson, S., Bergsma, D., Chambers, J. *et al.*, *Br. J. Pharmacol.* **125**, 1387-1392 (1998)

277P AGONIST-INDUCED [^{35}S]GTPγS BINDING MEDIATED BY THE hEdg2 RECEPTOR

E.J. Handford, J.A. Stanton, G. McAllister and M.S. Beer, Merck Sharp & Dohme Research Laboratories, Neuroscience Research Centre, Terlings Park, Harlow, Essex CM20 2QR, U.K.

Lysophosphatidic acid (LPA) is thought to be the endogenous ligand for the human Edg2 (hEdg2) receptor, a member of the Edg GPCR super family. Studies carried out by An *et al.*, (1998a,b), indicate that several LPA related analogues are also able to elicit hEdg2 receptor mediated responses.

In this study the functional effects of LPA and four related analogues, namely lysophosphatidylethanolamine (LPE), lysophosphatidylglycerol (LPG), lysophosphatidylcholine (LPC) and phosphatidic acid (PA) have been investigated at the pertussis toxin (PTX)-insensitive hEdg2 receptor-rGiα1 fusion protein transiently expressed in HEK cells using agonist-induced [^{35}S]GTPγS binding (Stanton *et al.*, this meeting). The fusion protein was constructed to overcome the problems associated with the almost ubiquitous LPA endogenous response seen in mammalian cell lines. Treatment of transfected cell membranes with PTX allowed the development of an assay devoid of non-Edg2 receptor mediated LPA effects.

Membranes from PTX pre-treated (100ng/ml, 20hrs prior to harvesting) HEK cells transiently expressing the hEdg2 receptor-rGiα1 fusion protein were homogenised in 20mM HEPES, 10mM EDTA buffer (pH 7.4 at RT) and centrifuged at 48,000xg for 15 min. The pellet was re-suspended in 20mM HEPES, 0.1mM EDTA buffer (pH 7.4 at RT) and re-spun at 48,000xg for 15min. The final pellet was re-suspended in 20mM HEPES, 100mM NaCl, 10mM $MgCl_2$ buffer, pH 7.4 at RT. Agonists were prepared in 1% fatty acid free BSA (final concentration of 0.1%). Membranes (2.5mg wet weight) were pre-incubated with 1μM GDP and agonist for 20min at 30°C followed by 15min on ice. [^{35}S]GTPγS (100pM) was added and the tubes incubated for a further 30mins at 30°C. The incubation was terminated by filtration and radioactivity measured.

LPA (oleoyl) was the most potent and efficacious compound tested yielding a pEC_{50} value of 6.7±0.1 (mean ± SEM, n=4). LPG (oleoyl) was slightly less efficacious (84±3% of the LPA response) with a much weaker potency (pEC_{50} 5.0±0.1, mean ± SEM, n=4). PA (dioleoyl), and LPE (oleoyl) were even weaker partial agonists compared to LPA (efficacy values of 64±3%, and 29±2% of the maximal LPA response respectively) but had similar potencies to LPG (pEC_{50} values of 5.2±0.1, and 5.0±0.1 respectively, mean ± SEM, n=4). LPC (oleoyl) was essentially inactive up to a concentration of 100μM.

LPE, LPG and LPC are analogues of LPA where ethanolamine, glycerol and choline have been attached to the phosphate group of the parent compound. This study indicates that the glycerol and ethanolamine, unlike choline, are relatively well tolerated although LPE was less efficacious than either LPA or LPG. In addition the study indicates that PA which has two acyl side chains is also reasonably well tolerated yielding an efficacy of 64% compared with LPA. This result reflects the findings reported by An *et al.*, (1998b) in which PA was found to be a partial agonist with respect to LPA.

This experimental procedure has therefore been used to monitor, with confidence, hEdg2 receptor-mediated responses in a mammalian cell line. Investigations as to the effects of several LPA analogues indicate that modifications to the phosphate group of LPA as well as the presence of two acyl side chains is tolerated for functional activation of this receptor subtype.

An S., Bleu T., Zheng Y. and Goetzl E.J. (1998a) *Mol. Pharmacol.* 54, 881-888.

An S., Bleu T., Hallmark O.G. and Goetzl E.J. (1998b) *J. Biol. Chem.* 273, 7906-7910.

Stanton J.A., Handford E.J., Salim K., McAllister G. and Beer M.S., this meeting

---

278P LPA-INDUCED [^{35}S]GTPγS BINDING MEDIATED BY MOUSE AND HUMAN HEDG2 RECEPTORS

J.A. Stanton, E.J. Handford, K. Salim, G. McAllister and M.S. Beer. Merck Sharp & Dohme Research Laboratories, Neuroscience Research Centre, Terlings Park, Harlow, Essex CM20 2QR.

Most mammalian cell lines are responsive to lysophosphatidic acid (LPA) the endogenous ligand for the Edg2 receptor (Hecht *et al.*, 1996). One approach to overcome interference by non-Edg2 receptor mediated responses, when monitoring Edg2 mediated LPA responses in recombinant receptor cell lines is to develop an assay using a hEdg2 receptor-pertussis toxin-insensitive rGiα1 subunit fusion protein. To this end, transient expression studies, investigating LPA-induced [^{35}S]GTPγS binding in HEK cells transiently expressing the mEdg2 receptor co-expressed with the rGiα1 subunit (untagged or epitope tagged with either HA or myc at the N terminus (N)), the hEdg2 receptor co-expressed with the rGiα1 subunit (untagged or HA(N) or myc(N) epitope tagged) and a pertussis toxin (PTX)-insensitive hEdg2 receptor- rGiα1 fusion protein, were carried out.

Cells were homogenised in 20mM HEPES, 10mM EDTA buffer (pH 7.4 at RT) and centrifuged at 48,000xg for 15 min. The pellet was resuspended in a 20mM HEPES, 0.1mM EDTA buffer (pH 7.4 at RT) and re-spun at 48,000xg for 15 min. The final pellet was resuspended in 20mM HEPES buffer containing 100mM NaCl and 10mM $MgCl_2$, pH 7.4 at RT. Membranes (2.5mg wet weight) were pre-incubated with GDP (1μM) and LPA (in assay buffer containing 1% fatty acid free BSA to give a final assay concentration of 0.1%) for 20 mins at 30°C followed by 15 mins on ice. [^{35}S]GTPγS (100pM) was added and tubes incubated for a further 30 min at 30°C. The incubation was terminated by filtration and radioactivity measured. LPA dose-dependently increased [^{35}S]GTPγS binding in all transfected cells. The responses seen with the rGiα1 subunit alone and mock transfected HEK cells, however, were very weak and probably reflect activation of an endogenous receptor. Varying levels of efficacy were seen in the remaining cell lines as shown in Table 1 (results are arithmetic means ± SEM, n ≥ 6, n/d = not done).

Table 1 Potency and efficacy values for LPA-induced [^{35}S]GTPγS binding

	Mouse		Human	
	pEC_{50}	Emax(%)	pEC_{50}	Emax(%)
Edg2	8.1±0.2	14±3	7.7±0.1	23±3
Edg2+rGiα1	7.9±0.2	16±2	7.6±0.1	44±6
Edg2+rGiα1HA(N)	7.9±0.2	27±3	7.5±0.1	62±5
Edg2+rGiα1myc(N)	7.7±0.1	20±2	7.4±0.1	63±6
Edg2-rGiα1 fusion	n/d		7.3±0.1	91±11

As anticipated the magnitude of the LPA-mediated response was improved following co-transfection of the hEdg2 receptor with the rGiα1 subunit. More surprisingly however, replacement of the native rGiα1 subunit with N terminal tagged rGiα1 subunits (HA or myc) resulted in an improved response. The response was even further enhanced with the hEdg2 receptor-rGiα1 fusion protein. This response was maintained following pre-treatment with pertussis toxin (100 ng/ml, 20 hours prior to harvesting) in contrast to the co-transfection studies where the response was dramatically reduced. The LPA potency values were comparable in all the transfected cell lines (Table 1).

This study, using the PTX pre-treated hEdg2 receptor-rGiα1 fusion protein, is the first definitive demonstration of LPA-mediated hEdg2 receptor activation in mammalian cells.

Hecht J.H., Weiner J.A., Post S.R. & Chun J. (1996) *J. Cell. Biol.*, 135, 1071-1083.

279P DILTIAZEM AND VERAPAMIL INHIBIT THE HUMAN α7-NICOTINIC ACETYLCHOLINE RECEPTOR

L.M. Houlihan & Isabel Bermudez. Department of Biological and Molecular Sciences, Oxford Brookes University, Gypsy Lane, Oxford OX3 OBP

Non-peptide calcium channel antagonists, such as diltiazem, inhibit exocytosis in chromaffin cells via a direct action on nicotinic ACh receptors in addition to L-type calcium channels. At present it is uncertain whether the α7 nicotinic ACh receptor (α7 nAChR) participates in exocytosis in chromaffin cells. This is partly due to the lack of information on the sensitivity of the α7 nAChR to L-type calcium channel antagonists. We have therefore investigated the effect of diltiazem on the Human α7 nAChR using ligand displacement and electrophysiological methods.

Mature female *Xenopus* frogs were sacrificed and the ovary lobes removed. Oocytes were manually defolliculated and injected with 50ng recombinant Human α7 nicotinic ACh receptor RNA and incubated overnight in low calcium Barth's medium. Electrophysiological recordings were made 1-4 days later with oocytes voltage clamped at -100mV to -60mV.

In oocytes expressing the Human α7 nAChR, diltiazem caused a concentration-dependent inhibition of ACh currents. Inhibition was reversible and non-competitive in nature. Previous exposure to diltiazem for 1 min caused a marked increase in potency from EC_{50} 7.2 ± 2.41μM (n=4) to EC_{50}. 1.0 ± 1.3μM (n=4; P<0.04). Current-voltage curves constructed with EC_{50} diltiazem concentrations showed that inhibition was not voltage dependent. Recovery of ACh currents from diltiazem inhibition were slower when pre incubation was performed. Curve fitting of recovery time data gave time constants of 13.9 ± 0.4 seconds (n=2), and 53.7 ± 10 seconds (n=3; P<0.02) for diltiazem with no incubation and 1min incubation, respectively. The data are consistent with the proposal (Herrero *et al*, 1999) that diltiazem promotes nicotinic ACh receptor transfer into, and stabilisation of, the 'deactivated' state.

To gain information on the diltiazem site of action the effect of increasing concentrations of diltiazem on the concentration-response curves of the competitive antagonist dihydro-β-erythroidine was studied. A strictly additive effect of diltiazem on the inhibition of ACh currents by these drugs was observed, suggesting that the diltiazem site is distinct from this drug's binding sites.

The Phenylalkylamine verapamil is known to inhibit chromaffin cell function in a similar manner to diltiazem. We have found that verapamil inhibits the α7 nAChR with an EC_{50} of 42.3 ± 5.3μM (n=7), and that diltiazem has an additive inhibitory effect when coapplied with verapamil. This suggests the two drugs do not share the same binding site. Given the similarity between the EC_{50} range for diltiazem inhibition of chromaffin cell nicotinic currents and the EC_{50} presented here, this study suggests that the Human α7 nAChR may play a role in diltiazem inhibition of adrenal medulla chromaffin cells.

Herrero C., Garcia-Palomero, E., Pintado, A., *et al* (1999) Br. J. Pharmacol. **127** 1375-1387

280P KERNEL DENSITY ESTIMATION AS A METHOD FOR DISPLAYING AND INTERPRETING TABULATED DWELL TIME DATA

R. Rosales[1], W.J. Fitzgerald[2] & S.B. Hladky[1] Departments of Pharmacology[1] and Engineering[2], University of Cambridge, Cambridge, CB2 1QJ Email: rr208@cus.cam.ac.uk; wjf@eng.cam.ac.uk; sbh1@cam.ac.uk.

Markov chain Monte Carlo methods are powerful tools that can be used with hidden Markov models in the analysis of single ion channel patch clamp records (Rosales et al, 1998, 1999). The Bayesian approach we have developed has emphasised signal restoration. As a consequence, the data is reduced to a set of possible sequences of dwell times at a finite set of possible conductance levels. These dwell times can be summarised by constructing a traditional histogram or by using a kernel density estimate (Bowman & Azzalini, 1997) of the probability density function (pdf). Kernel density estimation avoids both the loss of information inherent in grouping dwell times into bins and the need to adjust the plot to remove the distortions introduced when discrete time data are collected in logarithmically spaced bins (Stark & Hladky, 2000). The benefits of using kernel estimates are greatest when considering data sets with few observations or when using multi-dimensional plots that otherwise require many bins, i.e. whenever the number of counts per bin is expected to be small.

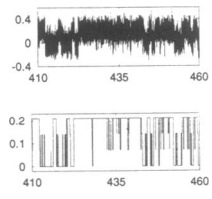

Left: 10^4 out of the 10^6 data points that were fitted to produce a list of dwell times. The theoretical trace is shown below. The levels at 0.14 and 0.2 are "open", those at 0 and 0.07 are closed.

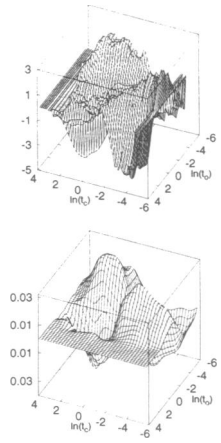

Right: Dependency-difference plots calculated from a histogram of the dwell times (top) or from the kernel estimates (bottom).

Magleby & Song (1992) introduced two-dimensional dependency difference plots to display the correlations between adjacent open and closed intervals. Peaks show events that are more frequent than predicted if the dwell times of open and closed intervals are independent; wells events that are less frequent. The figure compares a plot calculated from a kernel density estimate of the pdf with a plot calculated from a smoothed (but not adjusted) histogram produced when the pairs of adjacent open and closed dwell times are collected in logarithmic bins. The former is close to the theoretical shape in which brief closures (openings) are usually preceded by long openings (closings). Kernel density estimates are immediately and directly applicable to real patch clamp data sets including dwell time data generated through conventional methods.

Bowman, A. W. and Azzalini, A. (1997) Applied Smoothing Techniques for Data Analysis. Oxford Statistical Science Series, 18. Clarendon Press. Oxford.
Magleby, K. L. and Song, L. (1992). Proc. R. Soc. Lond. B. 249: 133-142.
Rosales R., Stark J. A., Hladky S. B. and Fitzgerald, W. J. (1998). Biophys. J. 74: A321.
Rosales R., Stark J. A., Hladky S. B. and Fitzgerald, W. J. (1999). Biophys. J. 76: A198.
Stark, J.A. and Hladky, S.B. (2000) Biophys. J. 78: in press.